NASA CR-72714

FINAL REPORT
Volume II

EVALUATION OF COATINGS FOR COBALT- AND NICKEL-BASE SUPERALLOYS

by

V.S. Moore, W.D. Brentnall, and A.R. Stetson

SOLAR DIVISION OF INTERNATIONAL HARVESTER COMPANY
2200 Pacific Hwy
San Diego, California 92112

prepared for

NATIONAL AERONAUTICS AND SPACE ADMINISTRATION

July 1970

CONTRACT NAS 3-9401

NASA Lewis Research Center
Cleveland, Ohio
Robert E. Oldrieve, Project Manager

NOTICE

This report was prepared as an account of Government sponsored work. Neither the United States, nor the National Aeronautics and Space Administration (NASA), nor any person acting on behalf of NASA:

A.) Makes any warranty or representation, expressed or implied, with respect to the accuracy, completeness, or usefulness of the information contained in this report, or that the use of any information, apparatus, method, or process disclosed in this report may not infringe privately owned rights; or

B.) Assumes any liabilities with respect to the use of, or for damages resulting from the use of any information, apparatus, method or process disclosed in this report.

As used above, "person acting on behalf of NASA" includes any employee or contractor of NASA, or employee of such contractor, to the extent that such employee or contractor of NASA, or employee of such contractor prepares, disseminates, or provides access to, any information pursuant to his employment or contract with NASA, or his employment with such contractor.

NASA CR-72714
Solar RDR 1474-3

FINAL REPORT
Volume II

EVALUATION OF COATINGS FOR COBALT- AND NICKEL-BASE SUPERALLOYS

by

V.S. Moore, W.D. Brentnall, and A.R. Stetson

SOLAR DIVISION OF INTERNATIONAL HARVESTER COMPANY
2200 Pacific Hwy
San Diego, California 92112

prepared for

NATIONAL AERONAUTICS AND SPACE ADMINISTRATION

July 1970

CONTRACT NAS 3-9401

NASA Lewis Research Center
Cleveland, Ohio
Robert E. Oldrieve, Project Manager

FOREWORD

Volume I of the Final Summary Report covered all experimental activities performed under NASA Contract NAS3-9401 during the period 27 June 1966 to 31 May 1968. This volume (Volume II) includes all additional experimental data generated on this program.

The program was the consequence of a contract initiated between Solar and the NASA-Lewis Research Center, Materials Contract Section, Materials and Structures Division, Cleveland, Ohio. It was conducted to evaluate the oxidation-erosion resistance and mechanisms of failure of nickel- and cobalt-base superalloys protected with commercially available coatings.

Technical direction was supplied by Robert E. Oldrieve, Project Manager of the NASA-Lewis Research Center. Salvatore J. Grisaffe served as technical advisor for the NASA Research Center.

Solar personnel who contributed to the experimental program and to the writing of this report are:

Mr. Victor S. Moore - Principal Engineer

Mr. William D. Brentnall - Metallurgy

Mr. Alvin R. Stetson - Program Director

Special recognition is granted to the team of technicians that operated the oxidation erosion rigs, Messrs. J. Lapping, D. Jader and A. Livingstone; to Messrs. C. Saucer and T. Johnson, who performed the instrumental analyses; and to Mr. R. Hutting for metallography.

The Solar report number is RDR 1474-3.

ABSTRACT

The final results of an oxidation-erosion rig evaluation of aluminide coatings applied by commercial vendors to IN-100 and B1900 nickel-base and X-40 and WI-52 cobalt-base alloys are presented. Tasks I and II of the program (Volume I, NASA CR-72359) resulted in the selection of two coatings per alloy for extended evaluation in Task III. In this task, as in the previous tasks, burner rigs were used that operated on JP-5 fuel and air producing a gas velocity of 0.85 (2000-2500 ft/sec) at the specimen's leading edge. One-hour heating cycles were used with three minutes air blast cooling. Results of testing at temperatures ranging from T_{max} of 1850° F to 2050° F indicate that coated B1900 has the longest oxidation life at all temperatures, followed by IN-100> X-40>WI-52, based on a weight change criterion. A metallurgical criterion, requiring retention of a continuous β-CoAl layer, interchanged the rating of coated X-40 and WI-52 alloys. The weight change criterion of failure indicated that coatings on nickel-base alloys provided more than twice the life of coating on cobalt-base alloys at comparable temperatures; however if rated on life per 0.001 inch of βMAl in the initial coating, the more protective coatings on cobalt- and nickel-base alloys exhibit approximately similar lives.

Metallurgical and microprobe data showed that the coatings with the higher aluminum content and comparable thickness had longer lives. Of additives identified, silicon appeared to be beneficial in the nickel-base alloy coatings for longer-term, low-temperature life, but not for short-term, high-temperature performance. Chromium was identified in all coatings, but large additions of this element were undesirable except for short-term performance at temperatures above 2000° F.

Extrapolating the life results obtained to 1600° F, all of the selected coatings on the four basis alloys would be protective for at least 10,000 hours.

SPECIAL NOTE: All of the temperatures reported in Volume II of this final report were obtained with chromel-alumel thermocouples insulated with MgO and contained in an Inconel 600 sheath. These thermocouples were imbedded within the test specimens during calibration and are believed to be essentially the same as the metal temperature. The temperatures during calibration for the tests in Volume I of the final report were obtained by surface thermocouples which, due to the high gas temperature (2500 to 2900° F), convective heating of the 0.040 inch diameter thermocouple sheaths and minimal contact area with the test specimen, provided an indicated temperature somewhat higher than the metal temperature. This temperature difference could be as high as 50° F on the test specimen. This change should be considered when comparing the data for Volume I with data from Volume II. For example, the 2050° F T_{max} noted in this volume is equivalent to 2100° F noted in Volume I.

PRECEDING PAGE BLANK NOT FILMED.

CONTENTS

PRECEDING PAGE BLANK NOT FILMED.

ILLUSTRATIONS

ILLUSTRATIONS (Cont)

ILLUSTRATIONS (Cont)

ILLUSTRATIONS (Cont)

ILLUSTRATIONS (Cont)

TABLES

1

INTRODUCTION

The increasing demands being placed on gas turbine blades and vanes by high turbine inlet temperatures are creating a condition by which protective coatings must be employed for even limited use. Currently, coatings are used primarily to extend the time between overhauls (TBO). With this widened role of the coating, a critical assessment of commercially available coatings for superalloys becomes a necessity. Proprietary attitudes which do not allow specifications to detail structure, composition, thickness, void concentration, and performance cannot be tolerated in future applications. Coatings should be procurable by specifications similar to those pertaining to the blade and vane alloys. Coatings can still be proprietary, but they must be capable of meeting a rigorous specification. For this program the vendors applied coatings to their own internal specifications.

The objective of this program was to analyze all salient properties of several selected commercially available protective coatings applied to cobalt- and nickel-base superalloys, and to determine the performance in oxidation-erosion rig testing. The program was not a critique of coating vendors, but rather of coatings. This report does not identify vendors. The contractor was not aware of the vendors or of which specimens were supplied by which vendors. Rather, the program emphasized the effects of variations between the coatings, such as coating chemistry, phases present, and thickness and roughness on the protection afforded in erosion rig testing. The coating vendors were asked to supply coatings of the composition and to the specifications which were current at the time of the procurement.

Properties evaluated in the program were:

- Surface roughness, as-coated
- Weight change, as-coated and after exposure
- Thickness, as-coated
- Chemical composition, as-coated and after exposure
- Coating and substrate hardness, as-coated and after exposure
- Coating structure, as-coated and after exposure
- Coating phases, as-coated and after exposure

- Oxide structure after exposure
- Blade warpage after coating and cyclic testing

This comprehensive coating analysis, before and after oxidation-erosion rig testing, should provide a clearer insight into the mechanism of coating failure and should indicate the direction to be taken for the development of the next generation of superalloy coatings.

The program includes the following alloys:

Nickel-Base	Cobalt-Base
IN-100	X-40
B1900	WI-52

Three commercially available coatings for each alloy were evaluated.

The coating evaluation program was divided into three major tasks:

Task I - Procurement and Inspection of Program Alloys and Coatings, and Rig Calibration

Task II - Initial 100-Hour Tests on all Coating-Alloy Systems

Task III - Long-term Testing of Selected Coating Alloy Systems

Volume I of the summary report, issued on January 31, 1969 (Ref. 1), includes all of the activities in Tasks I and II and the initial activities in Task III. Volume II includes a detailed description of the prominent feature of all of the coatings, the final results of oxidation-erosion testing, the metallurgical evaluation of the mechanisms by which coatings fail and the metallurgically determined life of the coatings.

SPECIAL NOTE: All of the temperatures reported in Volume II of this final report were obtained with chromel-alumel thermocouples insulated with MgO and contained in an Inconel 600 sheath. These thermocouples were imbedded within the test specimens during calibration and are believed to be essentially the same as the metal temperature. The temperatures during calibration for the tests in Volume I of the final report were obtained by surface thermocouples which, due to the high gas temperature (2500 to 2900° F), convective heating of the 0.040 inch diameter thermocouple sheaths and minimal contact area with the test specimen, provided an indicated temperature somewhat higher than the metal temperature. This temperature difference could be as high as 50° F on the test specimen. This change should be considered when comparing the data for Volume I with data from Volume II. For example, the 2050° F T_{max} noted in this volume is equivalent to 2100° F noted in Volume I.

2

SUMMARY

The oxidation-erosion resistance of commercially available coatings on nickel- and cobalt-base superalloys under simulated gas turbine operating conditions were determined in this program under special environmental conditions and at various maximum temperatures between 1845° F and 2050° F*. The special conditions were the use of low sulfur JP-5 fuel (sulfur ~ 0.07 percent) and essentially sea-salt-free air. Gas velocity used in the test at the specimen's leading edge was Mach 0.85 (2000 to 2250 ft/sec). All cycles presented in this report were constant at 60 minutes in the oxidation-erosion rig flame and three minutes in an air blast. Some data were presented in Volume I for rapid cycling (three minutes in the flame and two minutes air cool), but none of the coating systems exhibited thermal fatigue cracking in 2400 cycles. This type of testing was, therefore, discontinued in favor of the one-hour cycles as a means of determining coating life. Evaluation of coating performance was established by weight change, surface appearance, changes in microstructure and thickness, surface X-ray diffraction and electron beam microprobe analysis.

Two nickel-base (IN-100 and B1900) and two cobalt-base (X-40 and WI-52) alloys each with three different coatings were subjected to rig testing. The coating vendors and the processes and chemistries used by the vendors were unknown to Solar personnel. Uncoated specimens were supplied by Solar to NASA-Lewis who, in turn, had them coated by their selected vendors. The specimens were then returned by NASA personnel to Solar with no vendor identifying marks.

The coated specimens were identified at Solar by letter code numbers B, C, D (IN-100); F, G, H (B1900); J, K, L (X-40); and N, O, P (WI-52). Uncoated specimens of each alloy were identified as A, E, I and M, respectively.

In the work summarized in Volume I (Ref. 1), the coatings had all been analyzed for initial composition, weight change during coating application, structure and thickness. All coatings were primarily β-NiAl or β-CoAl with only several showing elemental additions other than Al that could not be attributed to the substrate. For example, C and F had minor additions of silicon and D and G were of the duplex type with major additions of chromium. The D coating appeared to have the chromium deposited after the aluminum and the G coating prior to the aluminum. Possible other additions such as Ti and Fe were also noted.

---

*See Special Note on page 2.

In Tasks I and II of this program (results are reported in Volume I), the alloys and coatings were procured and characterized and initially screened in 100-hour rig tests at temperatures to 2090° F (2140° F surface thermocouple). From these tests, two coatings per alloy were selected for long-term testings. These coatings were:

IN-100 - B and C

B1900 - F and H

X-40 - J and L

WI-52 - O and P

This volume primarily presents data on the above coatings after exposure to one-hour cycles to a Tmax of 1845° F (Series 1), 1950° F (Series 2), and 2050° F (Series 3) internal temperatures. The other coatings - D, G, K and N - are also included to a lesser extent because spares were required in rig testing as specimens were removed from test as they reached the point of failure. The failure criterion for specimens was a loss of an average of 20 mg per blade and was established by the NASA Program Manager. From the metallurgical evaluation of the coatings after test, this criterion usually was at a point beyond the breakdown of the continuous βMAl to either γ' or γ. The very thick D coating (0.0055 inch), however, could fail the weight loss criterion while maintaining a continuous β-NiAl layer.

A summary of the life of the coating-substrate alloy combinations at various temperatures is presented in Figures 1 to 3. Figure 1 displays the life of the coatings based on the 20 mg average weight loss criterion; Figure 2 presents the coating life based on loss of a continuous βMAl layer; and Figure 3 presents the coating life per 0.001 inch of initial coating thickness (average thickness used for this calculation) based on loss of the continuous βMAl criterion of failure. The data used to compute thickness is very minimal because a maximum of three specimens were sectioned to determine the "as-received" thickness. The results in Figure 3 should, therefore, be weighed somewhat less than the results in Figures 1 and 2.

On the nickel-base alloys, the F and H coatings exhibited the best overall performance using both the weight loss and loss of continuous βMAl criteria for failure. The F and H coatings were protective to between 1765° F and 1805° F for 3000 hours (Fig. 2). The F coating exhibited a slightly flatter life-temperature curve indicating a potentially longer life for this coating at lower temperatures. The B and C coatings exhibited a 3000-hour potential life at 1750° F. Both the D and G chromium-rich coatings exhibited the highest temperature capability in short-time exposures, i.e., 100 hours at 2090° F. Both coatings, however, showed steeper life-temperature curves due to coating spalling and variable coating performance.

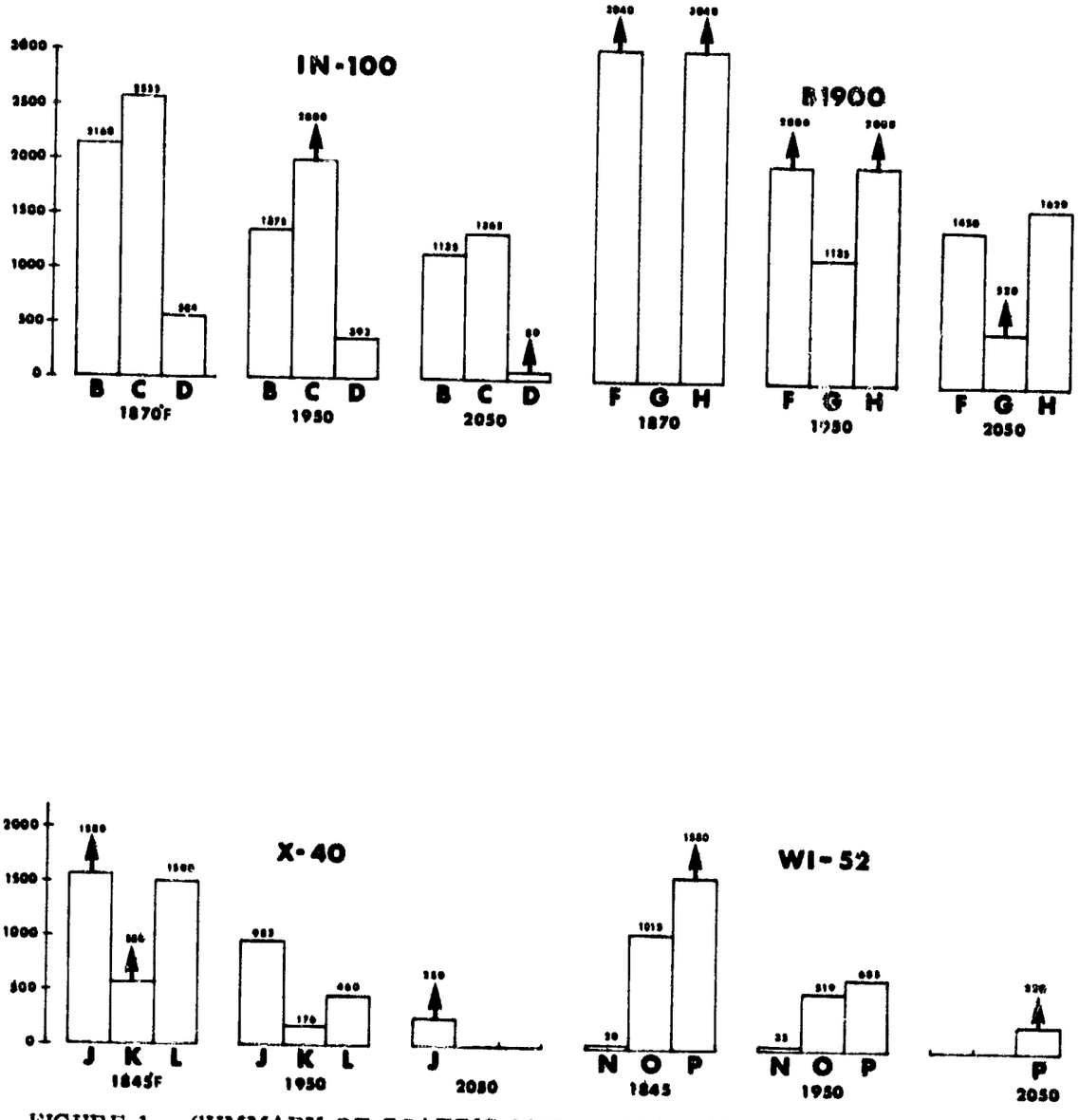

FIGURE 1. SUMMARY OF COATING LIFE BASED ON WEIGHT LOSS DURING TESTING

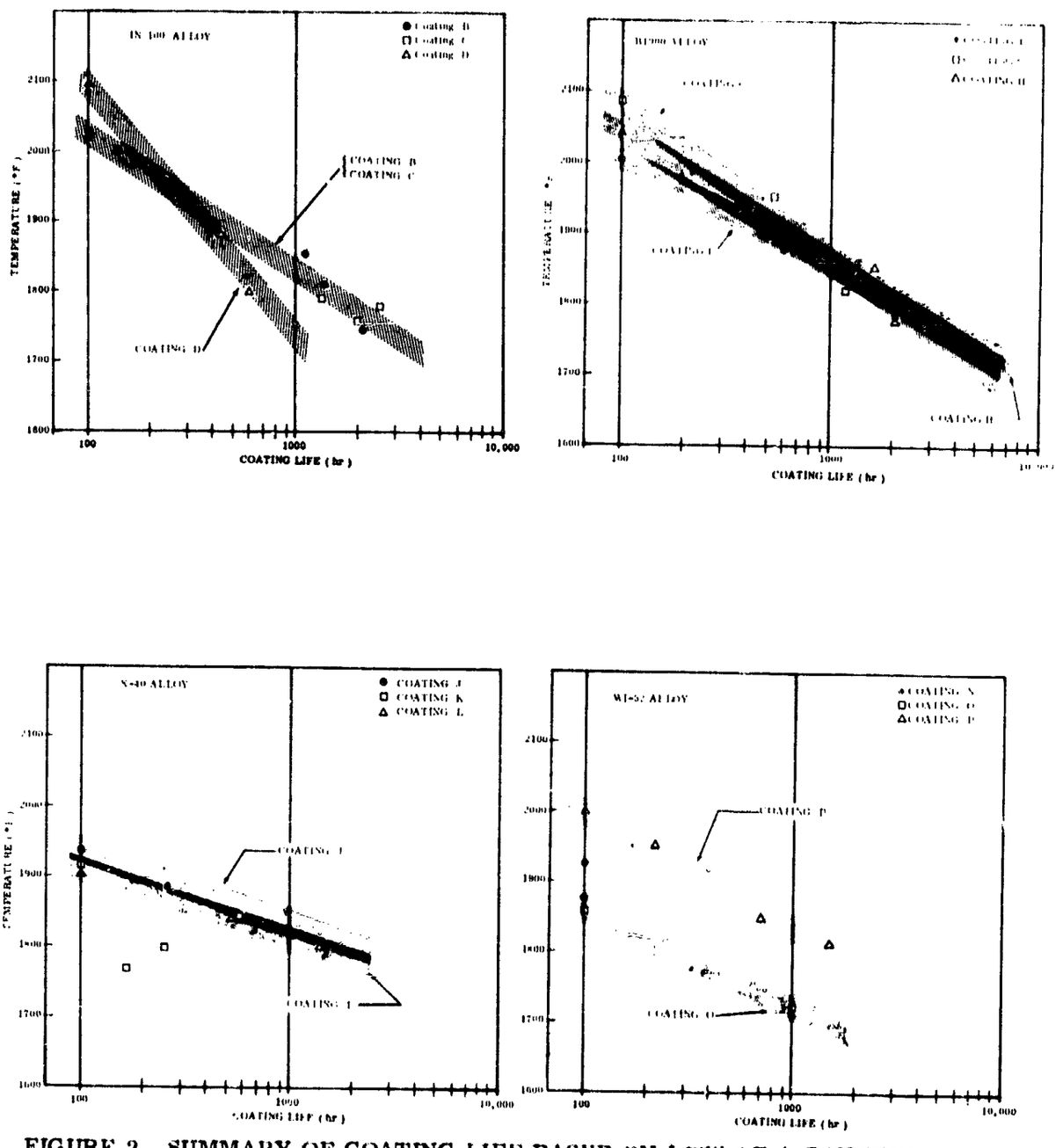

FIGURE 2. SUMMARY OF COATING LIFE BASED ON LOSS OF A CONTINUOUS βMAl LAYER

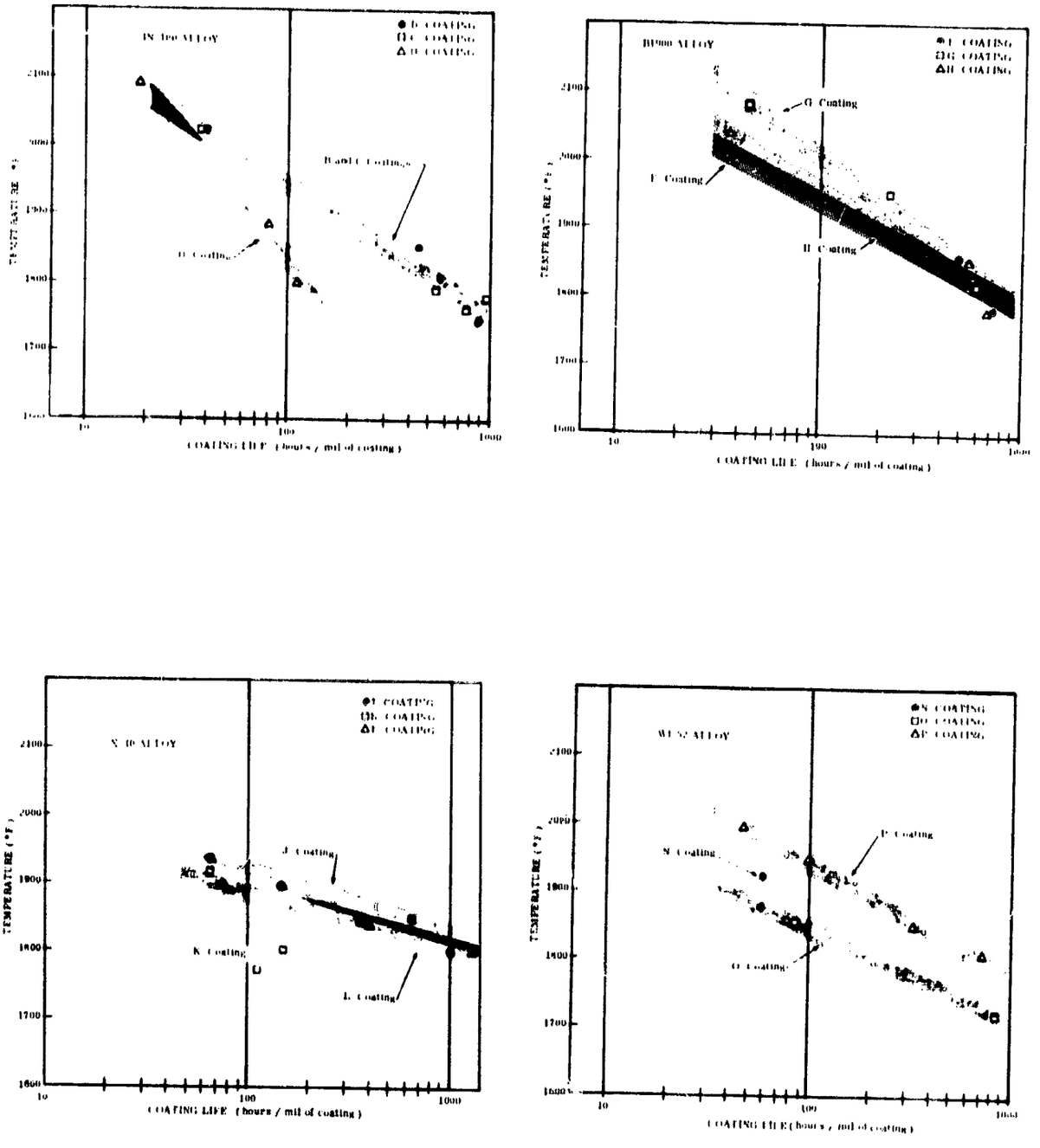

FIGURE 3. SUMMARY OF COATING LIFE PER 0.001-INCH OF COATING THICKNESS; Based on Loss of a Continuous βMAl Layer

The J coating exhbited the highest temperature capability over the entire temperature range of the three coatings on X-40 alloy. The extrapolated temperature for a 3000-hour life expectancy (Fig. 2) was approximately 1800° F. The L coating showed a slightly lower temperature capability of about 1765° F. Considerable scatter in the data for the K coating was no doubt related to the variation in coating thickness. On the WI-52 alloy, the P coating showed distinctly better performance than the N or O coatings. A 3000-hour life at 1800° F was exhibited which compared favorably with the J coating life on X-40 alloy. A higher temperature capability (2000° F) in the short-time, 100-hour tests, however, was apparent for the P coating. For a 3000-hour life of the O coating, the maximum temperature capability appeared to be 1660° F. Poorest performance was exhibited by the N coating on WI-52 alloy in the previous Task II tests and very little additional evaluation was performed on this coating system. Data are included that show the temperature capability for a 100-hour life to range from 1875° F to 1925° F.

Figure 3 presents the coating life data from Figure 2 normalized to show the hours per mil of coating thickness. For a Tmax of 1850° F, the normalized coating life was:

Coating	Hours/mil	Coating	Hours/mil
B	300	J	500
C	300	K	---
D	90	L	275
F	450	N	---
G	550	O	90
H	450	P	400

These data showed on the basis of hours/mil that the coatings on the cobalt-base alloys were capable of providing protection nearly equivalent to those on the nickel-base alloys. Comparing Figures 2 and 3, the curves show that the coating thickness was the most significant parameter lending itself to improvement for long-term protection of cobalt-base alloys.

Elements that were intentionally added to the coatings could only be unambiguously identified in several of the coatings on nickel-base alloys. Even after short-term thermal exposures, the coatings on cobalt-base alloys became structurally very similar.

The presence of large amounts of chromium was identified in the D and G coatings. The presence of chromium-rich phases in contact with the oxidizing environment caused spalling and the formation of the relatively poorly oxidation resistant γ solid solution. An intermediate zone of α chromium in the G coating was apparently effective as a diffusion barrier to restrict interdiffusion of nickel and aluminum.

Small percentages of added silicon were shown to be present in the best performing coatings on IN-100 and B1900, and it was hypothesized that the presence of silicon resulted in a decreased spalling rate of the protective αAl_2O_3.

In general, a large reservoir of aluminum correlated with extended coating life. This was noted particularly for the coatings on cobalt-base alloys where, for a similar coating thickness, a hyperstoichiometric aluminide composition (with respect to aluminum) performed better than a hypostoichiometric composition. The problem of obtaining a thick coating high in aluminum without exterior cracking and spalling appeared to be related to the degree of supersaturation of the aluminide with chromium from the substrates.

An interesting contrast in the diffusional stability of aluminide coatings on nickel alloys compared to cobalt alloys was exhibited. Degradation (aluminum dilution) of the coatings on nickel-base alloys clearly occurred by interdiffusion of nickel and aluminum across the interface in addition to loss by Al_2O_3 formation. An extensive region of γ' phase was formed in the substrate alloy and formation of γ' in the βMAl occurred progressively starting at the original coating/metal interface.

Extensive diffusion inwards of aluminum was not identified in the cobalt alloy systems and the initially thinner aluminide layers showed better stability and life than might have been expected by comparison with the nickel alloy systems. The presence of a continuous $M_{23}C_6$ interface zone may have acted as a "built in" diffusion barrier in the cobalt alloy systems, preventing inward diffusion of aluminum. Lower aluminum solubilities and different phase relationships (no intermediate γ' type phase in the Co-Al system) may also have been partly or largely responsible for the observed differences.

PRECEDING PAGE BLANK NOT FILMED.

3

TEST SPECIMENS AND TESTING TECHNIQUES

The procurement of the alloys, coatings and receiving inspection tests were reported in detail in Volume I of the final report. The only items that will be repeated are (1) the specimen identification code that is used when discussing performance of the various coating-alloy combinations, (2) a summary of the average coating thickness and average weight gain after coating for each combination, and (3) the chemical composition of the four program alloys.

3.1 TEST SPECIMENS

The chemical analyses of the four program alloys (IN-100, B1900, X-40 and WI-52) are shown in Table I. The analytical results performed at Misco are in good agreement with the nominal alloy compositions.

The selection and the procurement of the coatings for use in this program were made by the NASA Program Manager. A total of 12 coating-alloy combinations was included in the program; three coatings on each of the four alloys. The coating phase of the program was handled as follows:

- After receiving, inspection testing and individually identifying all of the as-cast blades at Solar, the blades were shipped to Lewis Research Center. NASA, in turn, shipped the blades to the selected coating vendors. After coating, the specimens were returned to NASA, repacked and then returned to Solar without any markings to show the source of the coating. The identity of the coating vendors is unknown to Solar.

Alloy and coatings were identified at Solar using the letter and number code system shown in Table II.

Figure 4 summarizes the average weight gain and the coating thickness (as determined metallographically) measurements made on specimens returned by the coating vendors. It should be noted that all specimens were weighed at Solar before shipment to NASA and after return to Solar by NASA. Since the specimens were not weighed at the coating vendors after their cleaning or preparation operations, the weight gains shown may be lower than actual values, depending upon the amount of substrate material removed.

TABLE I

CHEMICAL ANALYSES OF PROGRAM ALLOYS

Alloy and Heat	Composition (weight percent)															
	C	Mn	Si	P	S	Cr	Ni	W	Fe	Co	Mo	Al	Ti	Zr	B	Others
IN-100 RU082	0.18	<0.1	<0.1	--	0.003	10.15	Bal.	--	0.36	14.95	3.27	5.40	4.75	0.078	0.013	V 1.0
B1900 MG070	0.11	<0.1	0.15	--	0.007	7.75	Bal.	<0.1	0.09	9.95	5.90	6.01	1.07	0.086	0.010	Cb 0.1 Ta 4.22 Cu 0.007
X-40 12V5068	0.50	<0.1	0.29	0.008	0.017	25.50	10.75	7.55	0.12	Bal.	--	--	--	0.16	<.002	N 0.02
WI-52 MF199	0.47	0.31	0.41	0.013	0.013	20.75	0.29	10.8	2.04	Bal.	--	--	--	--	--	Cb + Ta 1.90

Note: Chemical Analyses were made by Misco Division of Howmet Corporation.

TABLE II

SPECIMEN IDENTIFICATION CODE

Code Letter	Remarks
A	Uncoated IN-100 alloy
B	Coated IN-100 alloy
C	Coated IN-100 alloy
D	Coated IN-100 alloy
E	Uncoated B1900 alloy
F	Coated B1900 alloy
G	Coated B1900 alloy
H	Coated B1900 alloy
I	Uncoated X-40 alloy
J	Coated X-40 alloy
K	Coated X-40 alloy
L	Coated X-40 alloy
M	Uncoated WI-52 alloy
N	Coated WI-52 alloy
O	Coated WI-52 alloy
P	Coated WI-52 alloy

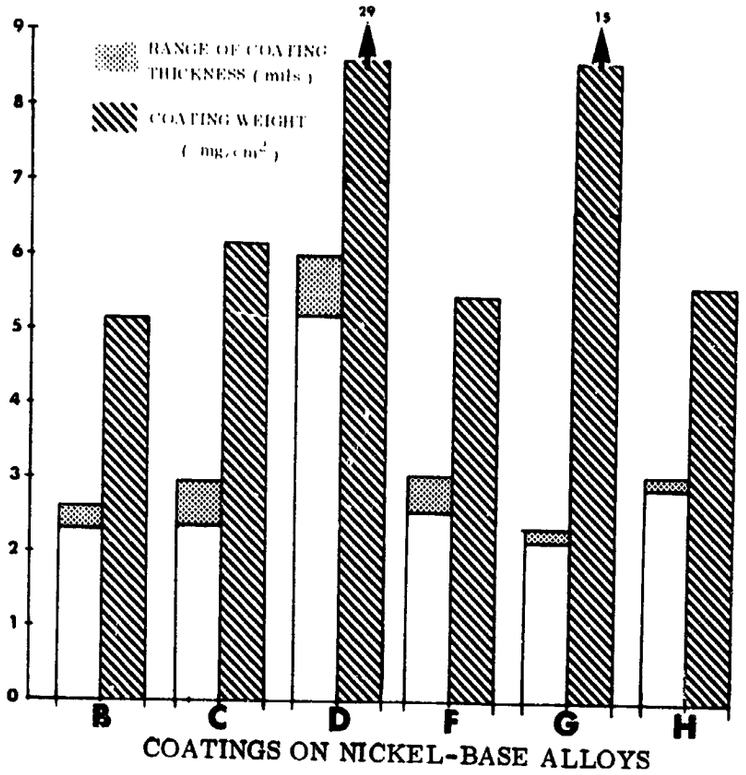

COATINGS ON NICKEL-BASE ALLOYS

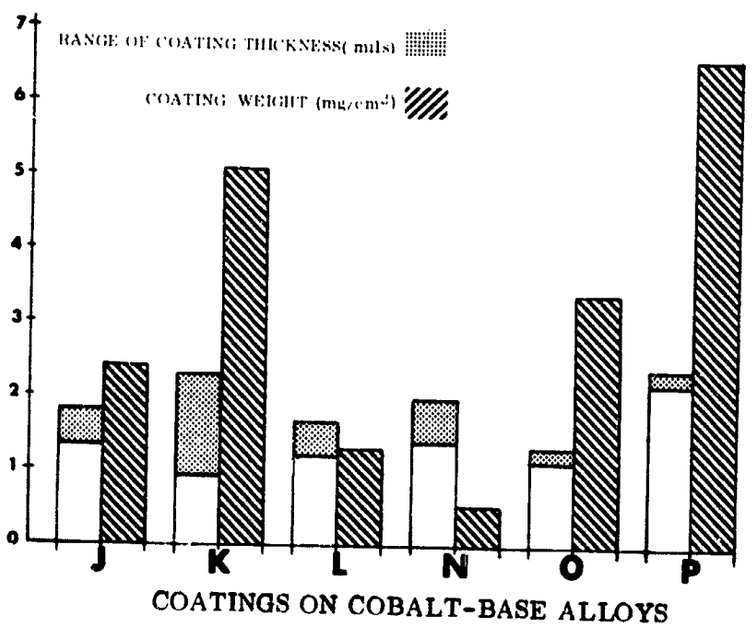

COATINGS ON COBALT-BASE ALLOYS

FIGURE 4. SUMMARY OF COATING THICKNESS AND WEIGHT GAIN

In summary, on the nickel-base alloys, average coating thickness ranged from a low of 0.0022 inch to a maximum of 0.0055 inch (the D coating). On the X-40 and WI-52 alloys, the average coating thicknesses ranged from 0.0011 inch for the K coating to 0.0022 inch for the P coating. Extreme variations in coating thickness from side to side were noted for the K coating; the concave side gave an average value of 0.0011 inch and the convex side measured 0.0021 inch. Coating coverage was generally good, but spalling was noted with the D, G, K and O coatings.

Average weight gain for the coatings ranged from a maximum of 29 mg/cm^2 (coating D) to a low of 0.5 mg/cm2 for the N coating. Considerable weight gain and variation in weight was also exhibited by coating G (15 mg/cm2). The evaluation studies showed that the weight gain and thickness could be accounted for by the deposition of a significant amount of chromium in addition to the aluminum. Excluding the heavy D and G coatings, the average weight gain for the nickel-base alloys was 5.5 mg/cm^2. The average weight gain for the six coatings on the two cobalt-base alloys was slightly lower at 3.3 mg/cm^2.

3.2 OXIDATION-EROSION TESTING TECHNIQUES

This program used rig testing for the performance evaluation of the coated superalloys. This type of test has found wide acceptance in the gas turbine engine field and simulates more closely the turbine environment than laboratory furnace oxidation and oxyacetelyne torch tests. A detailed discussion of the turbine environmental simulators (often also called burner rigs) used for the oxidation-erosion tests is provided in the following paragraphs.

3.2.1 Turbine Environmental Simulators

Two Solar gas turbine environmental simulators used for the high velocity oxidation-erosion tests are shown in Figure 5.

Details of these simulators are similar in features to those of modern small gas turbine engine combustors. A straight-through, can-type combustor is used with atomization of JP-5 fuel from a single spray nozzle. A water-cooled, one-inch diameter stainless steel nozzle is used for long-time, trouble-free operation.

The major control items used to ensure reproducible rig operations are:

- Fuel flowmeters and pressure regulators
- Combustor air pressure regulators
- Airflow measuring equipment

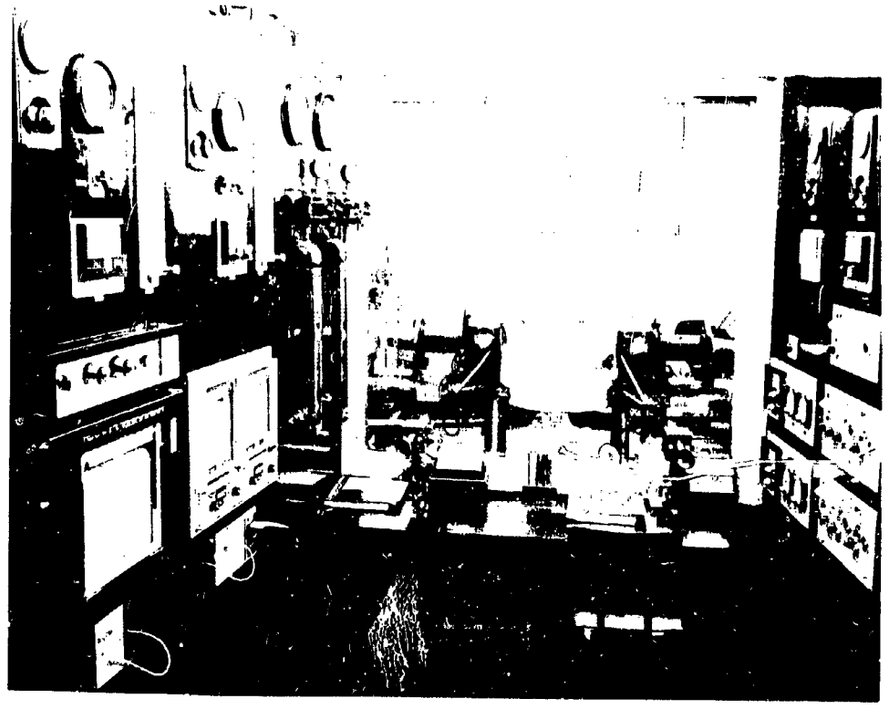

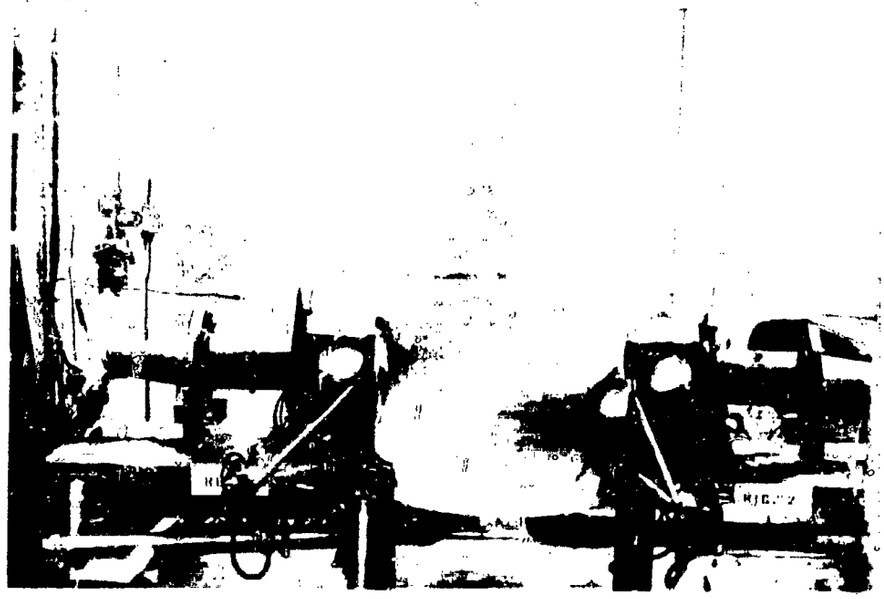

FIGURE 5. BURNER RIGS AND CONTROL ROOM

- Slip rings for continuous thermocouple temperature control
- Temperature recorder-controllers

During the rig tests, eight specimens were mounted in a holder (Fig. 6) which rotated at 1725 rpm. Rotation in the gas stream was required to ensure that all specimens experience the same test environment. The holder was positioned so that the leading edge of the specimens were one inch from the exit of the nozzle.

For all oxidation-erosion tests, the nozzle exit gas velocity was maintained above Mach 0.85, i.e., ranging from 2000 to 2250 ft/sec at the specimen location. Methods of determining hot gas velocity are described in detail along with sample calculations for typical test conditions in Volume I (Ref. 1).

Specimens were heated to the test temperature for one hour followed by cooling for three minutes in a room temperature air blast. Every 20 hours the specimens were removed from test for visual inspection and weighing.

3.2.2 Temperature Calibrations and Control Methods

Temperature is the major parameter that was carefully controlled to obtain quantitative, reproducible results in the oxidation-erosion tests. Control of the specimen metal temperature was effected by automatically adjusting and regulating the fuel flow to the combustor nozzle. Air flow was held constant by means of dome loading, diaphragm-type, high-capacity air regulators.

Specimen metal temperatures were continuously monitored, recorded and controlled throughout the test periods by means of a thermocouple inserted into a small hole in a test specimen. This hole was electrical discharge machined (EDM) through the base of the blade so that the thermocouple tip was at the center of the test section. One specimen in each group of blades (in the holder) was instrumented in this manner with a 0.040-inch diameter, Inconel sheathed, magnesium oxide insulated, chron el-alumel thermocouple. Output of the thermocouple was fed to a slip-ring assembly and then to a potentiometer-type strip chart temperature recorder and three-mode temperature controller. Any deviation between the temperature set point and the specimen temperature was sensed in the temperature recorder-controller, which continuously activated an electric-to-pneumatic converter thereby controlling a pneumatically operated fuel-flow control valve. Fuel flow was increased or decreased automatically as required to maintain the set temperatures.

To determine the maximum metal temperature distribution and the temperature gradient along the length and width of the simulated airfoil specimens, several methods of calibration were investigated during the program. These methods were:

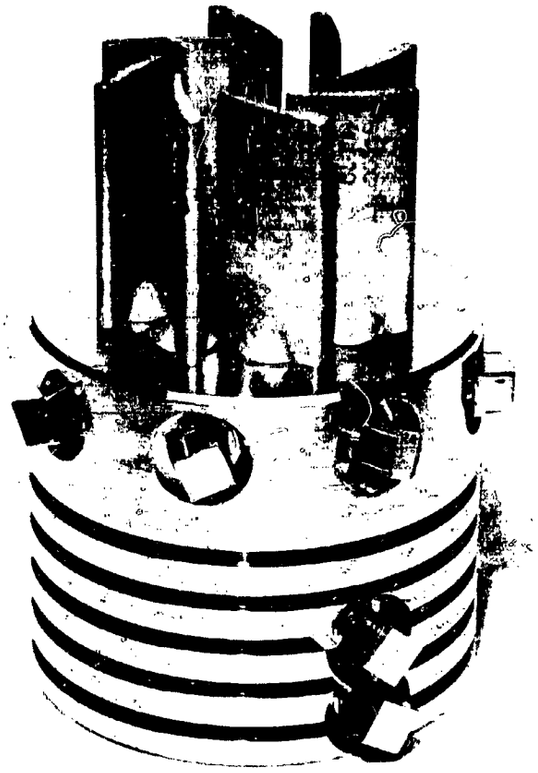

FIGURE 6. SPECIMEN HOLDER AND PADDLE WHEEL BLADES

Thermocouple:
0.040-inch diameter
Inconel sheath,
Type K, MgO insulation.

Tip shielded with
Inconel foil.

FIGURE 7. THERMOCOUPLE ON CONCAVE SURFACE OF TEST SPECIMEN

- The application of Templac paints and Thermindex paints.

- Pure metals were inserted into the blades. These included:

  - Small wires of silver (melting point 1761° F) (1234° K), gold (melting point 1945° F) (1336° K), and copper (melting point 1981° F) (1356° K) imbedded in the airfoil section of the blade.

- Thermocouples mounted on the surface of the specimen

Generally, the temperature-sensitive paints were not satisfactory due to the high velocity erosive conditions of the gas stream. The Templac paint was completely removed from the blade surfaces, and the Thermindex paints gave usable data only at the 1652° F (1173.3° K) temperature color change.

Melting points of the pure metals worked successfully, but the number of calibration points was limited.

The best results were obtained from the thermocouples mounted on the specimens. Small (0.040-inch diameter) Inconel sheathed thermocouples were spot-tacked to the concave surface of a blade, and readings were obtained using a slip-ring assembly. The tip of the thermocouple was shielded from direct flame radiation with a small piece of Inconel foil spot-tacked to the surface of the blade (Fig. 7). The temperature was determined at various locations on a test specimen airfoil over a control temperature range of 1450° to 1900° F. (The control thermocouple is located inside the blade at the center of the airfoil section.) The temperature distribution was determined for both test rigs, as the temperature gradients across the blades were somewhat different in each test rig. Even though the tip of the thermocouple was shielded from direct flame radiation and the high velocity gas stream, a small error existed using this calibration method.

At the completion of the oxidation-erosion tests, additional work was done on temperature calibration methods in order to define more accurately specimen metal temperatures for the tests at 1900°, 2000° and 2100° F.

An excellent temperature calibration method was developed wherein the small sheathed thermocouples were actually imbedded into the airfoil section of numerous blades at known locations. Correction factors for the surface temperature measurements were then determined by comparing the temperatures as determined by external and internal methods. The internal thermocouples were installed in the following manner:

- A small groove, 0.050 inch wide by 0.050 inch deep, was chemically milled into the concave surface of a blade so that the measuring

junction of the thermocouple was at a precisely known location (Fig. 8A).

- A 0.040-inch diameter Inconel sheathed thermocouple was inserted into this groove (Fig. 8B).

- The thermocouple junction was then spot-tacked in place, and the entire groove (and the thermocouple sheath) was filled in by plasma-arc spraying Nichrome powder (Ni-20Cr) (Fig. 8C).

- The concave surface of the blade was then carefully reground to the original surface contour (Fig. 8D).

The results of the blade temperature measurements made to establish calibration data for the 1900°, 2000° and 2100° F tests are shown in Figures 9 through 11. In Figure 9A, surface and internal temperatures are shown at eleven different locations on the concave surface of a specimen along with temperature curves for three thermocouples imbedded in the airfoil at the hottest location on the blade and for one surface thermocouple located at the "hot spot". Also included on this graph are curves drawn from optical temperature readings taken during the temperature calibration tests.

The test at 1900° F was originated and run based on surface temperature measurements. As shown in Figure 9A, a thermocouple control temperature of 1665° F was used throughout the duration of the test to maintain the 1900° F test temperature (this was later corrected to 1905° F T_{max}). Data from the internal thermocouple calibrations performed at the completion of the tests showed that the peak metal temperature was actually 1845° F or 60 degrees lower than that obtained by surface thermocouple measurements. Figure 9B shows the temperature distribution for the tests on the nickel-base alloys. T_{max} for these tests was 1820° F.

In all cases metal temperatures were maximum along the trailing edges of the blades and decreased rapidly towards the leading edge and shank area. Temperature variation generally exceeded 200° F from trailing edge to leading edge of the blades.

During the thermocouple temperature calibration tests, optical temperature measurements were also taken to ascertain whether or not a correlation could be made with the peak blade metal temperatures. The blades were viewed with a Pyro-Micro-Optical pyrometer (disappearing filament type) from two different optical paths. These optical paths (Fig. 12) were:

- Normal - In the midsection of the blades normal to the long axis of the blades.

- Edge - At a slight angle from the long axis of the blades sighted along the trailing edges of the blades.

Chem Mill Groove

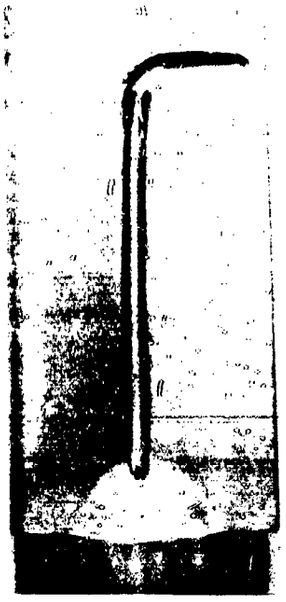

A

Install Thermocouple

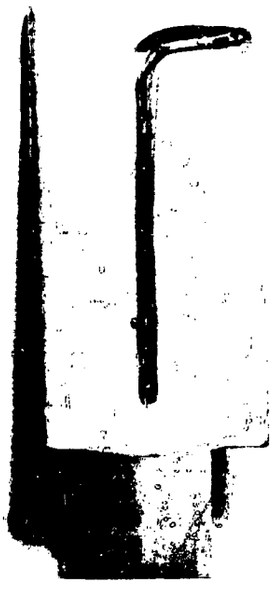

B

Magnification 1.5X

Plasma Arc Spray Ni-Cr

C

Clean-Up Surface

D

FIGURE 8. METHOD OF IMBEDDING THERMOCOUPLE IN SPECIMEN FOR TEMPERATURE CALIBRATION

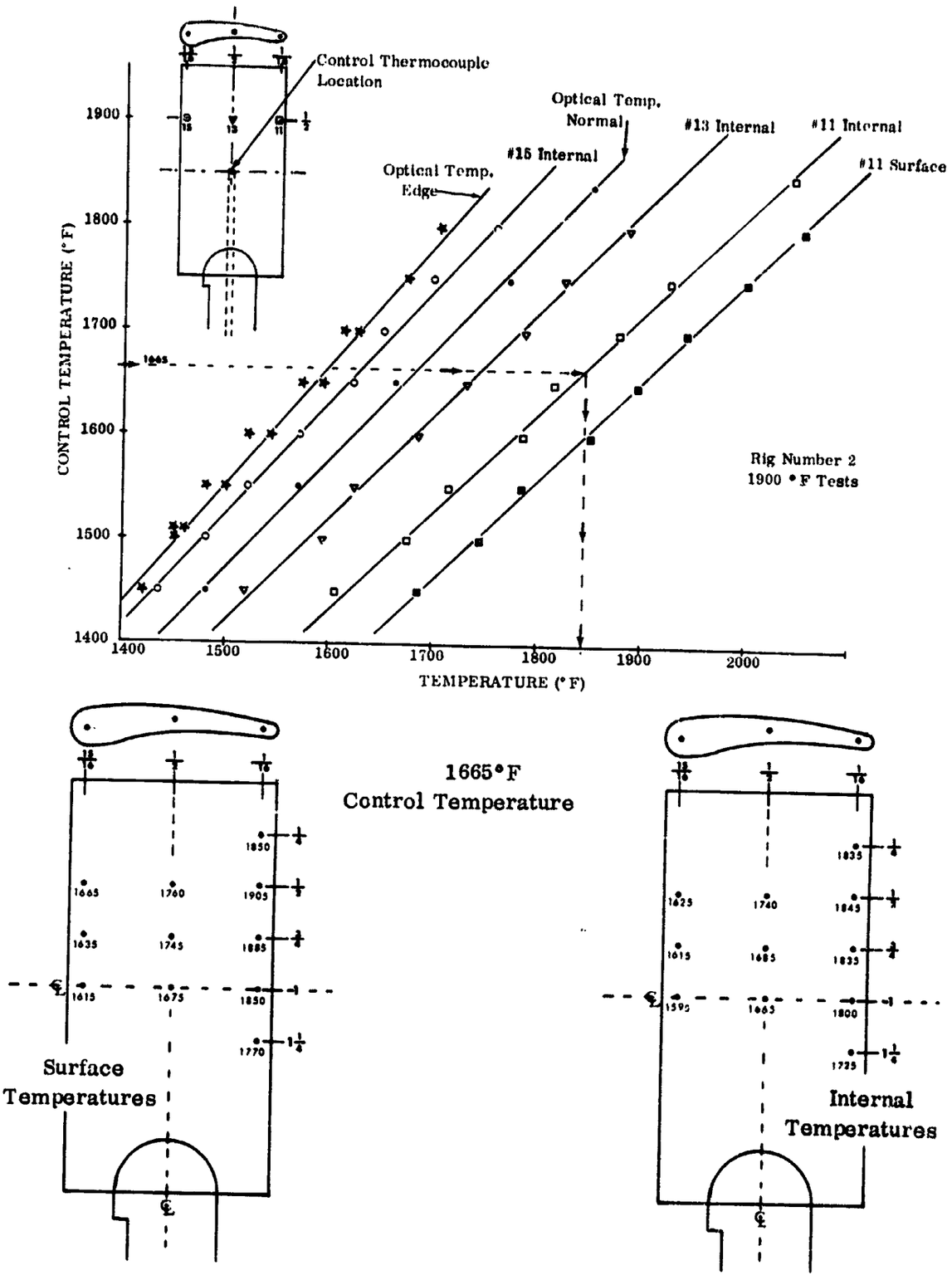

FIGURE 9A. TEMPERATURE CALIBRATION CURVES AND SPECIMEN TEMPERATURE DISTRIBUTION FOR SERIES 1 TESTS (T_{max} 1845° F) (X-40 and WI-52 Alloys)

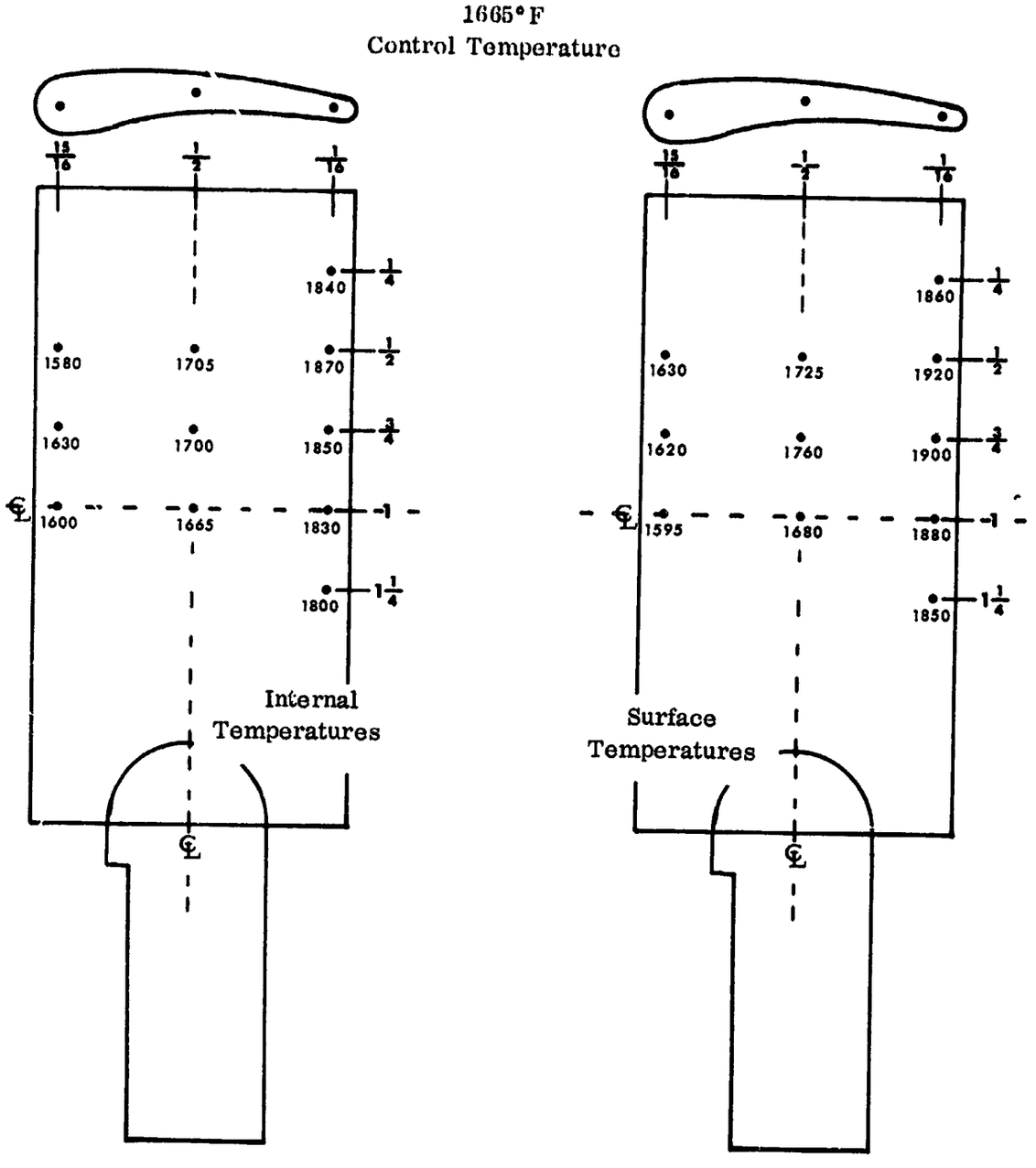

FIGURE 9B. SPECIMEN TEMPERATURE DISTRIBUTION FOR SERIES 1 TESTS (T_{max} 1870° F) (IN-100 and B1900 Alloys)

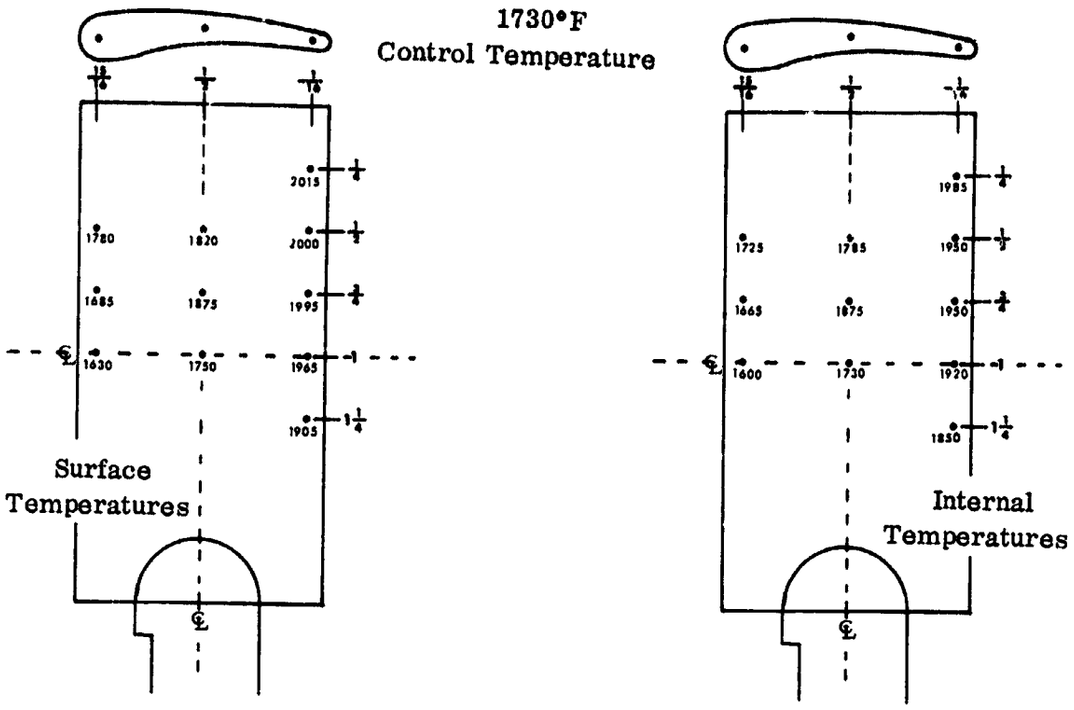

FIGURE 10. SPECIMEN TEMPERATURE DISTRIBUTION FOR SERIES 2 TESTS

The normal and edge optical temperature data for the 1900° F tests are shown plotted in Figure 9 along with the internal blade temperatures at the leading edge, mid-chord, and trailing edge across the hottest area of the blade.

For tests in this turbine simulator, the optical temperature normal readings are in good agreement with the control thermocouple temperature data obtained at the center of the blade (1665° F vs. 1680° F). If an optical pyrometer only was used for temperature control purposes (without regard to actual hot-spot metal temperatures), an optical control of 1900° F taken normal to the long axis of the blades would result in a maximum metal temperature of approximately 2060° F along the trailing edge of the blades.

The optical temperatures taken along the trailing edges of the blades were approximately 80° F lower than the optical normal temperature readings.

The internal and external temperature distribution for tests at the 2000° F temperature level are shown in Figure 10. For these tests, the actual peak metal temperature determined during the calibration tests was 1950° F, or 50° F lower than that obtained by surface thermocouple measurements.

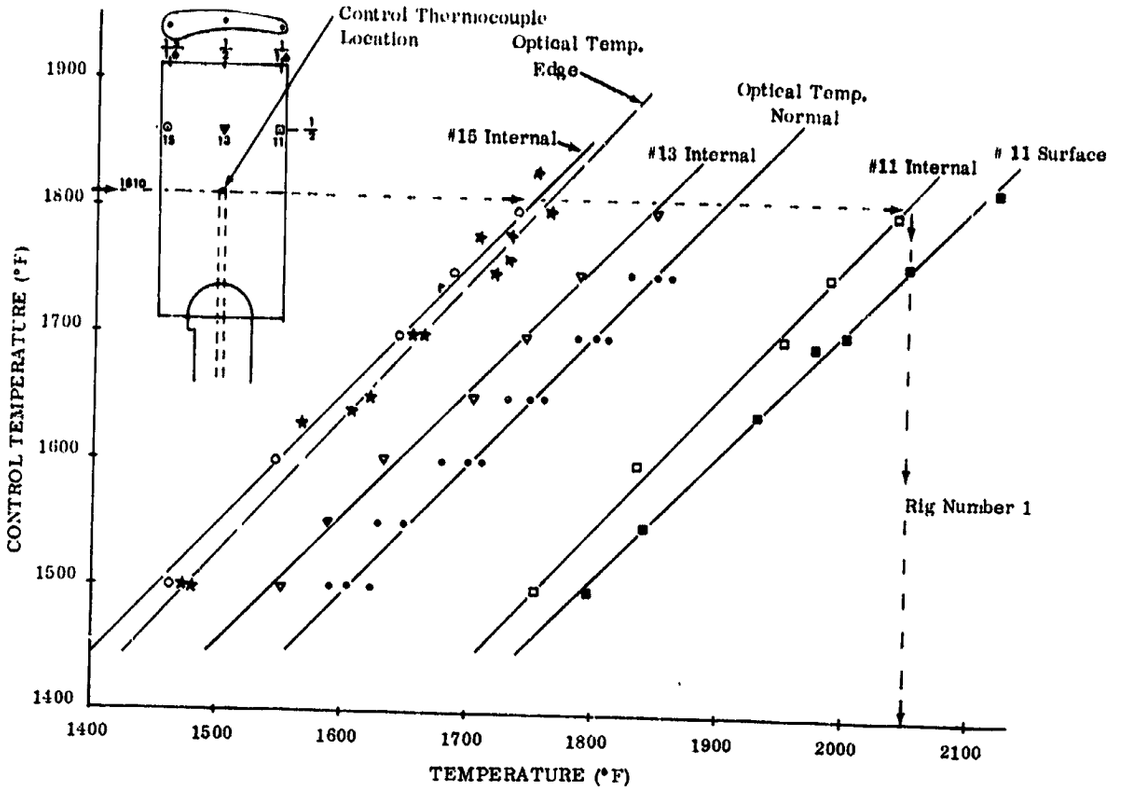

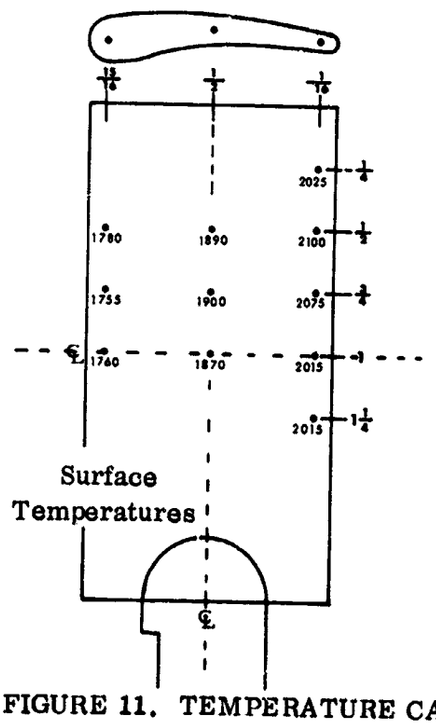

1810 °F
Control Temperature

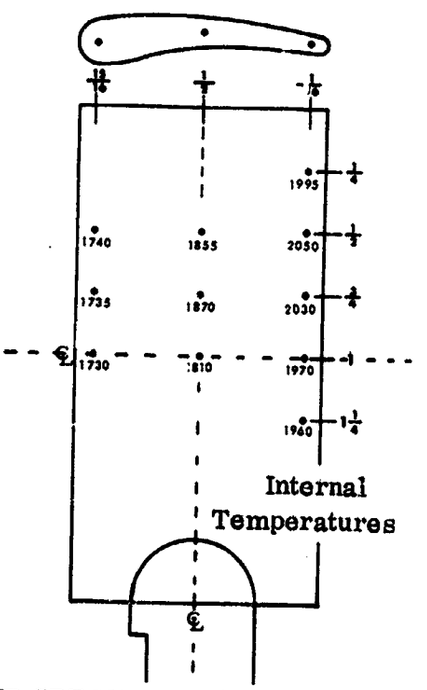

FIGURE 11. TEMPERATURE CALIBRATION CURVES AND SPECIMEN TEMPERATURE DISTRIBUTION FOR SERIES 3 TESTS

Figure 11 shows the specimen temperature distribution for the 2100° F test temperature level. In this turbine simulator test rig, a thermocouple control temperature of 1810° F produced a surface thermocouple temperature of 2100° F. The actual peak metal temperature, as determined by the internal thermocouple method, was 2050° F. Also shown in Figure 11 are the temperature curves for two other thermocouples imbedded into the airfoil section and optical temperature readings taken during the calibration tests.

In this particular test rig, which rotates in an opposite direction, the normal optical temperature data are approximately 100° F higher than the internal temperature at the midsection of the blades. This appears to be largely due to the luminous hot gas stream which is deflected over the surfaces of the blades. At this optical path, the optical pyrometer not only "sees" the blades but also this luminous hot gas stream.

The optical temperatures taken along the trailing edges of the blades were approximately 140° F lower than the optical normal temperature readings.

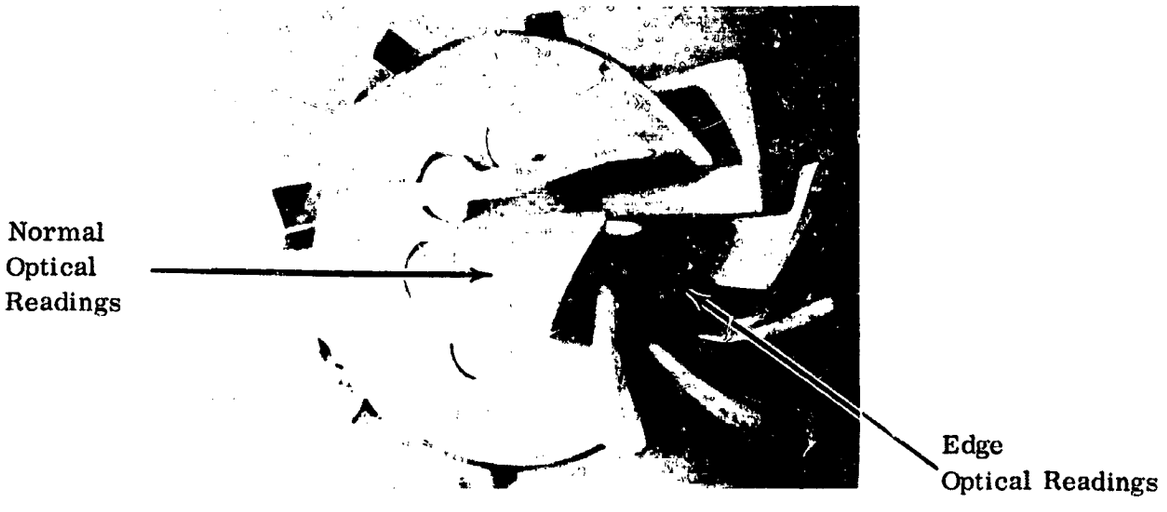

FIGURE 12. VIEWING ANGLES FOR OPTICAL PYROMETER TEMPERATURE MEASUREMENTS

4

TASK III
LONG-TERM OXIDATION-EROSION RIG TESTING

Additional oxidation-erosion rig testing was performed on most of the twelve coating systems to determine the performance of the coatings at lower temperature levels. These reduced temperatures resulted in considerably longer exposure times, particularly for the coated nickel-base alloys. The tests were performed as follows:

- Series 1 for up to 3000 hours on the coated nickel-base alloys and 1600 hours on the coated cobalt-base alloys. T_{max} during test was 1845° F for the cobalt-base alloys and 1870° F for the nickel-base alloys.
- Series 2 for up to 2000 hours on the coated nickel-base alloys and 1000 hours on the coated cobalt-base alloys. T_{max} during test was 1950° F.
- Series 3 for up to 1600 hours on the coated nickel-base alloys and 250 hours on the coated cobalt-base alloys. T_{max} during test was 2050° F.

For the long-term tests, the following criterion for blade failure was established by the NASA Program Manager:

- Specimens were considered to have failed and were removed from test when the average weight loss of the two blades was greater than 20 milligrams.

The 20-milligram weight loss value was selected based on results of the previous tests that showed visual coating degradation occurring at this level without catastrophic damage to the coated specimens. Substrate oxidation was also observed in the hot spot along the trailing edges of the coated cobalt-base alloys at this weight loss value. When pairs of specimens were withdrawn from test they were replaced with pairs of the remaining coating systems.

4.1 NICKEL-BASE ALLOYS

Tests on the nickel-base alloys were concentrated primarily on the B and C coatings on IN-100 alloy and on the F and H coatings on B1900 alloy. The D coating (on IN-100) and the G coating (on B1900) both exhibited extremely variable performance

in the Task II 100-hour screening test portion of the program. The latter two coatings were used several times as spares to "fill-in" the test specimen holder as other specimens were removed.

Weight change during testing, surface appearance after test, metallographic and electromicroprobe analyses after testing are included in the following sections.

4.1.1 Weight Change and Appearance

Curves of cumulative weight change plotted as a function of exposure time at temperature are presented for the tests run at the three temperature levels. These tests are discussed in ascending order of temperature as Series 1, 2, and 3 in the following sections. Photographs of the surface appearance of selected specimens after test are also included for each series of tests.

Series 1 - Oxidation-Erosion Tests (T_{max} 1870° F)

The weight change curves for the Series 1 tests on the B, C, D, F and H coatings are shown in Figure 13. Based on visual examination and an average weight loss of 20 mg, the B coated specimens were judged failed and removed from test after 2160 hours exposure. Both specimens exhibited coating spalling and substrate oxidation along the trailing edges on the concave surfaces of the blades. Specimen B35 after test (weight loss 23.5 mg) is shown in Figure 14.

At 2560 hours, the average weight loss of the two C coated specimens on IN-100 alloy was in excess of 20 mg; hence both specimens were removed from test. The two specimens exhibited spot-type failures along the trailing edge of the blades. Specimen C53 failed on the concave surface of the blade (Fig. 15A); whereas specimen C52 exhibited a failure on the convex surface (Fig. 15B). Note the two nodules on specimen C52 at the edge of the oxidation site. These nodules indicate either separation of the coating from the substrate (Kirkendall voids formation) or liquation. The nodules were first observed after approximately 900 hours total exposure in test. A review of the turbine simulator log books and weight changes for the other specimens in test did not indicate any abnormal operating conditions or over-temperature excursion.

After a total of 600 hours exposure, both D coated specimens were removed from test. The specimens exhibited considerable substrate oxidation and coating spall. Weight loss was quite rapid from about 500 hours to the conclusion of the test, as shown in Figure 13. Specimen D52 after test (weight loss 33.5 mg) is shown in Figure 16.

At 3040 hours total exposure, the remaining F and H coated specimens in test experienced an extreme over-temperature condition due to a malfunction of a

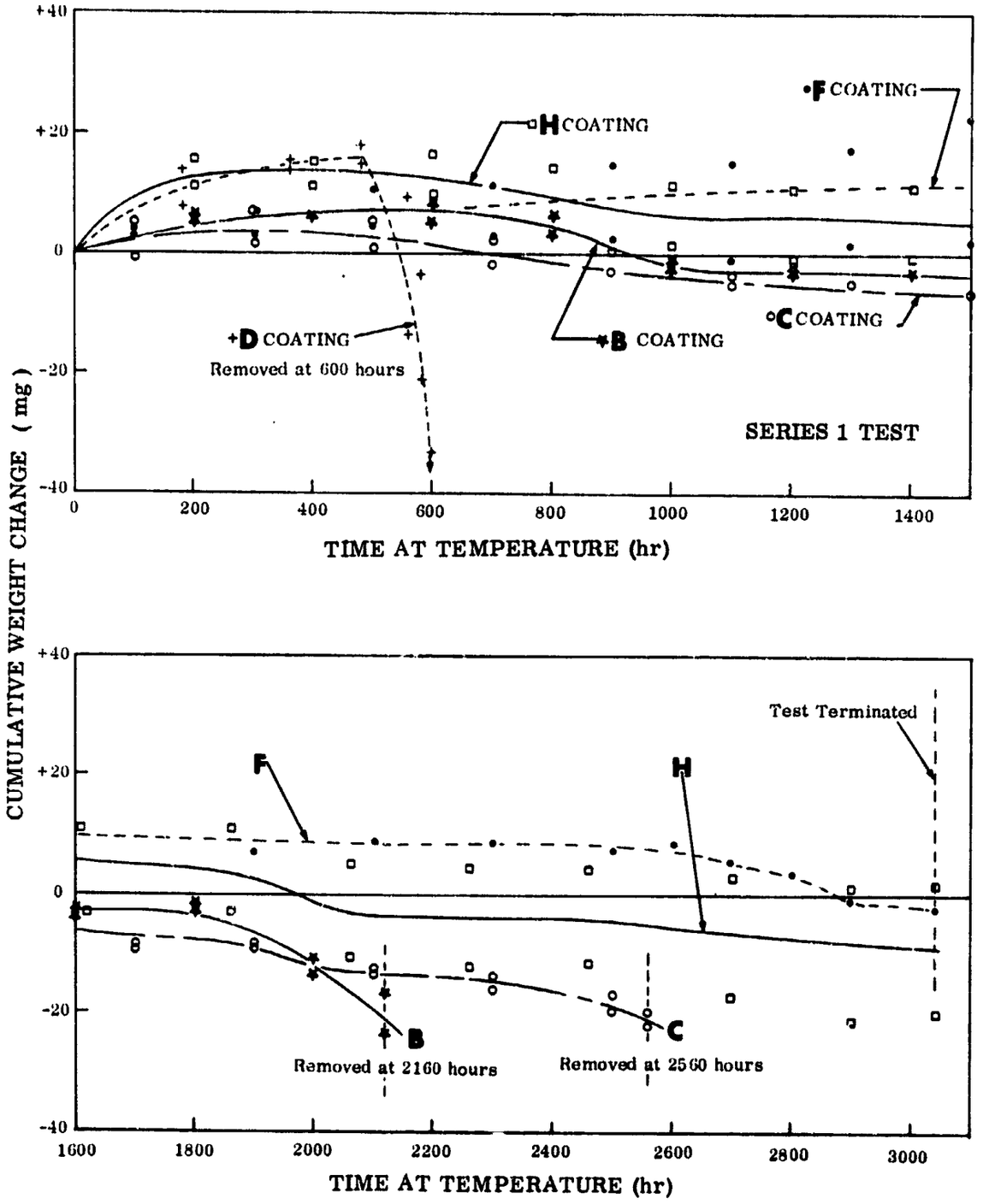

FIGURE 13. WEIGHT CHANGE VERSUS TIME FOR COATINGS B, C, D, F, AND H DURING SERIES 1 TEST (T_{max} 1870° F)

Weight Loss 23.5 mg

Concave Side of Specimen

Magnification: 1X

FIGURE 14. SPECIMEN B35 AFTER 2160 HOURS EXPOSURE; Series 1 Tests (T_{max} 1870° F)

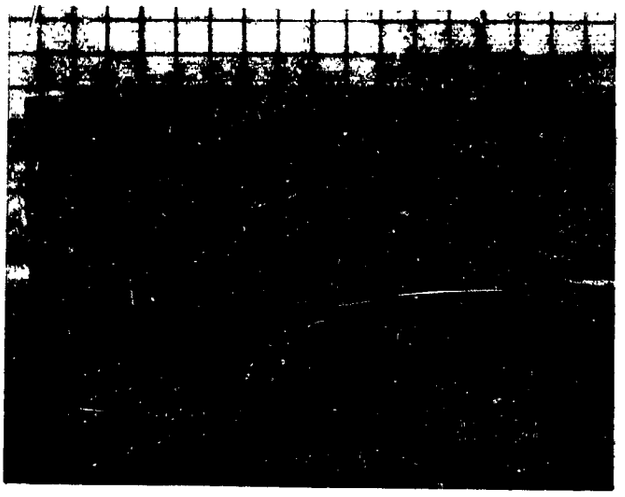

A

Specimen C53

Concave Side

Magnification: 2.5X

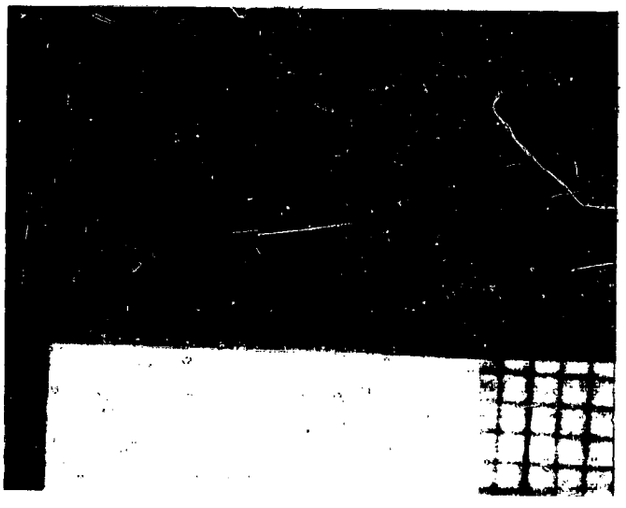

B

Specimen C52

Convex Side

Magnification: 2.5X

FIGURE 15. SURFACE APPEARANCE OF COATING C ON IN-100 ALLOY AFTER 2560 HOURS EXPOSURE; Series 1 Tests (T_{max} 1870° F)

Weight Loss 33.5 mg

Concave Side of Specimen

Magnification: 1X

FIGURE 16. SPECIMEN D52 AFTER 600 HOURS EXPOSURE; Series 1 Tests (T_{max} 1870° F)

temperature controller, and the test was concluded. The F and H specimens were slightly melted and the molten material was deposited over the surfaces of the adjacent specimens in the holder. During the last 300 hours in the test, one of the H coated specimens exhibited a nearly constant weight loss of approximately 20 mg. Only minor coating loss was visually apparent, however, on this specimen. The other H coated specimens in test appeared unchanged except for the typical white/grey Al_2O_3 surface appearance. Both F coated specimens after 3000 hours exposure did not show any evidence of coating deterioration. Specimens F3 and H54 after the over-temperature exposure are shown in Figure 17.

Series 2 - Oxidation-Erosion Tests (T_{max} 1950° F)

The weight change curves for the six coatings in the Series 2 oxidation-erosion test on nickel-base alloys are shown in Figures 18 and 21. At approximately 1300 hours exposure, the B coating started to fail quite rapidly and was removed from test after 1400 hours total exposure.

At the completion of 2000 total hours exposure, the C, F and H coatings exhibited no visible evidence of failure. There was no indication of coating spalling or substrate oxidation. The surface appearance of these three coatings after test is shown in Figure 19. The H coating had the largest weight loss in the test, 15 mg, with the C coating next at 12 mg. The F coated specimen continued to show a steady weight gain from approximately 1400 hours on, but this gain was entirely due to an oxide buildup on the round shank of the specimen. This shank oxidation is only apparent on the uncoated B1900 alloy (code letter E) and on the F coated specimens, which do not have any coating on the shanks (Fig. 20).

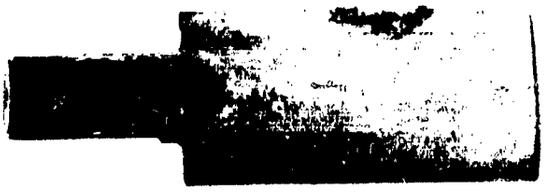

Total Exposure 3040 Hours

Convex Surface

Magnification: 1X

A

Total Exposure 3040 Hours

Convex Surface

Magnification: 1X

B

FIGURE 17. SPECIMENS F3 AND H54 AFTER OVER-TEMPERATURE EXPOSURE; Series 1 Tests (T_{max} 1950° F)

X-ray diffraction analysis of the oxide on the shank indicates that it is primarily NiO with minor amounts of substrate elements also present, i.e., Mo, Cr and Ti.

The three coatings visually appeared to be in excellent condition after the long-time exposure. Therefore, these three coatings were subjected to metallographic examination to determine if any metallurgical changes resulted from the long-term exposure. Results are reported in Section 4.1.2.

Figure 21 shows the weight change versus time curves for the D and G coated specimens. These coatings were introduced into the test as other coatings failed and were removed from test. Results of the tests on the four G coated specimens (B1900 substrate) showed the oxidation life (time to 20 mg weight loss) to range from 810 hours

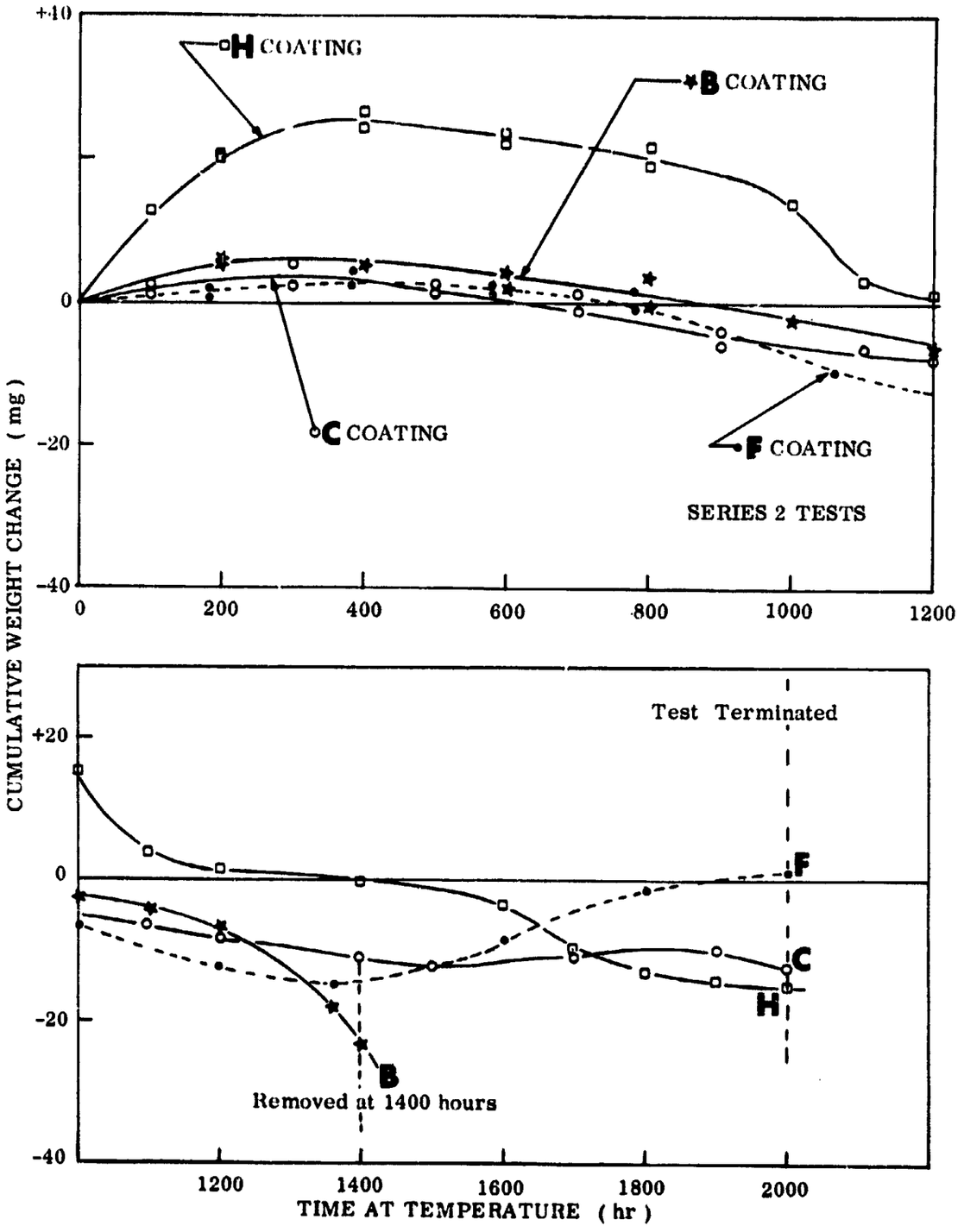

FIGURE 18. WEIGHT CHANGE VERSUS TIME FOR COATINGS B, C, F AND H DURING SERIES 2 TESTS (T_{max} 1950° F)

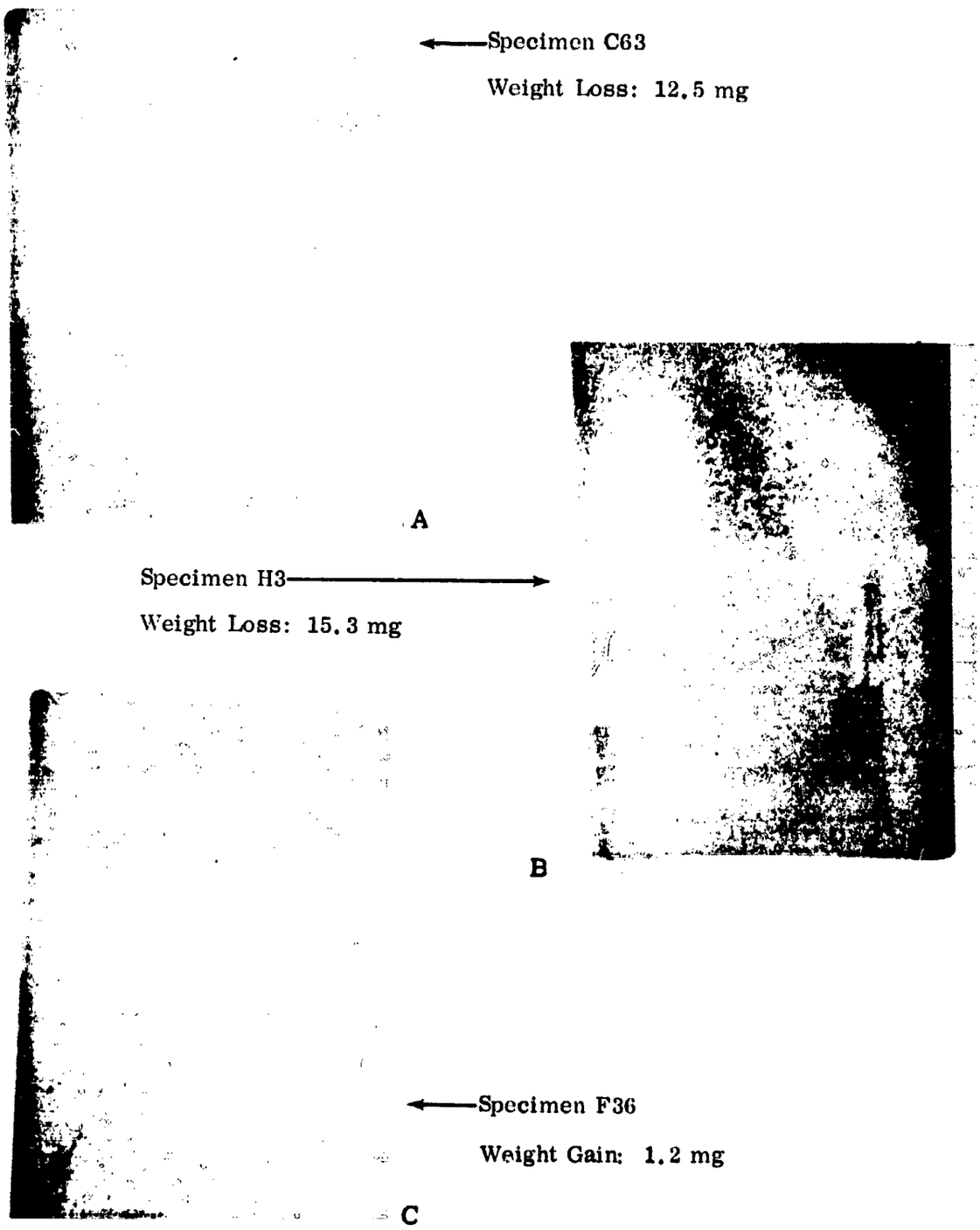

Magnification: 2.3X

CONCAVE SURFACE OF BLADES

FIGURE 19. SURFACE APPEARANCE AFTER 2000 HOURS EXPOSURE; Series 2 Tests (T_{max} 1950° F)

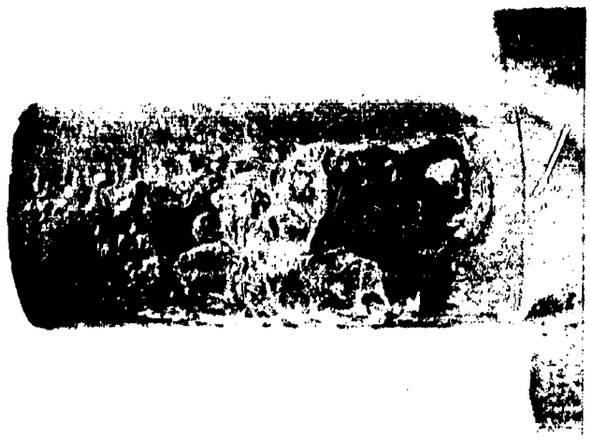

Magnification: 2.6X

FIGURE 20.

OXIDE ON UNCOATED SHANK OF SPECIMEN F3; B1900 Alloy Substrate

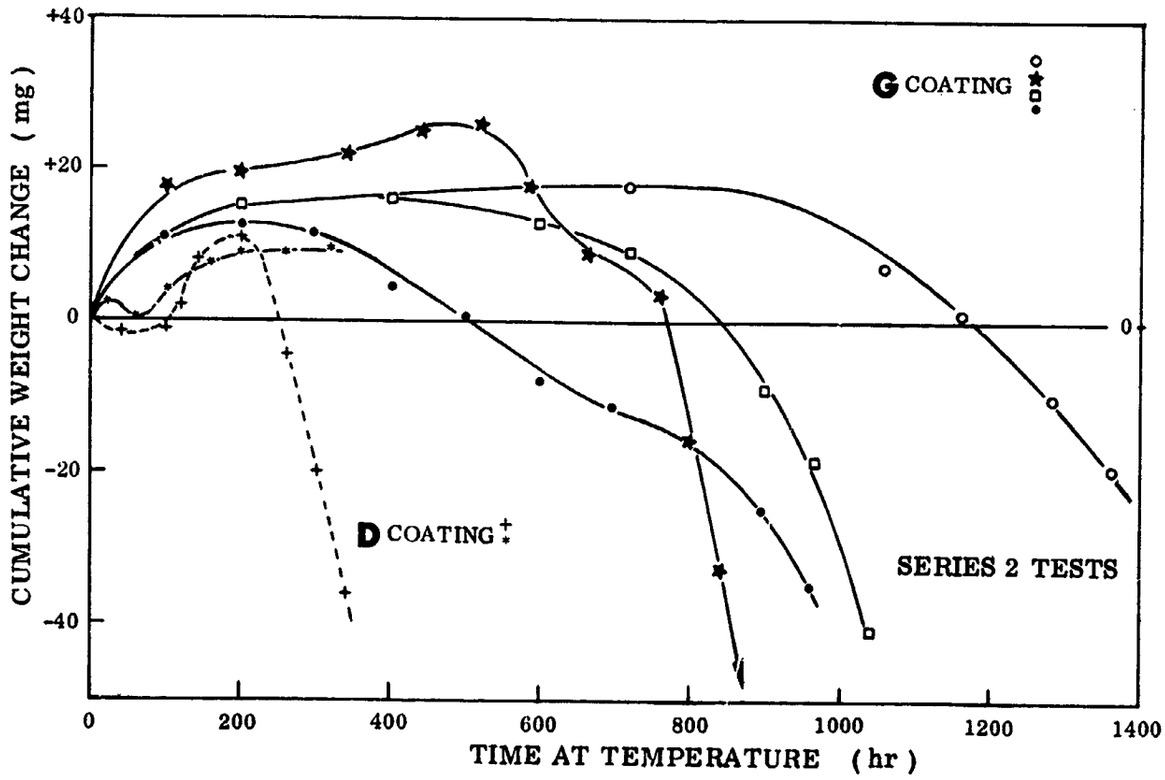

FIGURE 21. WEIGHT CHANGE VERSUS TIME FOR COATINGS D AND G DURING SERIES 2 TESTS (T_{max} 1950° F)

(specimen G54) to a high of 1360 hours for specimen G42. All four specimens exhibited coating spalling near the trailing edge on the concave side during the course of the test. For specimen G54, spalling was observed at approximately 520 hours exposure; for G37 at 600 hours; for G42 at 720 hours; and G48 at about 360 hours. Surface appearance of specimen G42 and G54 are shown in Figure 22.

Two D coated IN-100 alloy specimens were also included in the Series 2 test. Specimens D34 and D63 exhibited the usual coating spalling and subsequent weight gain-weight loss type curves previously exhibited by this massive coating system. Specimen D34 (Fig. 22) had lost 20 mg of weight after 300 hours exposure; whereas specimen D63 still showed a weight gain of approximately 10 mg after 300 hours exposure. Two D coated specimens included in a previous test at 2000° F exhibited similar performance with coating lives of 371 and 413 hours exposure for the specimens.

Series 3 - Oxidation-Erosion Tests (T_{max} 2050° F)

The weight change curves for the Series 3 tests on the B, C, F, G and H coatings are shown in Figure 23. At approximately 700 hours exposure, the B coating (on B1900 alloy) started to fail. Coating spalling and substrate oxidation was apparent along the trailing edges on the concave surfaces as shown in Figure 24A. After 1000 hours total exposure the specimens started to fail quite rapidly and were removed from test after 1100 hours exposure. The surface appearance after test is shown in Figure 24B.

Coating C (on IN-100 alloy) was removed from test when the average weight loss of the two specimens reached approximately 20 mg. One small spot on the trailing edge of specimen C54 was the only visual evidence of coating failure on these two specimens (Fig. 25).

The surface of the F coating after 1400 hours total exposure is also shown in Figure 25. Visual examination of the specimens did not show any evidence of coating degradation although the average weight loss was 20 mg.

At 1620 hours total exposure, the test was terminated when the two H coated specimens lost an average of 20 mg. The surfaces of the specimens after test (Fig. 25) appeared quite smooth in the hot test area and somewhat rough and mottled in the cooler regions toward the leading edge and shank areas of the blades. No coating defects, however, were apparent.

Two G coated specimens were included in the test as fill-ins when failures occurred in the other coating systems. One G specimen exhibited coating spalling and substrate oxidation very early in the test (loss of 20 mg in 300 hours); whereas the other specimen did not show any evidence of coating spalling or substrate oxidation after a total of 520 hours exposure.

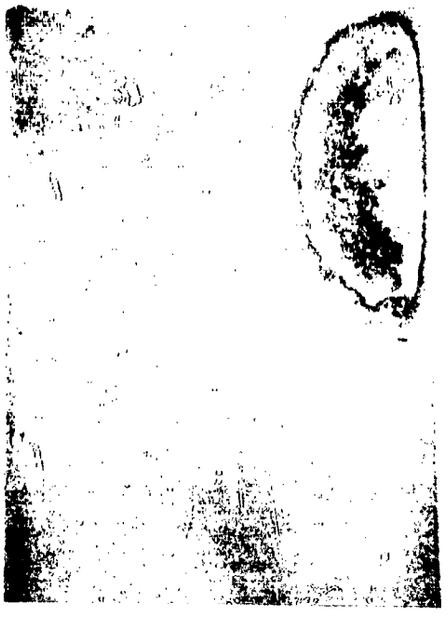

←Specimen G42 After 1360 Hours Exposure

Weight Loss: 19.3 mg

A

Specimen D34 After 340 Hours Exposure →

Weight Loss: 35.3 mg

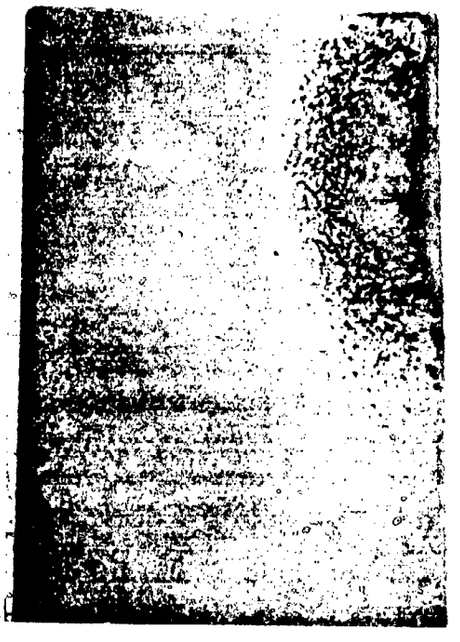

B

← Specimen G54 After 960 Hours Exposure

Weight Loss: 122.6 mg

C

Magnification: 2.3X

CONCAVE SURFACE OF BLADES

FIGURE 22. SURFACE APPEARANCE OF COATINGS D AND G AFTER SERIES 2 TESTS (T_{max} 1950° F)

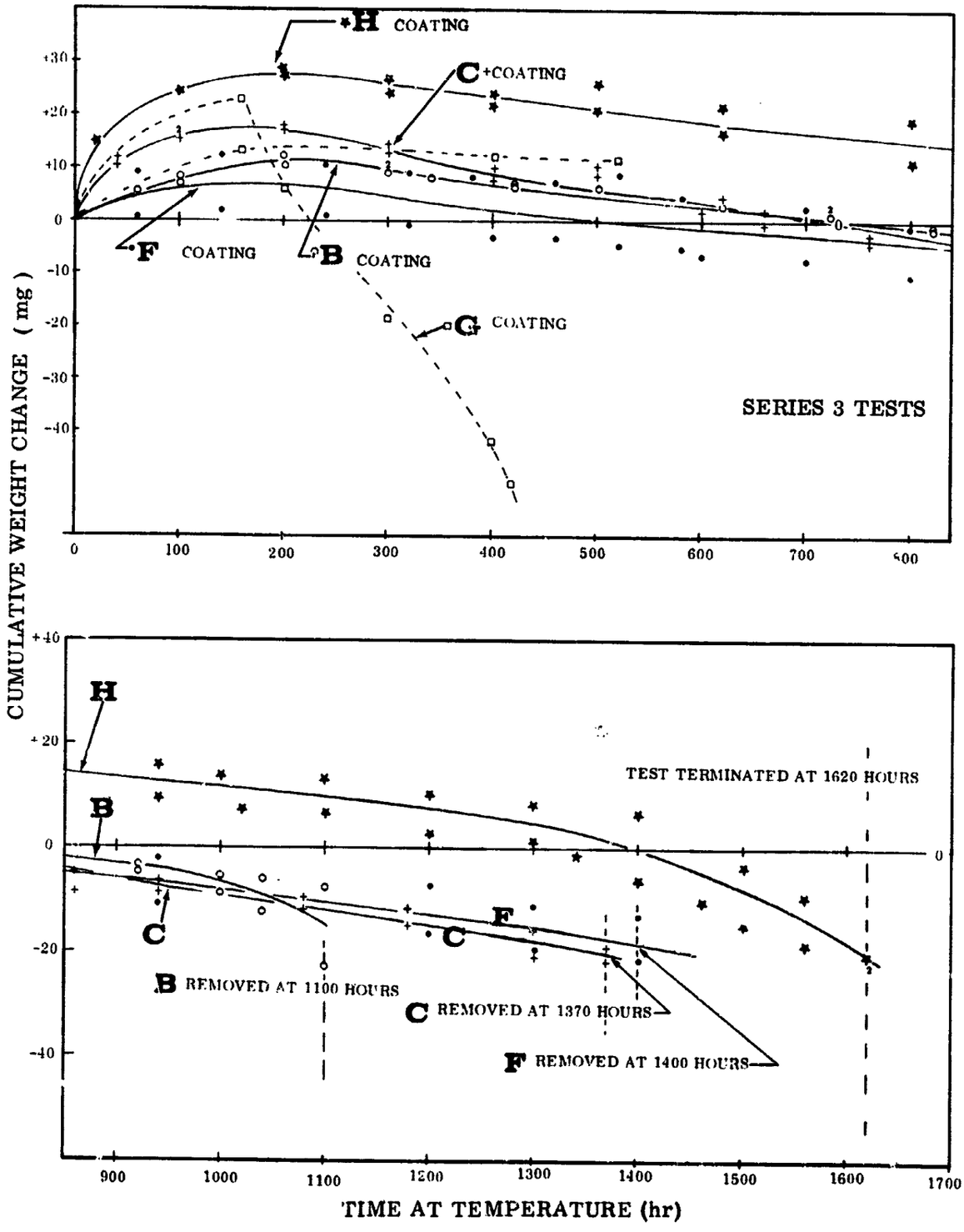

FIGURE 23. WEIGHT CHANGE VERSUS TIME FOR COATINGS B, C, F, G AND H DURING SERIES 3 TESTS (T_{max} 2050° F)

A

Specimen B52

700 Hours Exposure

Weight Gain: 1.7 mg

Concave Surface

Magnification: 2.3X

Coating Spalling

B

1100 Hours Exposure

Weight Loss: 22.8 mg

Concave Surface

Magnification: 2.3X

FIGURE 24. SURFACE APPEARANCE OF COATING B AFTER SERIES 3 TESTS (T_{max} 2050° F)

A

Specimen C54

1370 Hours Exposure

Weight Loss: 18.9 mg

Concave Surface

Magnification: 2.2X

B

Specimen F32

1400 Hours Exposure

Weight Loss: 13.4 mg

Concave Surface

Magnification: 2.2X

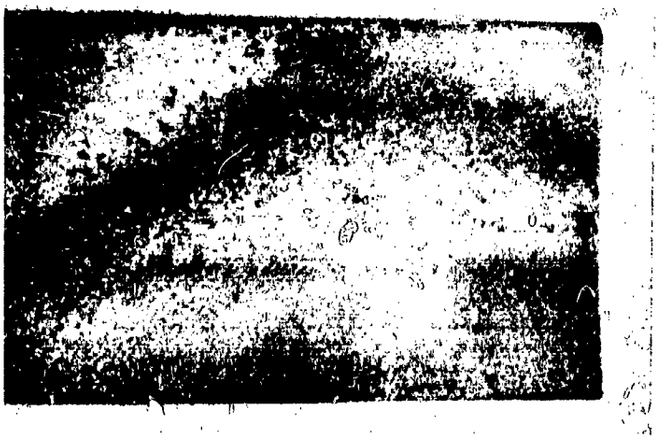

C

Specimen H38

1620 Hours Exposure

Weight Loss: 20.1 mg

Concave Surface

Magnification: 2.2X

FIGURE 25. SURFACE APPEARANCE OF SPECIMENS IN SERIES 3 TEST (T_{max} 2050° F)

4.1.2 Coating Evaluations - Nickel-Base Alloys

In accordance with the previous work and experimental techniques (Ref. 1), extensive evaluations of the structural changes occurring in coatings and matrix alloys (coating induced) were made using metallography and electron microprobe analysis. Table III shows the exposure times and temperatures for the particular specimens which were evaluated. Those coatings which failed, according to the 20 mg weight loss criterion, are indicated in the table.

The blades were sectioned for metallurgical and microprobe analyses studies through the hottest parts during the test. The temperature profiles, along the cross sections, for the Series 1, Series 2 and Series 3 tests are shown in Figure 26.

Because of the known temperature gradients which existed between the leading and trailing edge locations, it was possible to correlate structural changes with temperature. A metallographic failure criterion was proposed by NASA personnel based on the first observable discontinuities in the βMAl phase. A typical structure corresponding to this definition is shown in Figure 27. Such a definition in practice has different significance for aluminide coatings on cobalt-base alloys as compared to those on nickel-base alloys under oxidation-erosion conditions. This point is brought out in the discussions of coating degradation. Metallographic and microprobe data are presented for each coating in the following paragraphs. Not all of the microprobe analyses which were performed are included in this section in order to avoid unnecessary repetition. The additional data are included in Appendix A and will be referred to as required throughout this section.

TABLE III

OXIDATION-RIG EXPOSURES OF COATED NICKEL ALLOY SPECIMENS ANALYZED BY METALLOGRAPHY AND ELECTRON MICROPROBE

Test Temperature °F (Max.)**	Exposure Times (Hours)					
	IN-100 Alloy			B1900 Alloy		
	Coating			Coating		
	B	C	D	F	G	H
1870	2160 (f)	2560 (f)	603 (f)	3040 (f)*	545	3040 (f)*
1950	1400 (f)	2000	440 (f)	2000	1360 (f)	2000
2050	1100 (f)	1370 (f)	80	1400 (f)	440 (f) 520	1620 (f)

(f) = Coating failure based on 20 mg weight loss

* Failures due to rig malfunction ** Imbedded thermocouple

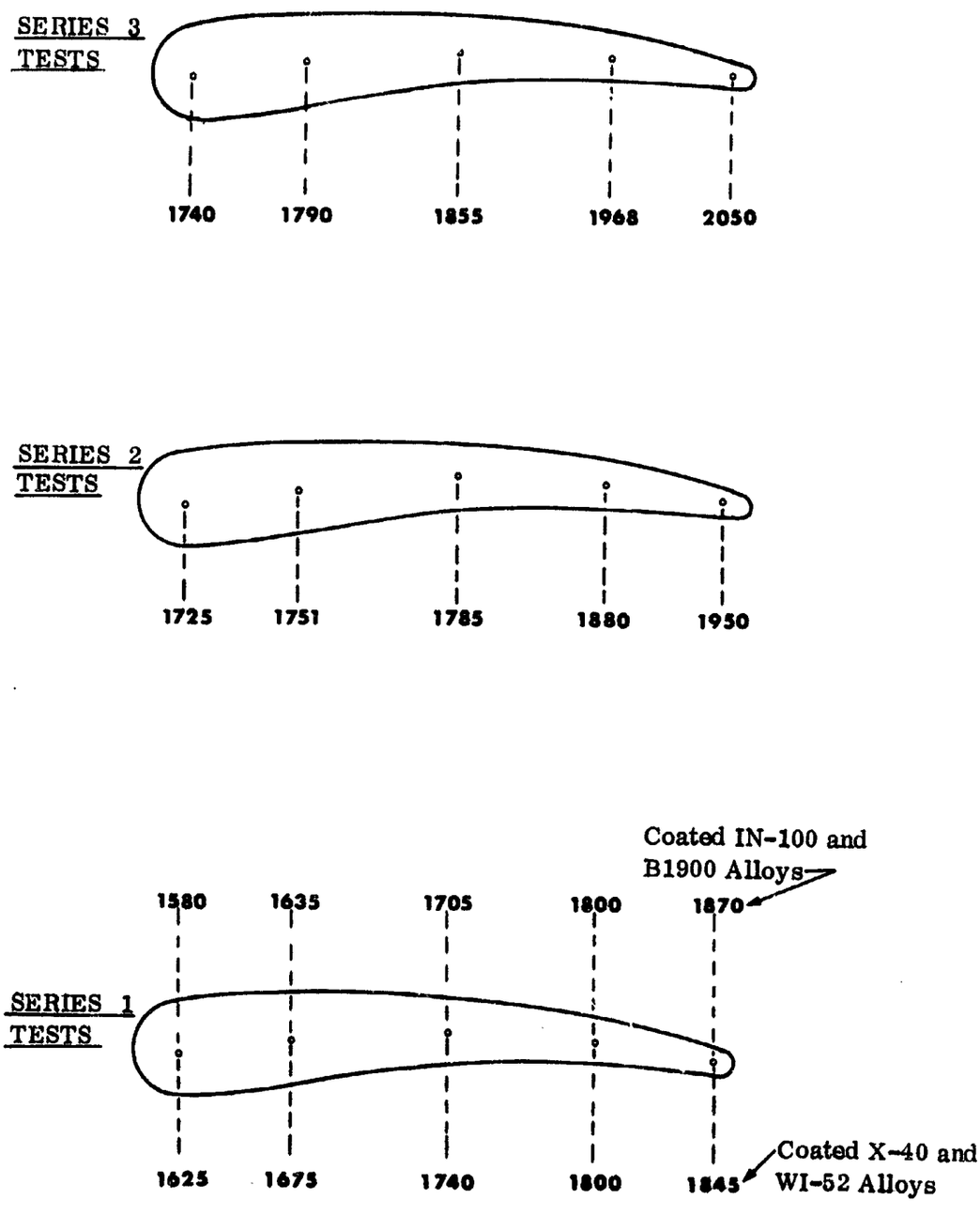

FIGURE 26. TEMPERATURE PROFILE ACROSS AREA SECTIONED FOR ANALYSIS

FIGURE 27. METALLOGRAPHIC FAILURE CRITERION FOR ALUMINIDE COATINGS ON NICKEL-BASE ALLOY

B Coating on IN-100

The microscopic appearances of specimen cross sections after 2160 hours in Series 1 tests and 1100 hours in Series 3 tests are shown in Figures 28 and 29. Both specimens had failed according to the weight loss criterion. The appearance at the leading edges of both specimens was similar, but only the Series 1 specimen showed evidence of substrate attack at the trailing edge locations. Such a difference correlated well with the amount of residual γ' phase, which is seen in the high-magnification photographs in Figure 30. None of the βMAl coating phase was retained in either

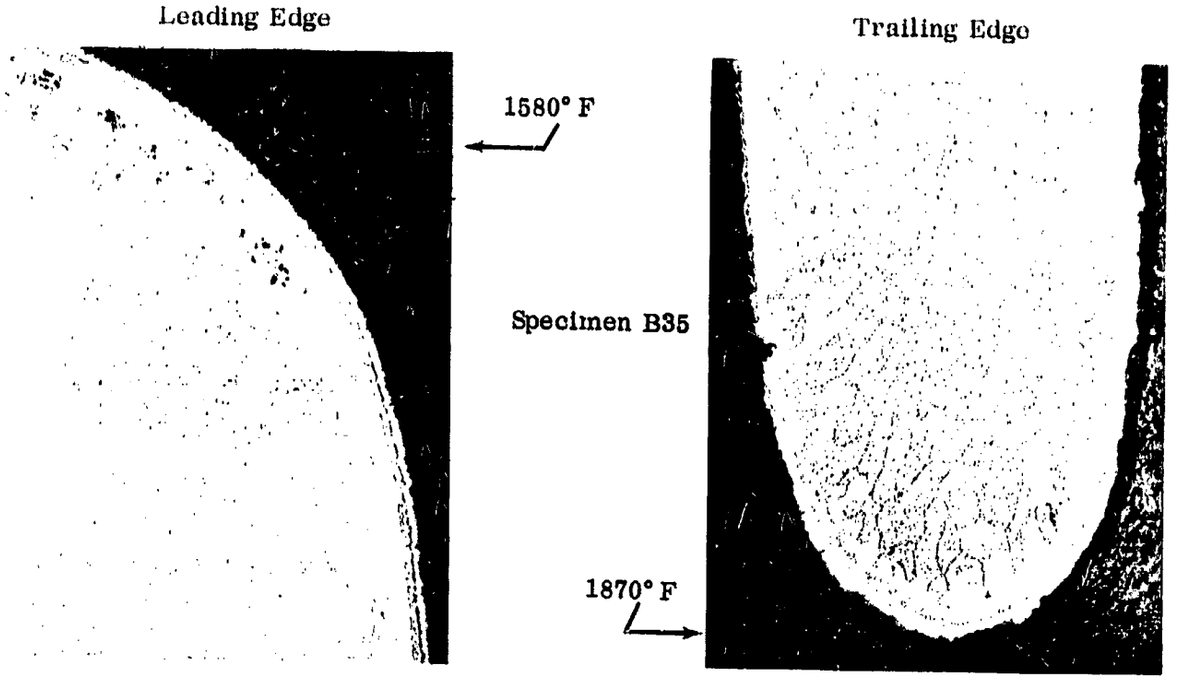

FIGURE 28. SPECIMEN AFTER 2160 HOURS (SERIES 1 TESTS); B Coating on IN-100 Alloy

Etchant: Oxalic Acid-Electrolytic

Magnification: 40X

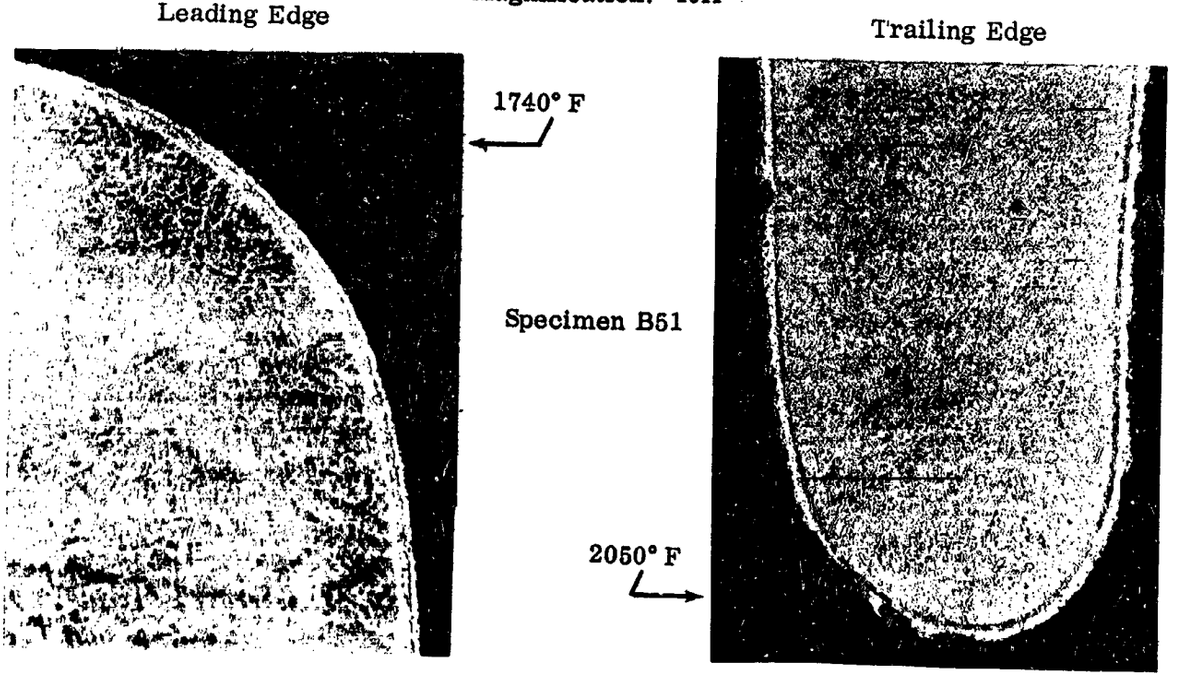

FIGURE 29. MICROSTRUCTURE AFTER 1100 HOURS IN SERIES 3 TESTS: B Coating on IN-100 Alloy

specimen at these hottest locations, but the Series 3 test specimen (B51) had a continuous band of γ' M_3Al phase, which was formed progressively during degradation of the aluminum-rich βMAl, and was still affording oxidation protection to the substrate. From Figure 30A, it can be seen that twice as long an exposure (2160 hours) at the lower temperature was sufficient to cause aluminum depletion down to the level where the relatively poorly oxidation resistant γ solution was formed. With no aluminum-rich layer present, the oxidation process is characteristic of the uncoated alloy.

The electron microprobe analyses were determined using pure element standards and the Colby computer program (Ref. 9) to provide semi-quantitative results. Without alloy standards it is not possible to estimate the percentage that the electron microprobe analyses vary from absolute values. Microprobe analyses were conducted at the same location on all specimens, viz., the blade center, concave side. Figure 31 shows the structure and corresponding microprobe analyses of specimen B40 (1400 hours in Series 2 tests) at this location where the temperature during test was 1785° F. The structure shown in Figure 31 was characteristic of all the B coated specimens after long-term oxidation rig exposures at 1700° F to 1900° F. As shown in the previous work, phase compositions may be related (to a first approximation) to the binary Ni-Al equilibrium phase diagram (Fig. 32) by assuming that Co can substitute for Ni up to about 15 weight percent. Some knowledge of ternary and quaternary phase equilibria helps in understanding many of the phase separations but, obviously, some extremely complicated diffusional processes may occur where ten or more major coating and substrate elements are present.

Figure 31 shows that about 50 percent of the βMAl phase had been consumed in the B coating, and the remaining β was surrounded by the white etching γ' phase. Probe area number 1 in Figure 31 was in the oxide and the major metallic element was aluminum, indicating Al_2O_3. Area number 2 gave an analysis in atomic percent of 54.9Ni, 12.4Co, 31.0Al, 2.8Cr, 6.8Si and 5.8Ti. Reference to the 1000° C isothermal section of Taylor and Floyd's Ni-Cr-Al (Ref. 1) diagram would give a composition corresponding to $\beta + \gamma'$. However, the Ni-Al-Si diagram of Guard and Smith (Ref. 2) shows an extended γ' region up to about 29 atomic percent Al and up to 15 atomic percent Si and, therefore, the analyses would appear to be in agreement with reported phase equilibria. The composition of points 3 and 5 would place this phase in the center of a Ni-Al-Cr-Si quaternary βMAl phase. The granular or powdery phase along the center of the coating has been discussed previously, and the present data which show a high-titanium level and low total element count, and also the fact that a fluorescence similar to that noted with Al_2O_3 was observed during electron bombardment, indicate an oxide, presumably TiO_2. This may have been applied to prevent sintering of the pack media to the coating or may have been occluded during the coating process. Whatever this phase is it was extremely inert and appeared to play no part in the coating behavior. Probe area 7 was in a hard, brilliant white phase and gave analysis values

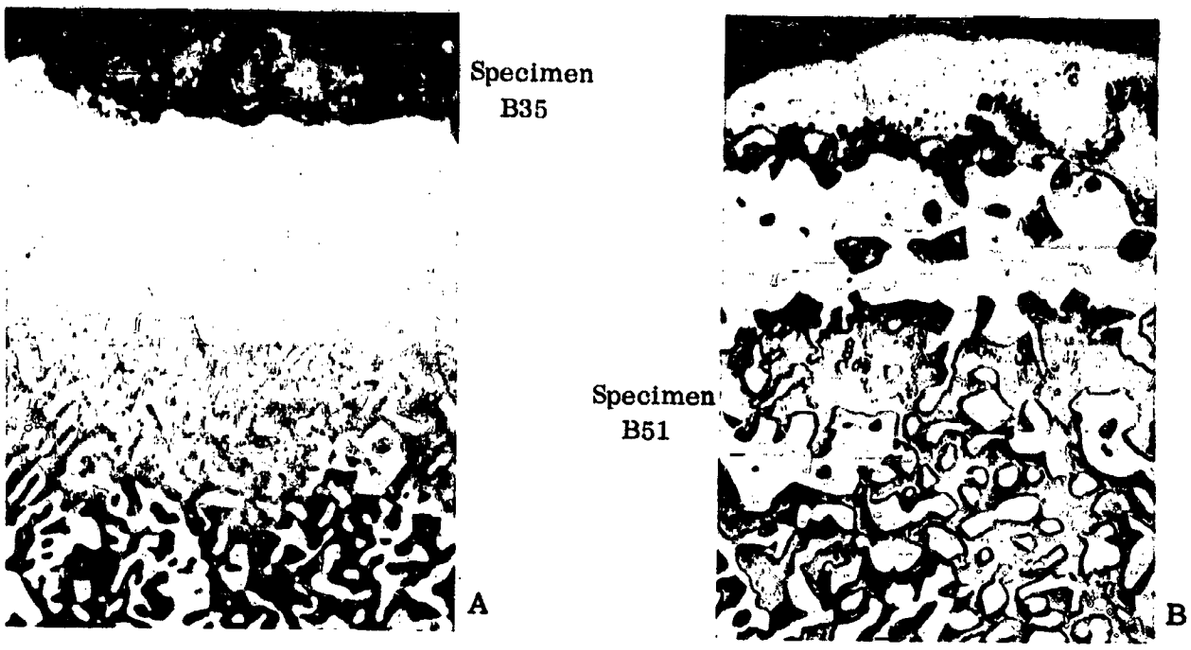

Magnification: 750X

Etchant: Oxalic Acid-Electrolytic

FIGURE 30. MICROSTRUCTURE OF B COATING AT TRAILING EDGE AFTER SERIES 1 AND SERIES 3 TESTS

of 3.3Al, 63.5Cr, 8.4Ni, 3.7Co, 1.4Si and 0.9Ti atomic percent. Previous analyses have shown segregation of Mo and Fe to these chromium-rich areas, which may account for the low, total element values since neither of these elements was determined in this particular analysis. The data therefore would tend to identify this phase as metastable α chromium.

The area shown in Figure 31 was at a temperature of 1785° F and the coating was close to failure based on the adopted metallographic failure criterion. Coating degradation occurs by Al loss from the surface and interdiffusion at the coating/matrix interface resulting in the formation of γ' (M_3Al). Because of the extensive γ' formation at the interface, diffusion inward of Al and diffusion outward of Ni must provide

Specimen No. B40

Test No. 35

Etchant: Oxalic Acid-Electrolytic

Magnification: 750X

Local Temperature: 1785° F

	Composition (wt %)						
	Al	Co	Cr	Ni	Si	Ti	Total
1	31.4	0.80	0.21	3.1	1.42	3.00	40.0
2	17.5	15.40	2.80	66.9	4.10	5.80	112.5
3	30.7	14.70	4.30	60.9	2.30	3.80	116.7
4	8.9	7.60	1.90	27.5	2.10	36.00	84.0
5	31.9	14.50	4.40	61.0	2.20	2.90	116.9
6	16.5	15.40	3.30	67.5	1.70	5.80	110.2
7	1.7	4.30	64.30	9.6	1.02	0.83	81.8
8	15.9	14.80	3.10	67.1	1.40	6.40	108.7
9	17.5	16.50	6.90	63.2	1.70	5.60	111.4
10	12.6	16.20	7.60	60.8	1.10	4.40	102.7

FIGURE 31. ELECTRON MICROPROBE ANALYSIS OF B COATING ON IN-100 ALLOY AFTER 1400 HOURS; Series 2 Test (T_{max} 1950° F)

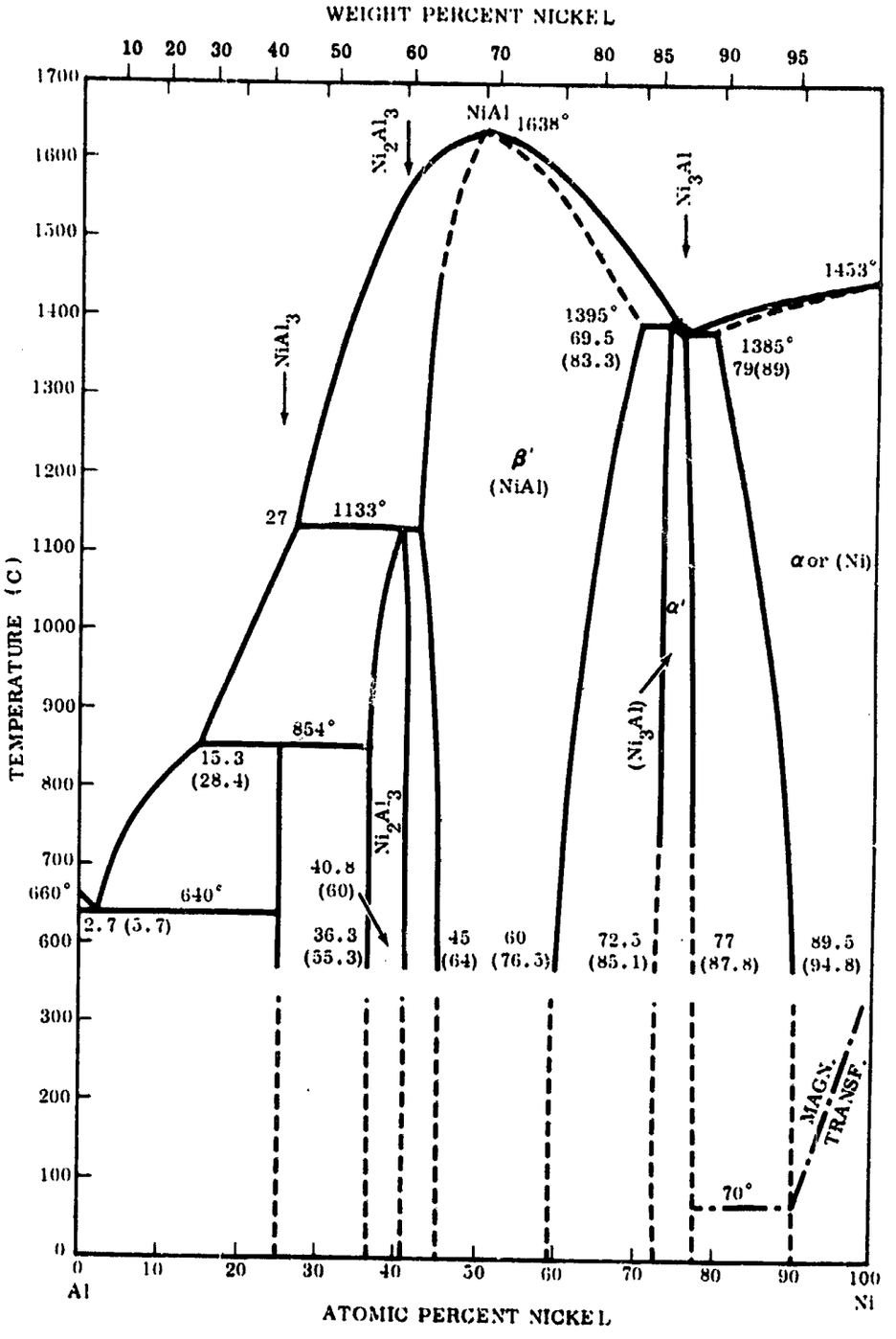

FIGURE 32. NICKEL-ALUMINUM PHASE DIAGRAM

a significant contribution to coating degradation. The γ' phase containing up to 15 weight percent Al (28 at. %) has significantly better oxidation resistance than γ solid solution and, therefore, protection is still being afforded to the substrate, under oxidation-erosion conditions, when all of the βMAl has been consumed. Kaufman (Ref. 3), however, has recently shown that under sulfidation conditions γ' is much less resistant to attack relative to NiAl than under oxidation conditions. Thus, loss of a continuous βMAl layer is probably a good practical definition of failure.

C Coating on IN-100

Figure 33 shows the low magnification and high magnification appearance of specimen C63 after 2000 hours exposure in Series 2 tests (T_{max} 1950° F). This appearance was characteristic of the three C coated specimens examined after long-term exposures in Series 1, 2 and 3 tests.

Full coating coverage was retained at the cooler leading edge, but the coating was completely consumed at the trailing edge. As shown in the high magnification photographs, a coarse, two-phase $\gamma + \gamma'$ structure was obtained at the trailing edge (1950° F location) with γ solid solution being the outer phase. At the leading edge (1725° F) a large amount of the βMAl was retained. Three major phases were noted in the coating at this location: β, γ', and a grey phase intermediate in etching rate between γ' and β. A thin, continuous layer of γ' was observable at the surface and a wide zone of γ' had formed at the interface growing into the matrix, which was again an indication of significant aluminum diffusion into the matrix. According to the weight change data, this specimen had not failed after 2000 hours. However, as shown by the photomicrographs, the coating was completely consumed at the trailing edge at this particular blade cross section.

Microprobe analyses were conducted on specimen C52 (2560 hours in Series 1 tests) and the data are shown in Figure 34. The temperature during test at this location was 1705° F. Similar data for the Series 3 test specimen are shown in Appendix A.

The three phases present in the coating are identified by probe areas 2, 3 and 4 in Figure 34. Point 2 gave compositions in atomic percent of 47.3Al, 44Ni, 12.3Co, 3.8Cr, 6.3Si and 0.26Mo which, combining the nickel and cobalt as one constituent, would correspond to a point in the center of a hypothesized quaternary Ni-Al-Cr-Si βMAl field (constructed from Guard and Smith's ternary diagrams). Similarly, point 3 corresponds to the quaternary γ phase. The probe data indicated that silicon was present in the oxide (probe area 1). The grey-brown phase (point 4), intermediate in color between the β and γ', was apparently silicon-rich (15.1Al, 25.9Si, 10.7Cr, 11.5Co, 33.3Ni atomic percent) and the analyses would appear to place it close to the $\beta + \psi$ phase field in the hypothesized Ni-Si-Cr-Al quaternary. The ψ phase was reported

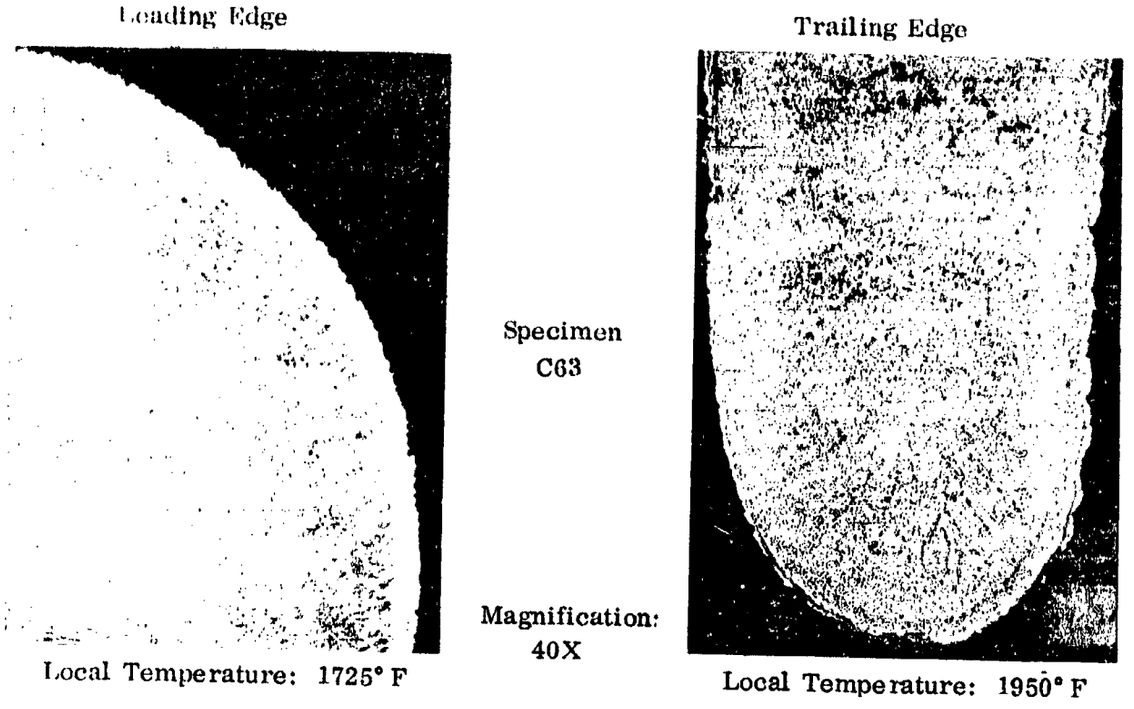

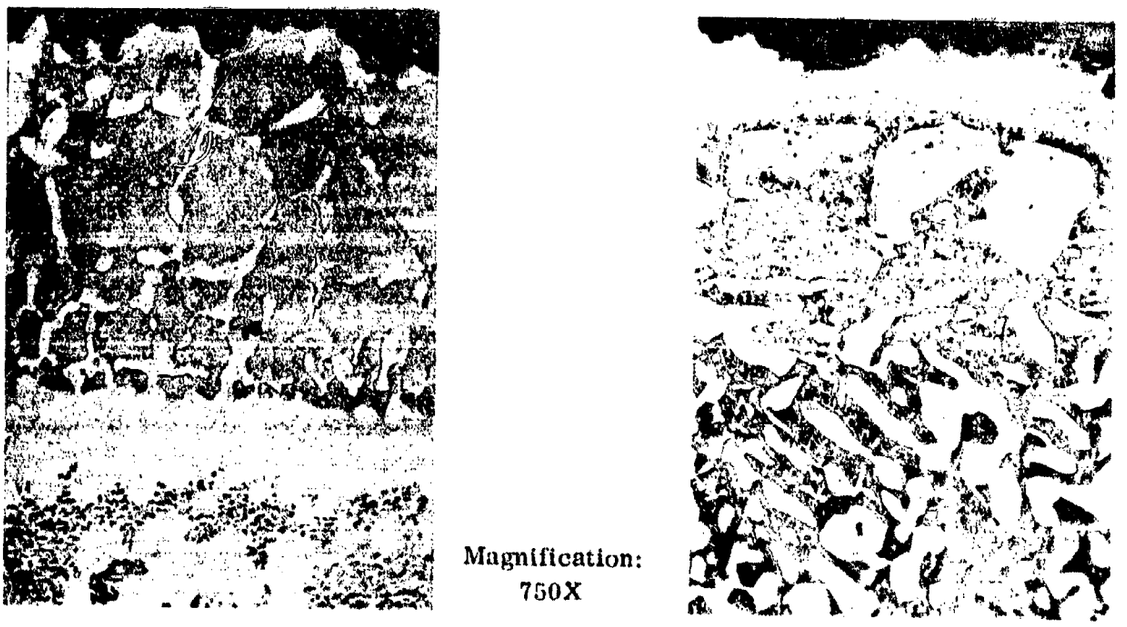

FIGURE 33. MICROSTRUCTURE AFTER 2000 HOURS IN SERIES 2 TEST; C Coating on IN-100 Alloy (T_{max} 1950° F)

29

Specimen No. C52

Test No. 32

Etchant: Oxalic Acid-Electrolytic

Magnification: 750X

Local Temperature: 1705° F

	Composition (wt %)						
	Al	Co	Cr	Mo	Ni	Si	Total
1	8.8	4.7	8.8	0.90	8.1	4.8	36.1
2	29.5	16.8	4.6	0.57	59.6	4.1	115.2
3	14.6	16.4	2.9	0.72	65.7	3.8	104.1
4	8.5	14.1	11.6	0.01	40.8	15.2	90.2
5	30.1	16.9	4.8	0.54	60.0	4.0	116.3
6	12.1	15.1	9.8	0.92	60.2	2.9	101.0
7	12.0	18.1	7.3	1.10	61.6	2.8	102.9
8	7.2	19.3	8.6	1.40	61.6	1.5	99.6

FIGURE 34. ELECTRON MICROPROBE ANALYSIS OF C COATING ON IN-100 ALLOY AFTER 2560 HOURS; Series 1 Test (T_{max} 1870° F)

by Guard and Smith to be the most stable compound except for the NiAl in the ternary Ni-Si-Al system. A wide zone of γ' composition had developed at the coating-matrix interface (point 6). The relatively high concentration of silicon determined in the C coating would indicate that this was an intentionally added element.

D Coating on IN-100

The D coating on IN-100 was shown in the previous work to be the thickest coating applied to the nickel-base alloys (>0.005 inch), and was apparently applied in a two-phase process where a chromizing cycle constituted the final operation. A continuous chromium-rich phase at the surface was identified as Cr_3Al_2 by microprobe and X-ray diffraction analyses. The coating was shown to be subject to rapid oxidation and spalling of the chromium-rich layer when exposed to high temperatures (above 1750° F) and, in this respect, was more temperature sensitive than the more conventional coatings. Similar observations were made from the long-term test specimens.

Figure 35 shows the microscopic appearance of specimen D28 after 440 hours in Series 2 tests. The coating was intact at the leading edge location (1725° F), but had spalled and corroded away badly near the trailing edge (1950° F). Weight loss data indicates failure after 440 hours in the Series 2 tests (24 mg weight loss). Particles of a gold colored phase were observed in the oxidized Cr-rich areas. These were tentatively identified as chromium nitrides.

The microprobe data for specimen D52 (603 hours in Series 1 tests) are shown in Figure 36. As stated earlier, the original analytical data on the as-coated condition, which included X-ray diffraction analysis, identified the outer chromium-rich layer as Cr_3Al_2. Following long-term oxidation exposures, this layer became internally oxidized and porous, making the microprobe analysis of these areas difficult to interpret. Metallography indicated that there were two light etching phases in this outer layer. A high, total element concentration was obtained from probe area 1 - 35.6Al, 51.5Cr, 4.4Fe, 6.4Co and 7.4Ni in atomic percent - and it was not possible to identify the phase as α chromium or a chromium aluminide compound. The phase corresponding to point 3, however, could be identified as α chromium from the ternary diagram. Probe areas 2 and 4 gave compositions corresponding closely to stoichiometric (NiCo)Al. The white dispersed phase in the lower part of the coating (points 5 and 6) was also identified as α chromium. (As shown in the previous analyses, this phase contained up to 15 weight percent molybdenum which would, therefore, account for the low values in these analyses.) The other hard phase in the lower part of the coating, which appeared as irregularly shaped particles (point 7) was low in all of the elements determined in this series of analyses. Semi-quantitative microprobe traverses showed

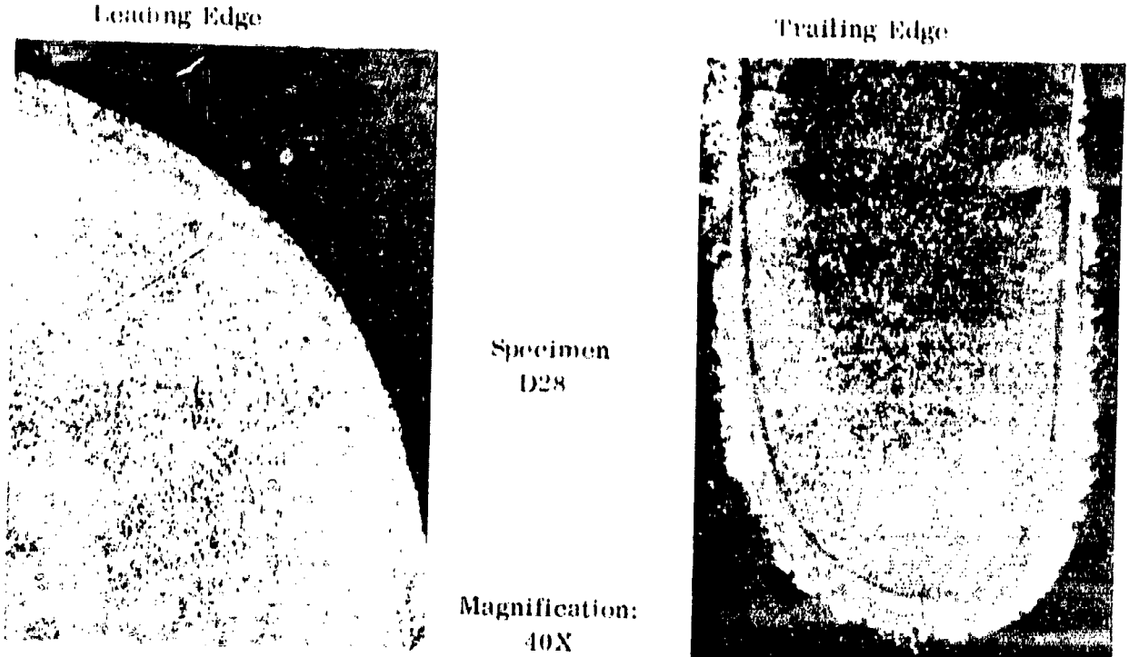

FIGURE 35. MICROSTRUCTURE AFTER 440 HOURS IN SERIES 2 TESTS; D Coating on IN-100 Alloy

that this phase was rich in titanium and carbon, which logically identified it as a MC carbide. A region of γ' was not formed at the interface as with the B and C coatings, but the exposure times were shorter for the D coated specimens.

The presence of a large amount of chromium was responsible for changing the phase relationships at the higher temperatures. As shown by Taylor and Floyd's Ni-Cr-Al, ternary system (Ref. 4), the presence of chromium suppresses the formation of γ', Ni_3Al, so that γ and βNiAl are in equilibrium with each other at temperatures down to about 1800°F (1000°C). The significance of this is that the phase adjacent to the βMAl and in contact with the oxidizing environment is now γ solid solution, which is high in chromium and low in aluminum compared to the γ' Ni_3Al phase, and which is less oxidation resistant by virtue of the formation of a spinel-type oxide rather than αAl_2O_3. Figure 37 is a photomicrograph of the trailing edge cross-section of the test specimen (1950° F location) in Series 2 tests and shows how rapid oxidation proceeded along the Ni-Cr-Al γ solid solution phase.

Specimen No. D52

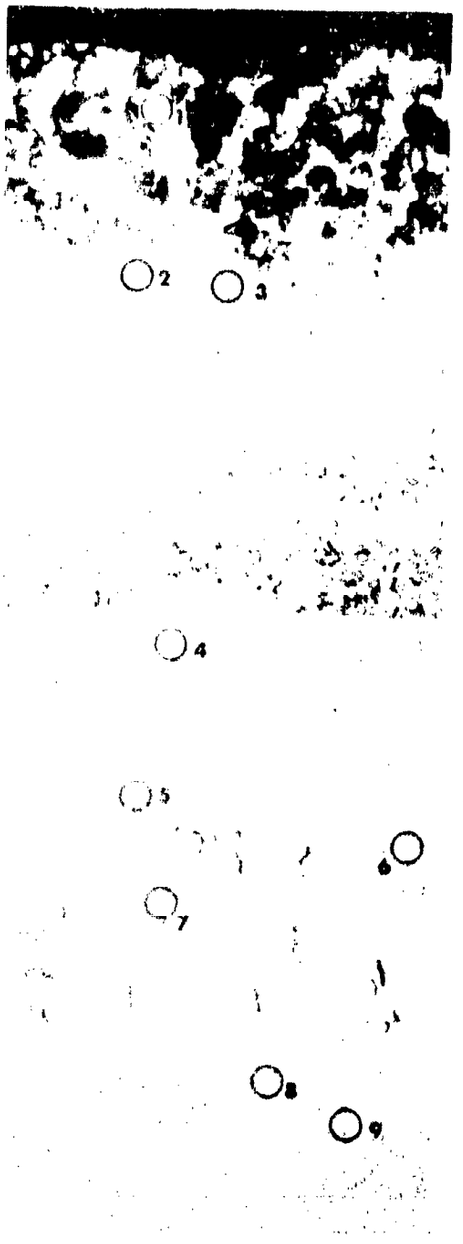

	Composition (wt %)						
	Al	Co	Cr	Fe	Ni	Si	Total
1	22.2	8.7	73.9	5.6	10.1	-	120.5
2	34.4	11.3	6.4	3.6	58.4	-	114.1
3	8.4	5.4	66.4	4.0	16.3	-	100.5
4	32.7	13.9	5.0	2.3	57.4	-	111.3
5	3.2	6.2	62.6	1.3	12.4	0.06	85.8
6	5.6	7.1	57.0	1.2	16.0	-	86.9
7	3.0	5.5	2.8	0.78	19.9	0.13	32.1
8	14.1	16.8	6.5	1.0	59.0	-	97.4
9	14.2	16.8	9.8	0.71	59.0	-	100.5
℄	12.2	17.6	8.7	0.19	61.2	0.40	100.3

Test No. 32

Etchant: Oxalic Acid-Electrolytic

Magnification: 750X

Local Temperature: 1705° F

FIGURE 36. ELECTRON MICROPROBE ANALYSIS OF D COATING ON IN-100 ALLOY AFTER 603 HOURS; Series 1 Tests (T_{max} 1870° F)

Specimen D28

Local Temperature: 1950° F

Trailing Edge

Exposure: 440 Hours

Magnification: 500X

Etchant: Oxalic Acid-Electrolytic

FIGURE 37. MICROSTRUCTURE OF D COATING AFTER SERIES 2 TEST (T_{max} 1950° F)

F Coating on B1900

Leading and trailing edge locations (1725° F and 1950° F, respectively) of the specimen exposed 2000 hours in Series 2 tests are shown in Figure 38. The thermogravimetric data for this specimen did not indicate failure after this exposure but, as can be seen from Figure 38, the coating was completely consumed at the trailing edge and the appearance was typical of exposed, uncoated B1900. At the leading edge the coating was about 50 percent consumed (in terms of remaining βMAl). Extensive γ' had formed both as isolated, irregular shaped particles in the MAl matrix and as a continuous zone at the interface. This type of γ' formation was typical of the coatings containing silicon. In the Series 1 tests, F and H coated specimens survived over 3000 hours, but unfortunately a failure in the temperature controlling equipment caused overheating and localized melting at 3040 hours. Metallography was performed on the specimens, but gross structural change had occurred in both substrate and remaining coating such that evaluation was of no practical significance.

Microprobe data for the Series 2 tests are shown in Figure 39. The temperature corresponding to this location during test was 1785° F. The structure shown in Figure 39 would exemplify coating failure based on the metallographic criterion of breakdown of the continuous βMAl layer. The γ' phase constituted the "coating" matrix and, in addition to the large islands of β, there were two other discernible phases, mostly close to the original coating matrix interface and usually in contact with each other. One of these resembled the high silicon phase, which was identified in the C coating, while the other appeared as white discrete particles. The light grey, high silicon phase was difficult to see under the microprobe, optical microscope (300X magnification) and, in fact, was only just visible at 1000X under the metallograph. Microprobe determination No. 5 was an attempt to analyze this phase, but, as was observed by the residual carbon spot, the analysis was performed partly on the white etching phase and partly on the high silicon phase. The values of 4.0Al; 10.1Si; 11.6Cr; 6.6Co; 26.1Ni and 2.6Ta (atomic percent) showed that the aluminum level was very low and that Si was concentrated in this area. Molybdenum was not determined, which may explain the low total element value. The other analyses identified the γ' and β phases and showed that the chromium concentration was quite low in the coating (~1.0 weight percent) compared to the original B1900 alloy composition (8 weight pe). As usual, cobalt was present to about the same level as in the matrix alloy in both γ' and β phases, while tantalum was apparently rejected from the βMAl. The earlier analysis on specimens tested for 100 hours showed that about 2.0 weight percent silicon and 6.0 weight percent chromium was present in both γ' and β phases. The later analyses indicated, therefore, that these two elements were progressively lost during the long-time oxidation exposures. Both metallography and microprobe analyses showed that substantial interdiffusion of Al and Ni occurred at the coating/matrix interface.

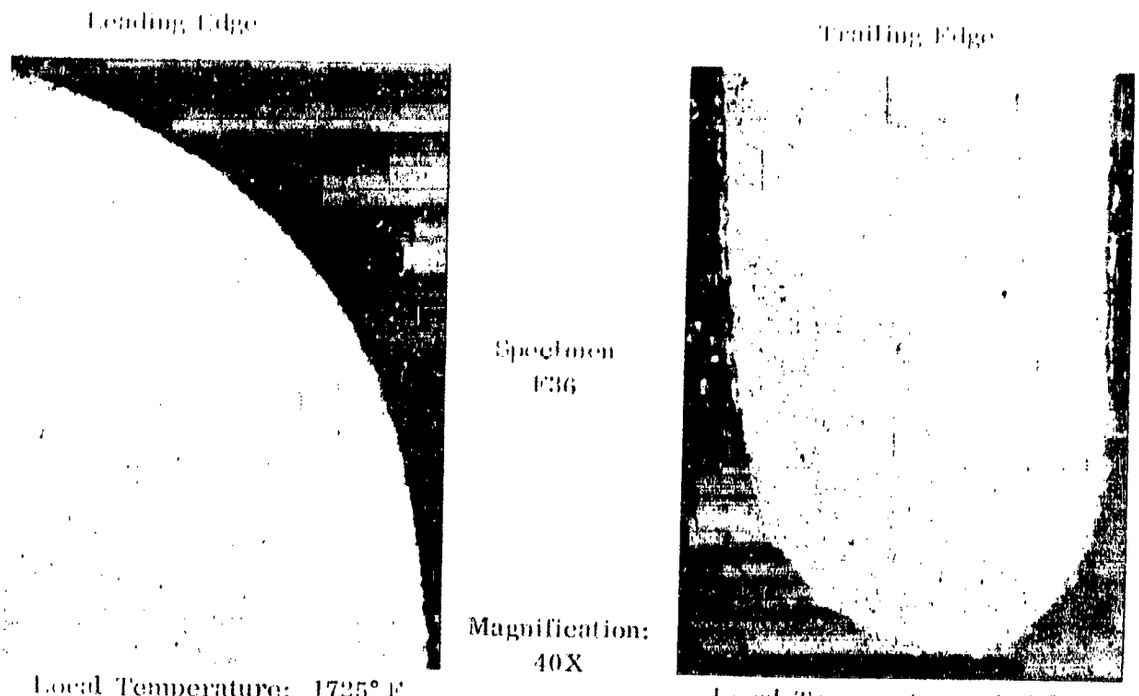

Etchant: Oxalic Acid–Electrolytic

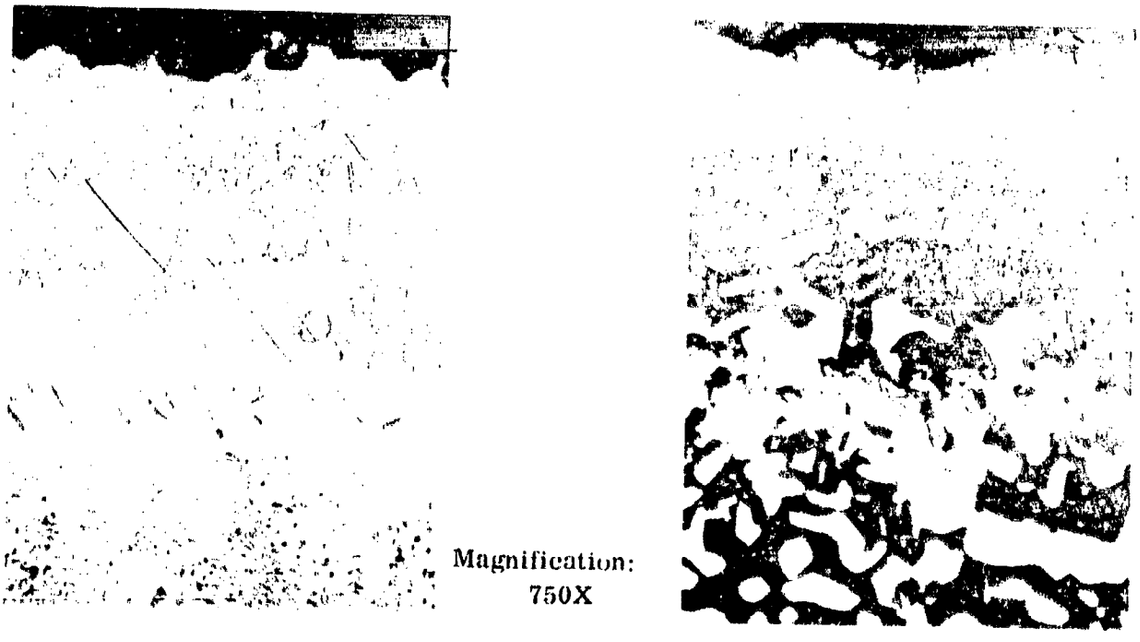

FIGURE 38. MICROSTRUCTURE AFTER 2000 HOURS IN SERIES 2 TEST; F Coating on B1900 Alloy (T_{max} 1950° F)

Specimen No. F36

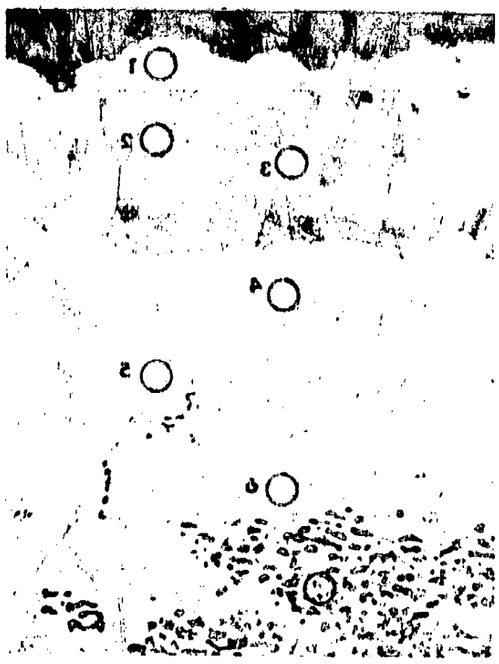

Test No. 35

Etchant: Oxalic Acid-Electrolytic

Magnification: 750X

Local Temperature: 1785°F

	Composition (wt %)						
	Al	Co	Cr	Ni	Si	Ta	Total
1	16.2	9.0	2.1	70.0	0.05	2.1	99.4
2	30.8	8.7	2.5	66.5	-	-	108.5
3	17.5	9.0	2.1	71.2	0.05	2.1	102.0
4	17.0	8.6	2.1	70.0	-	2.8	100.5
5	1.9	7.0	10.9	27.6	5.10	8.5	61.0
6	15.7	8.3	2.2	69.8	-	3.8	100.0
7	14.5	10.4	4.6	66.1	-	3.4	99.0
8	9.1	9.8	6.3	64.8	-	3.2	93.2

FIGURE 39. ELECTRON MICROPROBE ANALYSIS OF F COATING ON B1900 ALLOY AFTER 2000 HOURS; Series 2 Tests (T_{max} 1950° F)

G Coating on B1900

The G coating was previously shown to be more complex than most others applied to nickel-base alloys. The coating process apparently involved a chromizing cycle prior to aluminizing which produced a coating with a hard α chromium layer at the interface or along the center of the aluminide layer. The G coating was subject to void formation and spalling along the chromium-rich layer and the metallographic data indicated that this was a function of coating structure uniformity. Figure 40 shows the structure at leading and trailing edge locations (1725° F and 1950° F) of the specimen tested for 1360 hours at 2000° F. The aluminide layer was completely consumed at the trailing edge and the three phases, γ, γ' and α chromium, were visible in the residual coating layers. At the lower temperature location a fairly thick aluminide layer was retained. Chromium-rich phases were present throughout the coating in this particular specimen and were not as concentrated along the intermediate zone as in other specimens which were examined. Considerable scatter was observed in the performance of G coated specimens, and it was possible to relate this to the distribution of the chromium-rich phase. Wherever this phase made contact with the exposed surface and intermediate layer, rapid oxidation occurred beneath the βMAl layer and subsequent spalling occurred.

Specimens G59 and G36 provide a good example of the variation in coating performance. These specimens were rig tested simultaneously in a Series 3 test. Specimen G36 spalled badly and was removed from test after 440 hours, while G59 showed no signs of failure after 520 hours. All testing on the program was concluded at this point. Microprobe data for these two specimens are shown in Figures 41 and 42. The temperature corresponding to these locations during test was 1855° F. Phases positively identified from the data in Figure 41 were βMAl(2); αCr(3 and 5); and $\gamma' M_3Al$(6). The matrix analysis (8) at the centerline corresponded well with the known B1900 values. The second analysis (Fig. 42) was carried out to identify any compositional differences between G59 and G36, which could account for the early failure of specimen G36. The major difference was the presence of considerably more of the chromium-rich phase throughout the coating on specimen G36. The frequently observed presence of this phase, connecting the outer surface and intermediate layer, (point 1 in Fig. 42) was clearly responsible for oxidation and spalling. In contrast, the coating on G59 contained a narrower and more uniform α chromium layer which did not make direct contact with the oxidizing environment at any point. Figure 43 shows that βMAl was retained at the trailing edge (2050° F location) on this specimen after the 520 hours rig exposure. A point of significance in Figure 43 is that, although the remaining β MAl layer was quite thin at this location, extensive γ' formation had not occurred as was the case with the other coatings on nickel-base alloys. This implies that the chromium layer was an effective diffusion barrier to aluminum diffusing inwards and/or nickel diffusing outwards, preventing dilution of the βMAl phase by matrix/coating reactions. The aluminum depletion mechanism would be largely restricted to formation and spalling of αAl_2O_3. The formation of a wide band of γ solid solution at the interface was typical of the chromium-containing coatings as mentioned previously.

Leading Edge

Trailing Edge

Specimen
G42

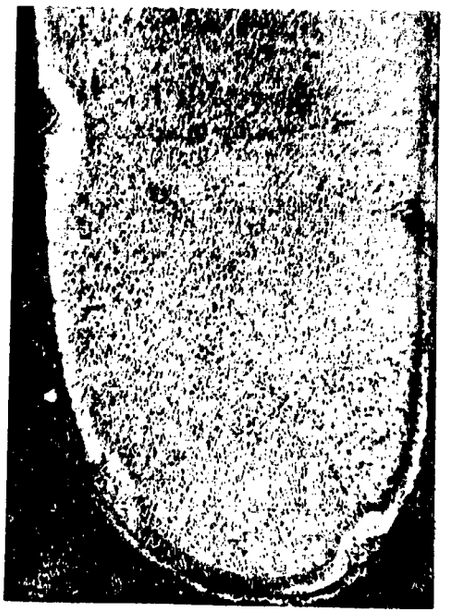

Magnification:
40X

Local Temperature: 1725° F

Local Temperature: 1950° F

Etchant: Oxalic Acid-Electrolytic

Magnification:
750X

FIGURE 40. MICROSTRUCTURE AFTER 1360 HOURS IN SERIES 2 TEST; G Coating on B1900 Alloy (T_{max} 1950° F)

Specimen No. G59

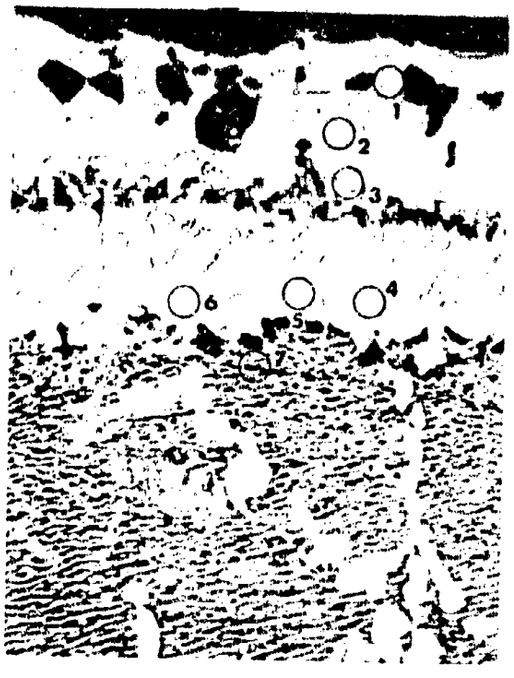

Test No. 37

Etchant: Oxalic Acid-Electrolytic

Magnification: 750X

Local Temperature: 1855° F

	Composition (wt %)						
	Al	Co	Cr	Mo	Ni	Ti	Total
1	22.1	8.3	6.8	1.8	69.0	0.12	108.1
2	27.3	7.5	7.6	1.7	65.8	0.12	110.0
3	0.3	2.4	81.0	9.8	4.5	0.09	98.1
4	15.4	8.7	11.6	1.9	53.5	1.00	92.1
5	9.8	3.8	69.5	13.5	5.1	0.31	102.0
6	12.4	7.9	8.6	1.8	60.3	0.65	91.7
7	9.6	9.4	7.2	7.2	58.6	0.63	92.6
8	7.9	9.9	8.2	6.1	68.3	1.10	101.5

FIGURE 41. ELECTRON MICROPROBE ANALYSIS OF G COATING ON B1900 ALLOY AFTER 520 HOURS; Series 3 Test (T_{max} 2050° F)

Specimen No. G36

Test No. 37

Etchant: Oxalic Acid-Electrolytic

Magnification: 750X

Local Temperature: 1855° F

	Composition (wt %)						
	Al	Co	Cr	Mo	Ni	Ti	Total
1	55.60	3.50	68.6	5.3	11.40	0.06	144.5
2	27.40	8.10	19.8	1.4	55.50	0.13	112.3
3	3.70	5.40	56.9	1.6	15.80	0.06	83.5
4	5.20	0.60	76.4	13.3	0.93	1.30	97.7
5	0.60	12.80	23.1	5.5	51.20	4.00	97.2
6	7.10	10.10	12.2	4.3	66.50	0.43	100.6
℄ 7	7.90	11.40	11.4	5.2	67.80	1.30	105.0

FIGURE 42. ELECTRON MICROPROBE ANALYSIS OF G COATING ON B1900 ALLOY AFTER 440 HOURS; Series 3 Test (T_{max} 2050° F)

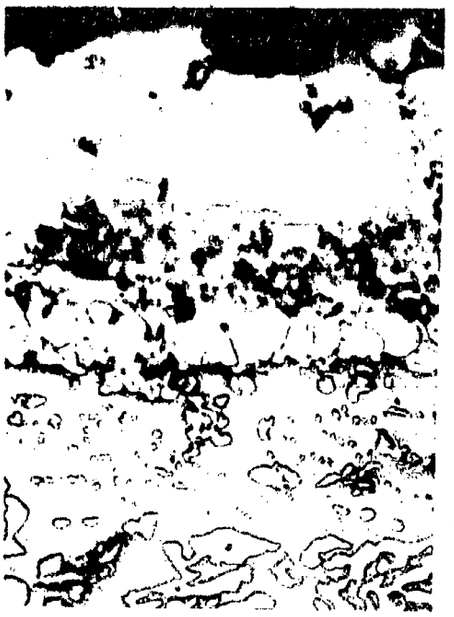

Specimen G59

Exposure: 520 Hours

Local Temperature: 2050°F

Etchant: Oxalic Acid-Electrolytic

Magnification: 750X

FIGURE 43. MICROSTRUCTURE OF TRAILING EDGE OF SPECIMEN G59

H Coating on B1900 Alloy

The H coating was one of the thicker coatings applied to the program alloys and exhibited good performance in the short-term, high-temperature tests. Specimen H3 had not failed, according to the thermogravimetric data, after 2000 hours in Series 2 tests. Metallography, however, showed that no coating was retained at the trailing edge location after this exposure. Figure 44 shows the appearance of the blade cross-section at the extreme temperature locations (1725° F and 1950° F). Although the surface appearance of this specimen was good at the completion of the test, the low magnification photograph of the trailing edge showed that oxidation-erosion sufficient to change the specimen profile had occurred. At the trailing edge the specimen surface was again typical of exposed, uncoated B1900. The remaining βMAl layer at the leading edge was quite thick and significantly less of the γ' phase had formed within the β, compared to the silicon containing coatings (e.g., C and F). The usual zone of γ' plus isolated precipitate particles had formed at the interface.

Figure 45 shows the combined metallographic-microprobe analysis which was performed on specimen H3 at the mid section (1785°F). The coating had failed at this

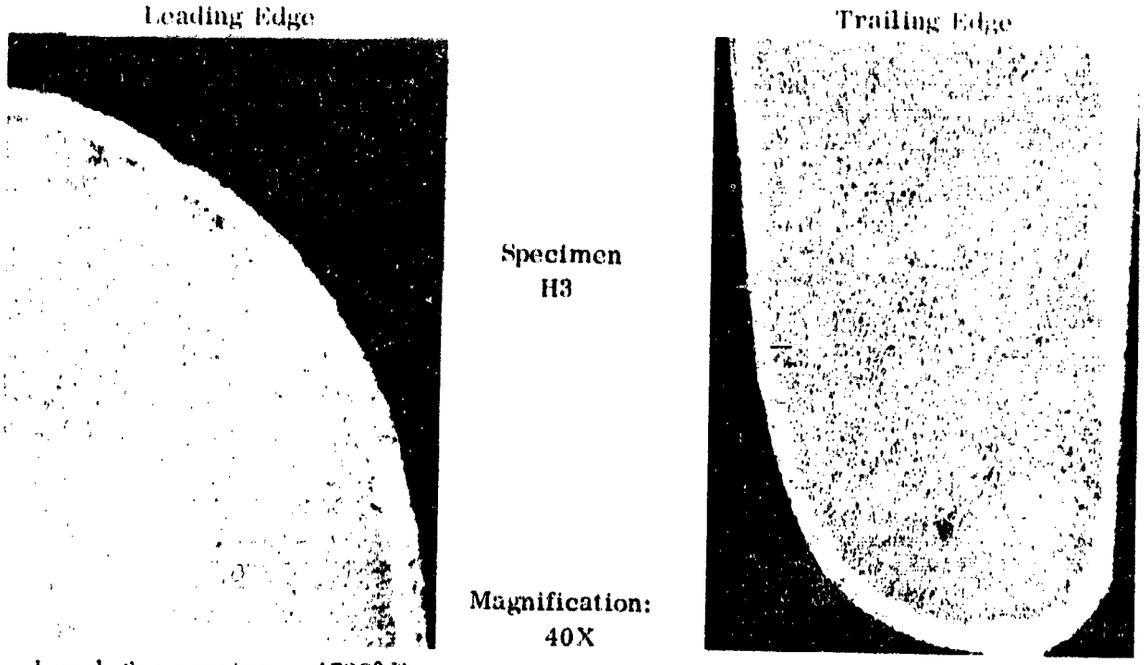

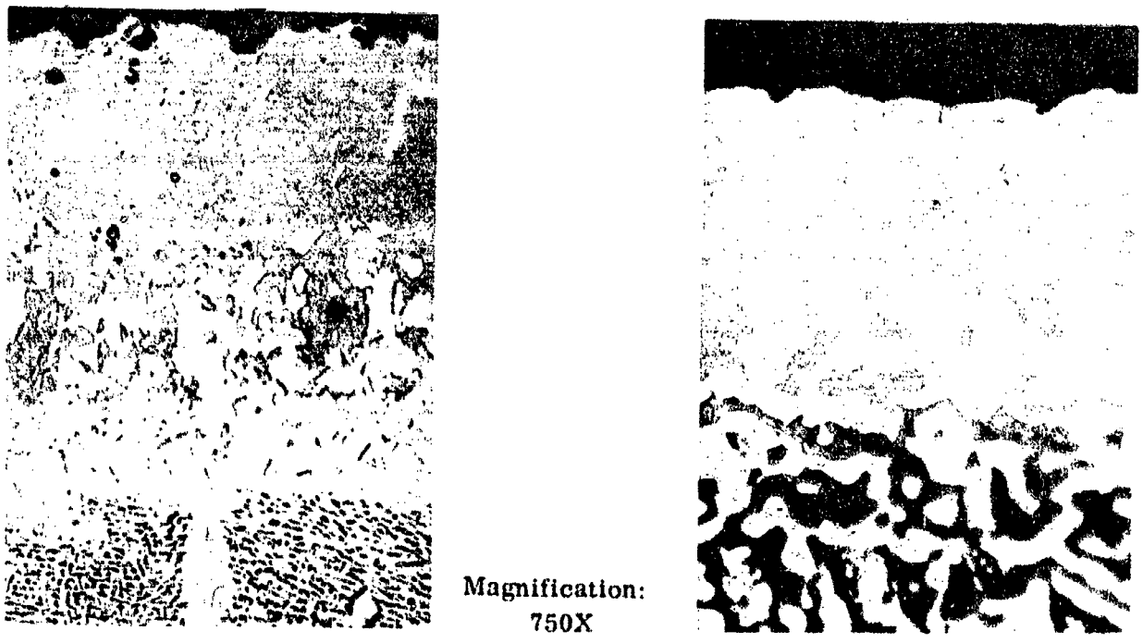

FIGURE 44. MICROSTRUCTURE AFTER 2000 HOURS IN SERIES 2 TEST; H Coating on B1900 Alloy (T_{max} 1950° F)

Specimen No. 113

Local Temperature: 1785° F

	Composition (wt %)						
	Al	Co	Cr	Ni	Si	Ta	Total
1	18.1	9.2	1.7	69.5	0.80	0.7	100.0
2	25.3	8.4	1.9	66.7	0.10	-	102.4
3	1.2	4.1	62.3	4.2	0.70	1.2	73.7
4	18.6	7.7	2.1	65.0	0.70	3.1	97.2
5	15.6	8.8	3.5	66.0	0.40	2.1	96.4
6	11.5	9.2	6.7	65.1	0.40	2.3	95.2

Test No. 35

Etchant: Oxalic Acid-Electrolytic

Magnification: 750X

FIGURE 45. ELECTRON MICROPROBE ANALYSIS OF H COATING ON B1900 ALLOY AFTER 2000 HOURS; Series 2 Test (T_{max} 1950° F)

location, according to the metallographic failure criterion, since βMAl no longer formed the coating-matrix phase. Phases which could be positively identified from these analyses were γ'M3Al (1,4) and βMAl (2). The phase corresponding to (3) was tentatively identified as αCr and showed 71 atomic percent Cr; since earlier analyses had shown segregation of molybdenum to this phase, the analyses would tend to agree with a Cr-Mo bcc solid solution. The matrix analysis (6) was in a predominantly γ' region, as determined by examination of the microprobe beam carbon residue spot, which explains the high aluminum level.

4.1.3 Comparison of Nickel-Base Alloy Coatings (see page 101 for Cobalt-Base Alloys)

The purpose of this program was to compare the structure and chemistry of a variety of commercially available coatings and to compare their relative performances in a simulated gas turbine environment. The chemistry of the coatings is, in most cases, related intimately to the chemistry of the substrate alloys and, therefore, comparisons of coating chemistry and performance must include consideration of the substrate alloy. The relative performances of the coatings are discussed below, and an attempt is made to relate these to structural and chemical differences.

Because of the large temperature gradient which existed between the leading and trailing edge blade locations, it was possible to observe a coating structure on the prepared cross sections corresponding to any exposure temperature between the two extremes - usually a range of about 200° F to 300° F. A coating failure criterion was established for the nickel-base alloy coating where the first appearance of a structure, such as shown in Figures 27 and 45, was taken as the failure point. Specimens from up to four tests were examined; therefore it was possible to obtain up to four points on a life-temperature plot for each coating. Since these data are limited, they were plotted as bands rather than as well-defined curves.

Figures 46 and 47 show the available data for the coatings on IN-100 and B1900 alloys. On IN-100 alloy the B and C coatings showed similar life in the 1750° F to 1850° F temperature range. The indicated temperature for 3000-hour life was between 1700° F and 1800° F with the C coating, perhaps having a slight temperature advantage. The D coating appeared to have the highest temperature capability in the short-term tests (2100° F, 100 hours), but exhibited a steeper slope on the coating life-temperature curves because of its spalling tendency.

From Figure 47, the F and H coatings had the highest temperature (between 1765 and 1805° F), 3000-hour life capability. The chromium-containing G coating appeared to have the highest temperature, 100-hour life capability (2100° F), but, similar to the D coating on IN-100, exhibited a steeper slope on the life-temperature curves. The data indicated a slightly higher 100-hour temperature for the H coating (2045° F) compared to the F coating (2000° F). On an overall basis, the F coating on B1900 alloy

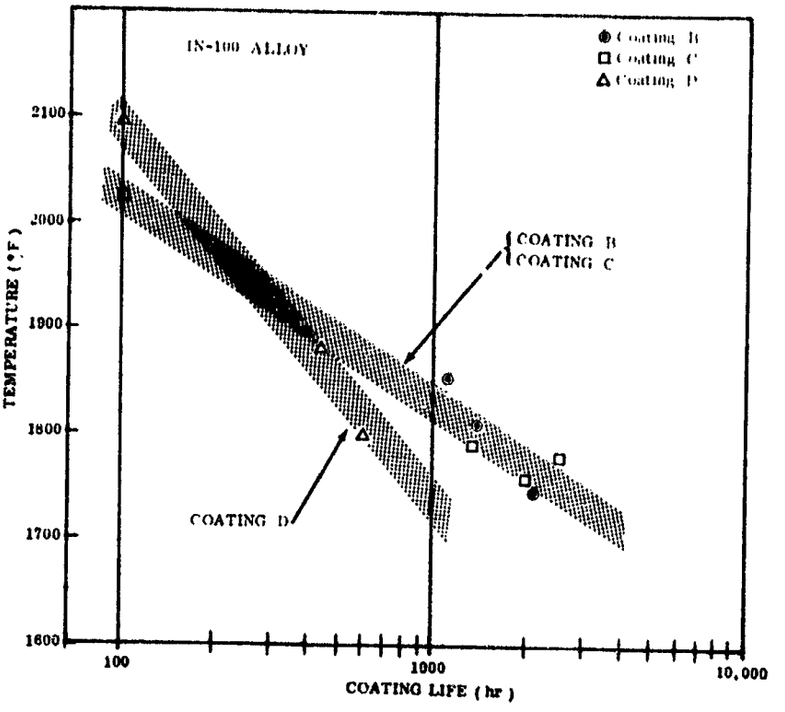

FIGURE 46. LIFE OF COATINGS ON IN-100 ALLOY

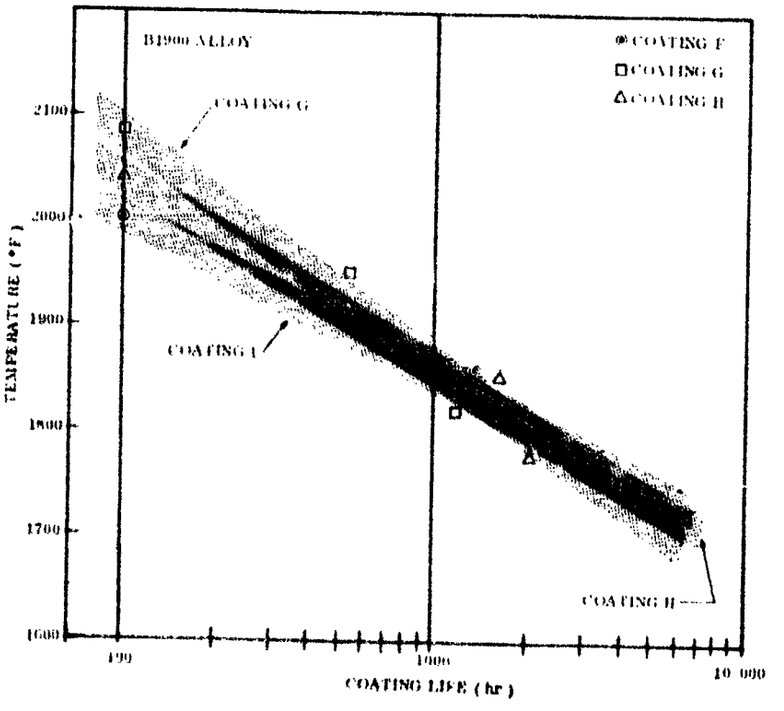

FIGURE 47. LIFE OF COATINGS ON B1900 ALLOY

appeared to have the highest temperature potential for 3000 hours life of all the coatings on the nickel-base alloys.

Structurally and chemically, there were many similarities between the F coating on B1900 and the C coating on IN-100. The presence of silicon in both coatings appeared to be related to the manner in which γ' was formed within the MAl layer. As pointed out previously, Guard and Smith's Ni-Al-Si diagram (Ref. 2) shows an extended γ' region to higher aluminum levels than in the binary. This could account for the extensive γ' formation within the aluminide layer in addition to the γ' formation at the coating-matrix interface, which occurred with all of the coatings. Providing the aluminum activity of the surface phase was sufficiently high to form the protective Al_2O_3, the oxidation rate was apparently unchanged. The aluminum reservoir, therefore, was the most important factor. The presence of silicon in the oxide may have been beneficial in terms of the spalling rate of αAl_2O_3. The solubility of SiO_2 in Al_2O_3 is known to be negligible in contrast to Cr_2O_3, which exhibits complete solubility. But the presence of a two-phase oxide, $Al_2O_3 + SiO_2$, could have improved plasticity which would tend to decrease spalling and, therefore, provide longer life for the coating. Silicon was also found in the B coating, but to lower levels than in C and F, and the grey etching phase was not observed. In many respects silicon was the most difficult element to analyze, and possible errors arising from such sources as silicon carbide grinding papers must be considered.

The D and G coatings were less conventional and apparently applied in two-step processes. Both coatings were shown to have serious limitations. The D coating on IN-100 spalled badly in the outer chromium-rich layer (initially $Cr3Al_2$) due to internal oxidation and/or nitride formation. The presence of chromium caused formation of a γ solid solution phase at the surface, which was stable in contact with βMAl. Oxidation proceeded more rapidly than if $\gamma' M_3Al$ had formed.

Apparent lack of control in the G coating process produced variations in the amount of chromium-rich phase present within the aluminide. Whenever the chromium-rich phase made contact with the oxidizing environment, accelerated oxidation and subsequent spalling occurred. Good performance was exhibited by one or two specimens in which the chromium layer was restricted to a narrow, continuous layer at the coating/metal interface or intermediate zone in the coating. Under these conditions, the chromium layer appeared to prolong the coating life by restricting aluminum and/or nickel diffusion across the interface. This coating is potentially a good performer, providing that better control of the application process is achieved. Ballistic impact properties should, however, be considered because of the apparent brittleness of the chromium layer.

The H coating on B1900 and C coating on IN-100 had similar lives and, on an overall basis, could be rated equally as second best performer. The data indicate that the C and F coatings were the "same" (i.e., applied by the same process); in which

case, the better performance of the F coating must be related to the substrate composition. The probe analysis showed that the elements, which entered and were retained, in the coating (in addition to nickel) were cobalt, chromium and titanium. Other elements such as molybdenum and tantalum, which represented significant compositional differences between the two alloys, did not enter the coating to any appreciable extent. It could not be determined conclusively which of the elements, Co, Cr and Ti, could contribute to more rapid degradation, but it is felt that the γ solid solution-forming elements, Co and Cr, could have caused slightly more rapid degradation of the C coating compared to the F coating by formation of the γ phase at high temperatures in preference to the more oxidation resistant γ' phase. The effect of the cobalt level in the substrate alloy on γ-forming tendency has been confirmed in a current program at Solar (contract N00019-68-C-0532). High cobalt alloys such as IN-100 formed a continuous γ layer at the coating-metal interface, while low cobalt alloys such as 713C formed a γ' interface layer when the same coating was applied. Redden (Ref. 5) noted the adverse effect of titanium in the substrate on the oxidation resistance of aluminide coatings. The poorer performance of the C coating on IN-100 compared to the F coating on B1900 may be in a large part due to the high concentration of titanium in the IN-100 alloy.

Silicon was not found in the H coating to any significant level, a fact which tends to support the conclusion that this element is beneficial to optimum coating life and may be related to a decreased spalling rate of protective Al_2O_3. However, a potential problem was shown to exist which was related to the presence of silicon. An incipient melting phenomenon was observed in specimen C52 which caused bulging of the coating at the trailing edge location (Fig. 48). Microprobe analysis and high magnification

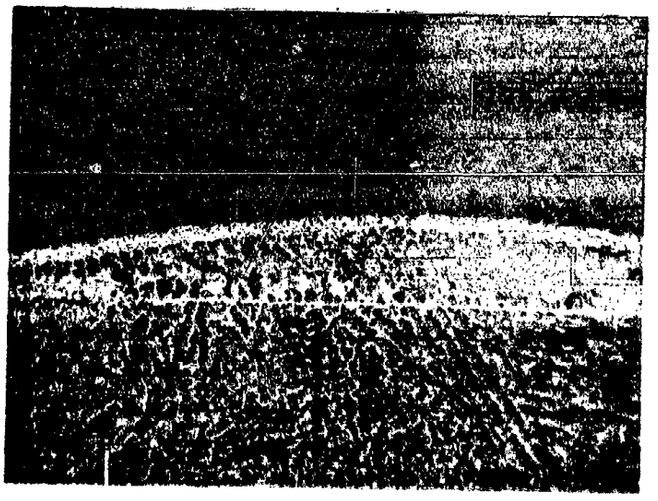

Magnification: 40X

FIGURE 48. SPECIMEN C52 AFTER 2560 HOURS AT 1870° F

metallography of this region is shown in Figure A-2 of Appendix A. The local temperature was about 1870° F. The metallography and probe data indicated that the incipient melting was associated with segregation of silicon. An excess of silicon, therefore, could result in a low melting point coating.

The formation of a γ' zone at the coating-matrix interface took place in all the coating/substrate combinations (nickel alloys). This layer was modified in the case of the chromium-rich coatings such that γ solid solution was formed at temperatures above 1800° F. At locations corresponding to temperatures of between 1700° F and 1800° F an acicular phase was formed within the γ' diffusion zone layer. Examples are shown in Figure 49. In the previous work, this phase was tentatively identified as acicular σ phase. In view of the work of Collins (Ref. 6) which showed that σ phase was not stable above about 1620° F in typical superalloys and, more recently, the work of Havalda (Ref. 7) which identified formation of acicular η from γ' in a Ni-Cr-Ti-Al alloy, a positive identification of the phase shown in Figure 49 could not be made without X-ray analysis on extracted particles. More important than the identification of the phase would be an evaluation of its effect on mechanical properties of the coated alloy.

4.2 COBALT-BASE ALLOYS

Tests on the cobalt-base alloys were concentrated primarily on the J and L coatings on X-40 alloy and on the O and P coatings on WI-52 alloy. These four coatings exhibited best performance on the cobalt-base alloys in the Task II, 100-hour screening tests. Specimens of the K coating (on X-40) and N coating (on WI-52) were used as required to fill in the test specimen holder. Weight change during testing, surface appearance after test, metallographic and electron microprobe analysis after testing are included in the following sections.

4.2.1 Weight Change and Appearance

Curves of cumulative weight change plotted as a function of exposure time at temperature are presented for the three temperature levels - Series 1, Series 2, and Series 3. Photographs are shown of the surface appearance of selected specimens after the oxidation-erosion tests.

Series 2 - Oxidation-Erosion Tests (T_{max} 1845° F)

The weight change curves for the Series 1 tests on the J, L, N, O, and P coatings are shown in Figure 50. Based on visual evidence of severe substrate

Specimen B51
1100 Hours at 1780° F
Magnification: 750X

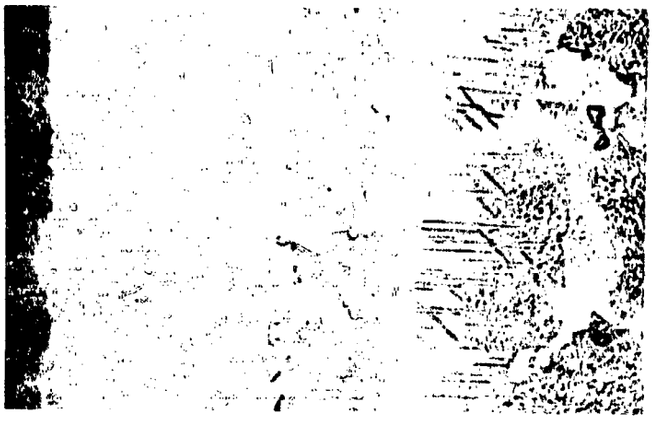

Specimen C48
1370 Hours at 1780° F
Magnification: 750X

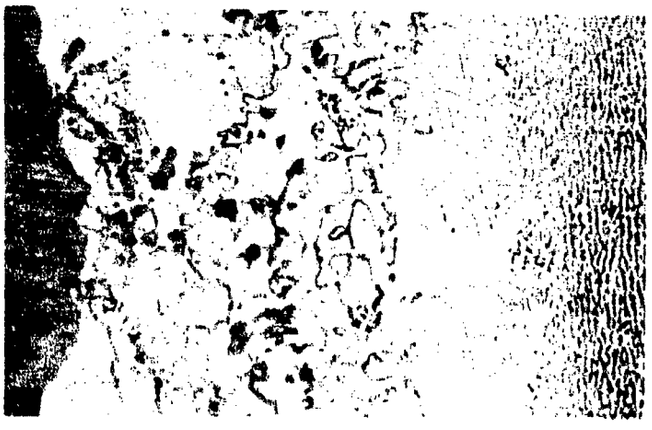

Specimen C46
545 Hours at 1750° F
Magnification: 750X

FIGURE 49. EXAMPLES OF ACICULAR PHASE FORMATION AT THE COATING/MATRIX INTERFACE OF COATINGS ON IN-100 AND B1900 ALLOYS

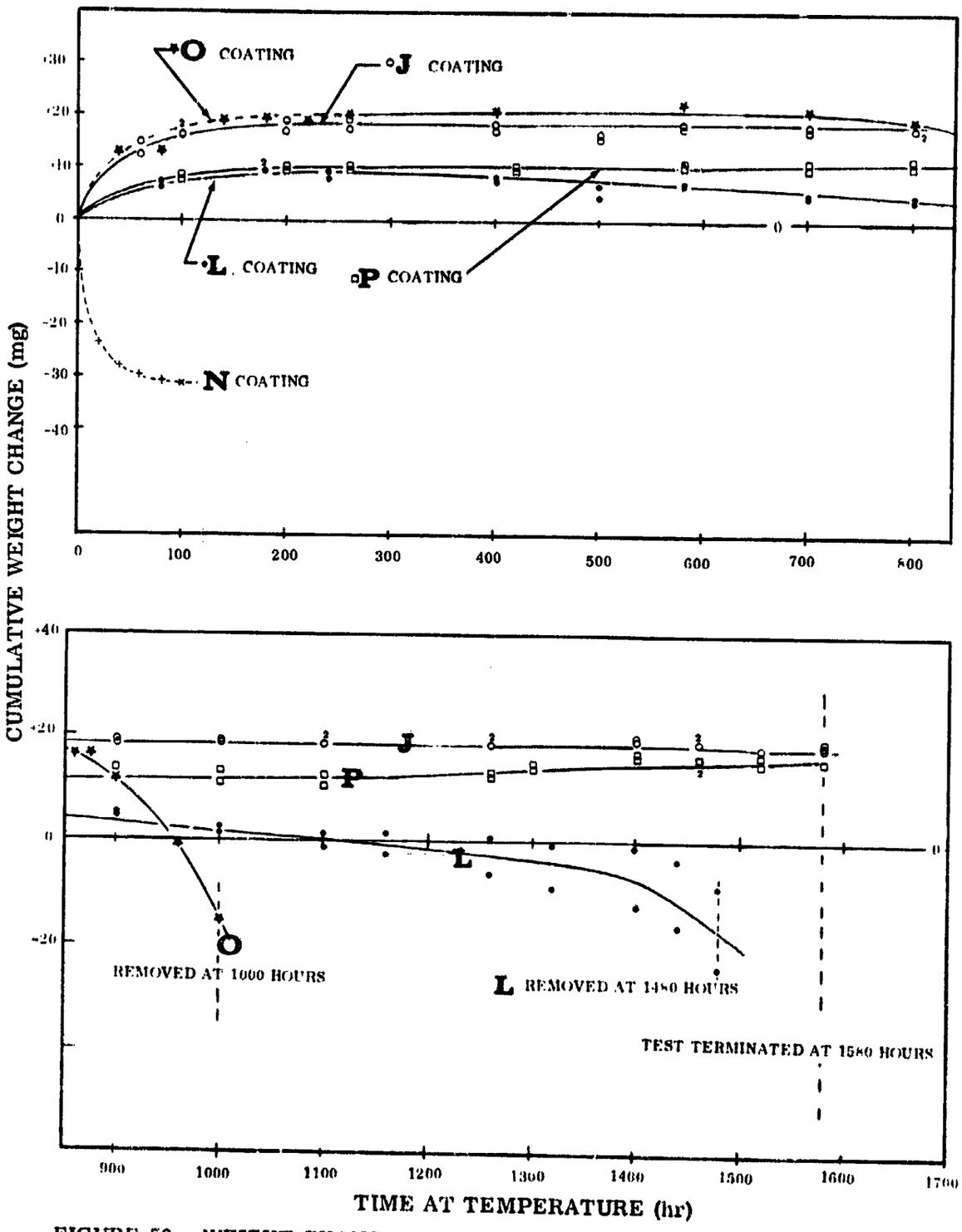

FIGURE 50. WEIGHT CHANGE VS. TIME FOR COATINGS J, L, N, O, AND P DURING SERIES 1 TESTS (T_{max} 1845° F)

oxidation and rapid metal loss, the O coating was removed from test after 1000 hours exposure. The first visual evidence of coating failure was observed at approximately 650 hours. At this time, a small area of spalled coating and blue-to-black oxide was apparent on the concave surface of the blade along the trailing edge (Fig. 51A). This area slowly increased in width and depth. After 860 hours of exposure the substrate oxidation was extremely rapid. Figure 51B shows this failed area on the concave surface after test.

The L coated X-40 alloy specimens exhibited slight coating spalling after approximately 500 hours total exposure. From 500 to 1400 hours, the specimens continued to slowly lose weight in a uniform manner. After approximately 1400 hours, both specimens exhibited a large increase in substrate oxidation and a correspondingly rapid weight loss. Specimens were removed from test after 1480 hours exposure. Figure 52 shows the surface appearance of the L coating after test.

Erosion-oxidation tests on the J and P coatings were terminated after a total of 1580 hours exposure. The coated specimens are shown in Figures 53 and 54. With both coatings, the specimens exhibited some evidence of coating loss, spalling and substrate oxidation. All failure sites occurred along the trailing edges on the concave surfaces.

Series 2 - Oxidation-Erosion Tests (T_{max} 1950° F

Results of the Series 2 tests performed on the J, K, L, N, O, and P coatings are shown in Figures 55 and 56. The J coating (on X-40 alloy) exhibited excellent performance in the test. At 994 hours the test was terminated when the average weight loss of the two specimens was in excess of 20 milligrams (one specimen had lost 34.4 mg and the other specimen had lost 16.3 mg). Visual examination showed substrate oxidation and erosion along the trailing edges of both specimens on the concave surface of the blades. One specimen after test is shown in Figure 57.

On the WI-52 alloy, coating P exhibited the best performance (as judged by weight loss and visual appearance only). The performance of this coating was somewhat better than the O coating and considerably better than the N coating. From the shape of the weight change curve for coating P, coating depletion and oxide buildup were essentially equal from 400 to 600 hours; aluminum depletion then reached a point at which α-Al_2O_3 could not be maintained and the specimens were oxidized quite rapidly. Specimens were removed from the test at 694 hours exposure (Fig. 58).

The O coating (on WI-52 alloy) exhibited a weight gain for approximately 330 hours similar to that shown by the J coating. However, from 330 to 475 hours, both specimens lost weight quite rapidly (0.12 mg/hr); from 475 hours on, the coating failed catastrophically in a manner similar to that observed during several 100-hour tests in Task II (Ref. 1). Specimens were removed from test at 519 hours when the

Specimen O42

650 Hours Exposure

Weight Gain: 21.4 mg

Concave Surface

Magnification: 2.3X

A

1000 Hours Exposure

Weight Loss: 15 mg

Concave Surface

Magnification: 2.3X

B

FIGURE 51. SURFACE APPEARANCE OF COATING O AFTER SERIES 1 TESTS (T_{max} 1845° F)

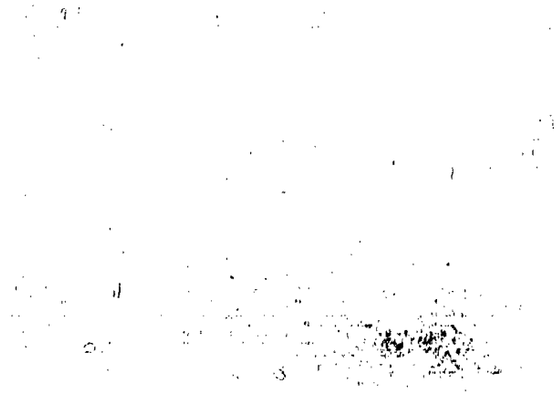

Specimen No. L47

1480 Hours Exposure

Weight Loss: 24.5 mg

Concave Surface

Magnification: 2.2X

FIGURE 52. SURFACE APPEARANCE OF COATING L AFTER SERIES I TESTS (T_{max} 1845° F)

Specimen No. J28

1580 Hours Exposure

Weight Gain: 17.9 mg

Concave Surface

Magnification: 2.2X

FIGURE 53. SURFACE APPEARANCE OF COATING J AFTER SERIES I TESTS (T_{max} 1845° F)

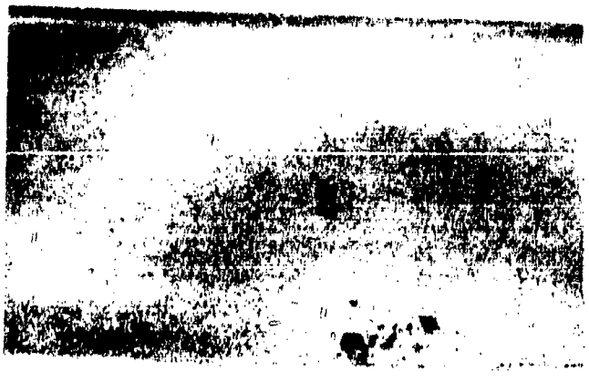

Specimen No. P48

1580 Hours Exposure

Weight Gain: 15.8 mg

Concave Surface

Magnification: 2X

FIGURE 54. SURFACE APPEARANCE OF COATING P AFTER SERIES 1 TESTS (T_{max} 1845° F)

average weight loss of the two specimens reached 20 milligrams. Specimen O45 after test is shown in Figure 59.

Coating L (on X-40 alloy) exhibited fair performance in the test. First observation of coating spalling and substrate attack was apparent after approximately 150 hours exposure. Specimens were continued in test to a total of 519 hours exposure. The surface appearance of specimen L45 after test is shown in Figure 60.

The results of the test on the K and N coatings (Fig. 56) show considerable difference in performance between specimens. It should be noted, however, that the K and N coatings consistently exhibited the poorest performance in all the previous oxidation-erosion tests. The extreme variation in oxidation protection for the K coating can probably be explained by the large variation in coating thickness side-to-side (Ref. 1).

Poorest performance was exhibited by the N coating on WI-52 alloy. Both specimens exhibited an immediate weight loss similar to that previously shown by this coating system in previous Task II tests. Exposure time for an average weight loss of 20 mg was only 35 hours.

Series 3 - Oxidation-Erosion Tests (T_{max} 2050° F)

The weight change curves for the Series 3 tests on the J and P coatings are shown in Figure 61. Surface appearance of specimens after approximately 250 hours exposure are shown in Figure 62.

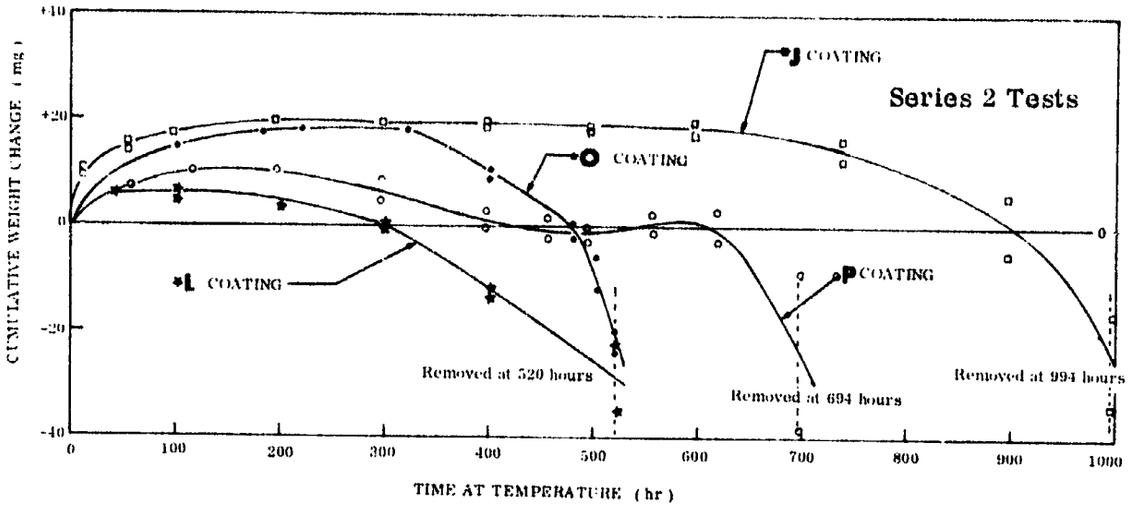

FIGURE 55. WEIGHT CHANGE VERSUS TIME FOR COATINGS J, L, O, AND P DURING SERIES 2 TESTS (T_{max} 1950° F)

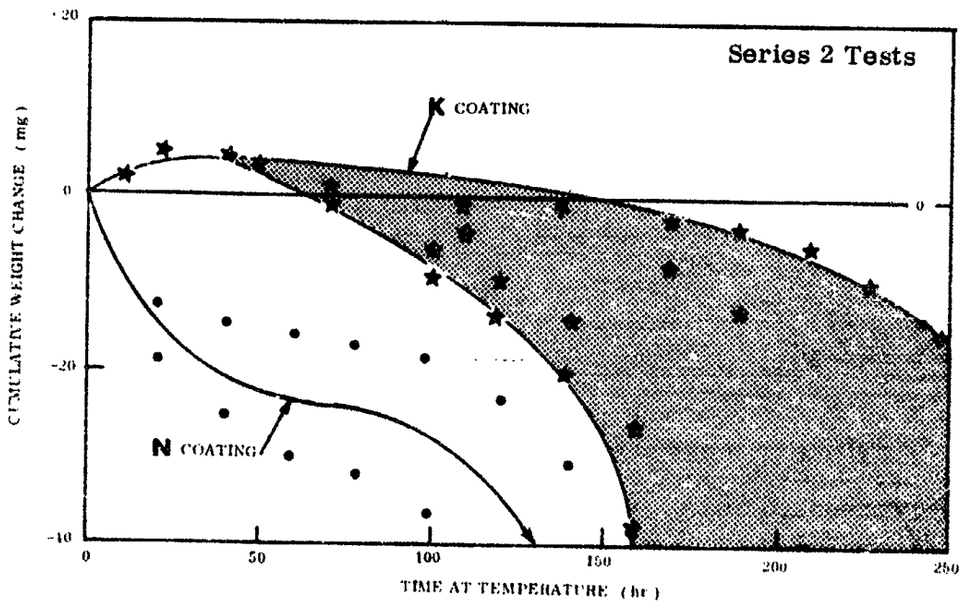

FIGURE 56. WEIGHT CHANGE VERSUS TIME FOR COATINGS K AND N DURING SERIES 2 TESTS (T_{max} 1950° F)

Specimen J2

994 Hours Exposure

Weight Loss: 34.4 mg

Concave Side

Magnification: 2X

FIGURE 57. SURFACE APPEARANCE OF COATING J AFTER SERIES 2 TESTS (T_{max} 1950° F)

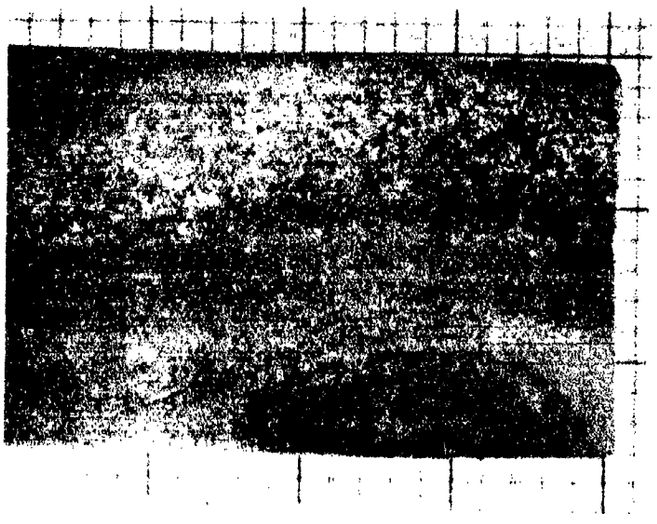

Specimen P29

694 Hours Exposure

Weight Loss: 47 mg

Concave Side

Magnification: 2.25X

FIGURE 58. SURFACE APPEARANCE OF COATING P AFTER SERIES 2 TESTS (T_{max} 1950° F)

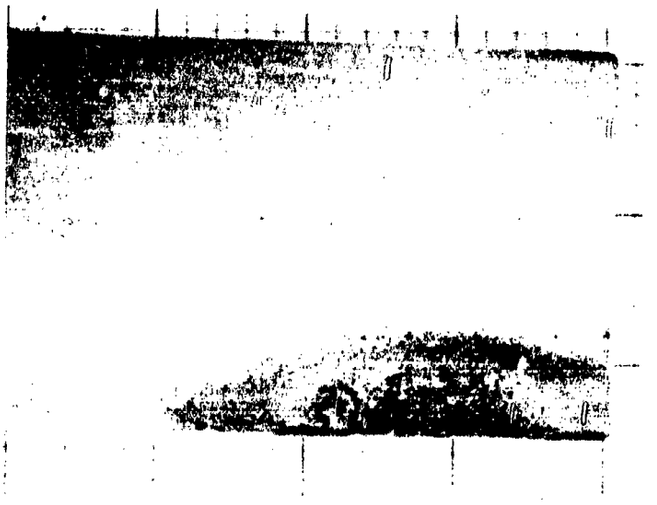

Specimen O45

520 Hours Exposure

Weight Loss: 23 mg

Concave Side

Magnification: 2.25X

FIGURE 59. SURFACE APPEARANCE OF COATING O AFTER SERIES 2 TESTS (T_{max} 1950° F)

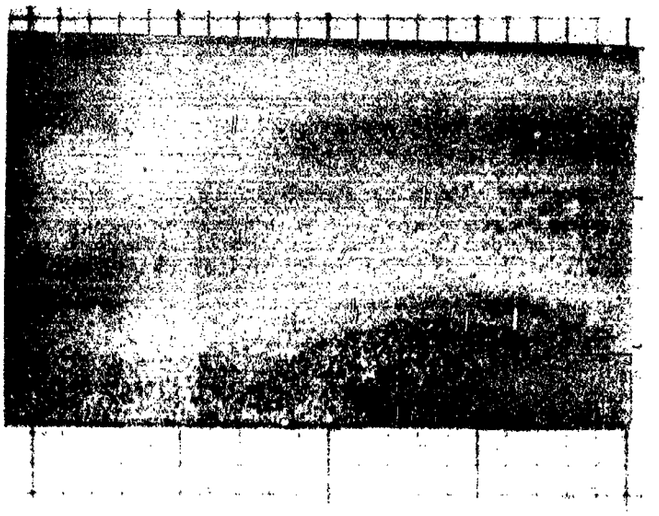

Specimen L45

520 Hours Exposure

Weight Loss: 35 mg

Concave Side

Magnification: 2.25X

FIGURE 60. SURFACE APPEARANCE OF COATING L AFTER SERIES 2 TESTS (T_{max} 1950° F)

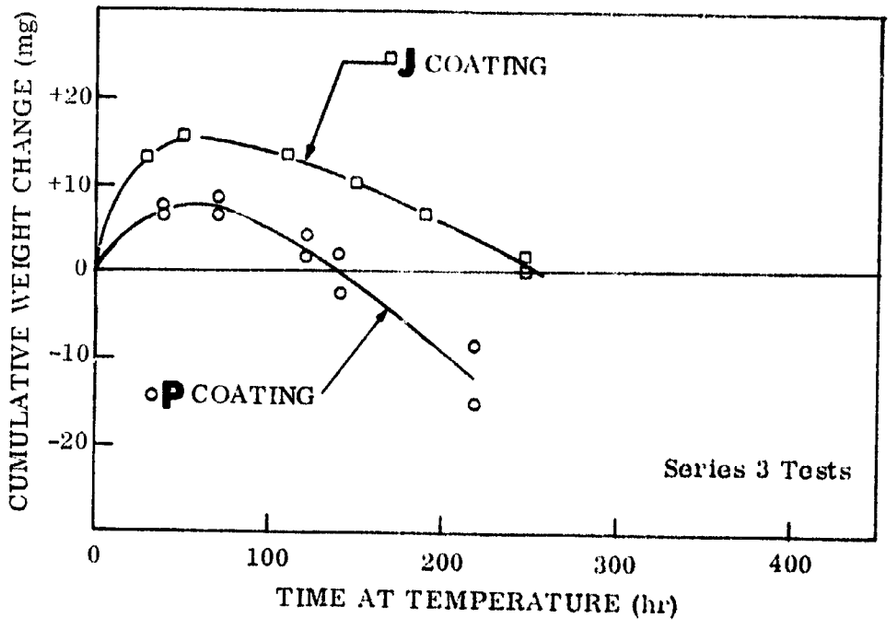

FIGURE 61. WEIGHT CHANGE VERSUS TIME FOR COATINGS J AND P DURING SERIES 3 TESTS (T_{max} 2050° F)

These two coatings were not tested to failure, i.e., 20 mg average weight loss. The specimens were inserted into the test as replacements for the C and F coatings as they failed and were removed from test. The entire test was terminated when the remaining two coated nickel-base alloy specimens (H coating on B1900 alloy) failed. From the shape of the weight change curves, it is apparent that the coatings both started to fail at approximately 70 hours total exposure. All specimens exhibited a maximum weight gain and the first appearance of blue oxide ($CoAl_2O_4$) was observed at this time. Weight loss from 70 hours exposure to the termination of the test was slower for the J coating (on X-40 alloy) due to the more oxidation resistant substrate alloy. Both coatings after test showed visual coating failure. The J specimens showed slight coating spall and some blue-black oxide; whereas the P specimens exhibited a large loss of coating and the subsequent appearance of black substrate oxide (Co_3O_4).

4.2.2 Coating Evaluations - Cobalt-Base Alloys

Table IV shows the exposure times and temperatures for the coated X-40 and WI-52 alloy specimens which were evaluated by metallography and microprobe analyses. Representative metallographic and microprobe analysis data are discussed in the following paragraphs. Additional microprobe data are included in Appendix A.

Specimen J50

250 Hours Exposure

Weight Gain: 0.4 mg

Concave Surface

Magnification: 2.2X

Specimen P50

220 Hours Exposure

Weight Loss: 15.5 mg

Concave Surface

Magnification: 2.2X

FIGURE 62. SURFACE APPEARANCE OF J AND P SPECIMENS AFTER SERIES 3 TEST (T_{max} 2050° F)

TABLE IV

OXIDATION-RIG EXPOSURES OF COATED COBALT ALLOY SPECIMENS ANALYZED BY METALLOGRAPHY AND ELECTRON MICROPROBE

Test Temperature °F (max.)*	Exposure Times (Hours)					
	X-40 Alloy			WI-52 Alloy		
	Coating			Coating		
	J	K	L	N	O	P
1845	1580	580	1480 (f)	100	1000 (f)	1580
1950	985 (f)	170 (f) 250 (f)	519 (f)	160 (f)	519 (f)	694 (f)
2050	250	--	--	--	--	220

f = Coating failure based on 20 mg weight loss
*= Imbedded thermocouple

The same metallographic failure criterion as used for the coatings on nickel-base alloys was adopted for the cobalt alloys to obtain coating life vs. temperature curves. Failure of the coating and noticeable substrate attack occurred over a much more localized region (temperature range) than with the nickel-base alloys. This fact can be related to the phase equilibria. The binary Co-Al system (Fig. 63) has no phase of intermediate aluminum level between βCoAl and αCo, analogous to the γ' in the Ni-Al system. (For the Ni-Al system, superior oxidation resistance was afforded by the γ' phase than the matrix composition.) At 1800° F, βCoAl containing 20 weight percent Al is in equilibrium with αCo containing only 5 weight percent Al. Thus, when the MAl phase in the coating has been consumed, rapid attack of the matrix occurs. Figure 64 shows a continuous sequence of microphotographs along an airfoil cross section moving toward the trailing edge and illustrates coating failure and substrate attack on X-40 alloy. The distance between the first observable discontinuity in the MAl layer (coating failure) and extensive substrate attack is less than 0.020 inch. An $M_{23}C_6$ interface layer was identified which apparently had good oxidation resistance. Coating failure on WI-52 alloy occurred in a similar manner, but the presence of MC carbides having poor oxidation resistance resulted in rapid interface attack and spalling once the MAl oxygen diffusion barrier was penetrated. In general, the coatings applied to the cobalt-base alloys were significantly thinner than those on the nickel-base alloys.

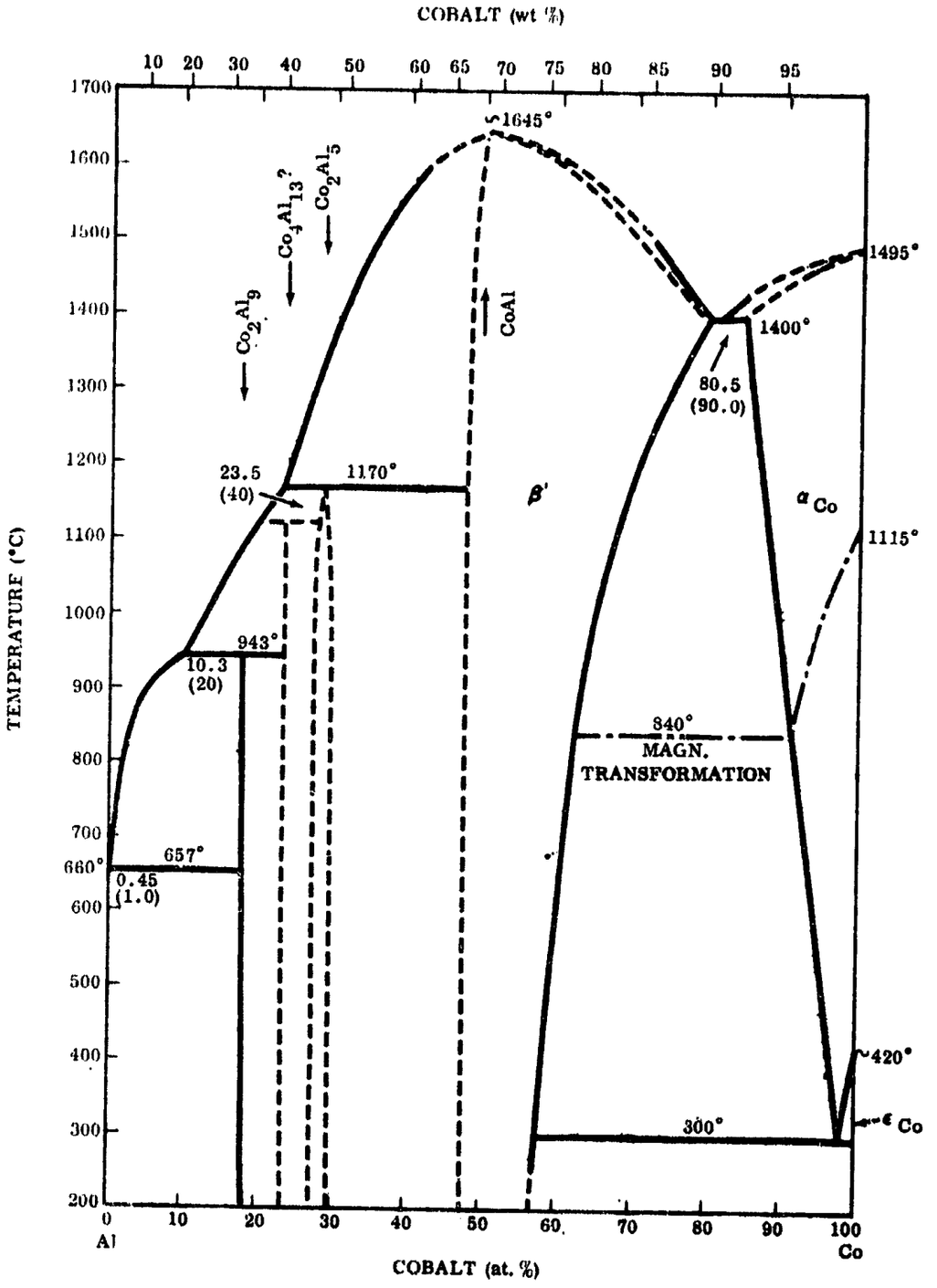

FIGURE 63. COBALT-ALUMINUM SYSTEM

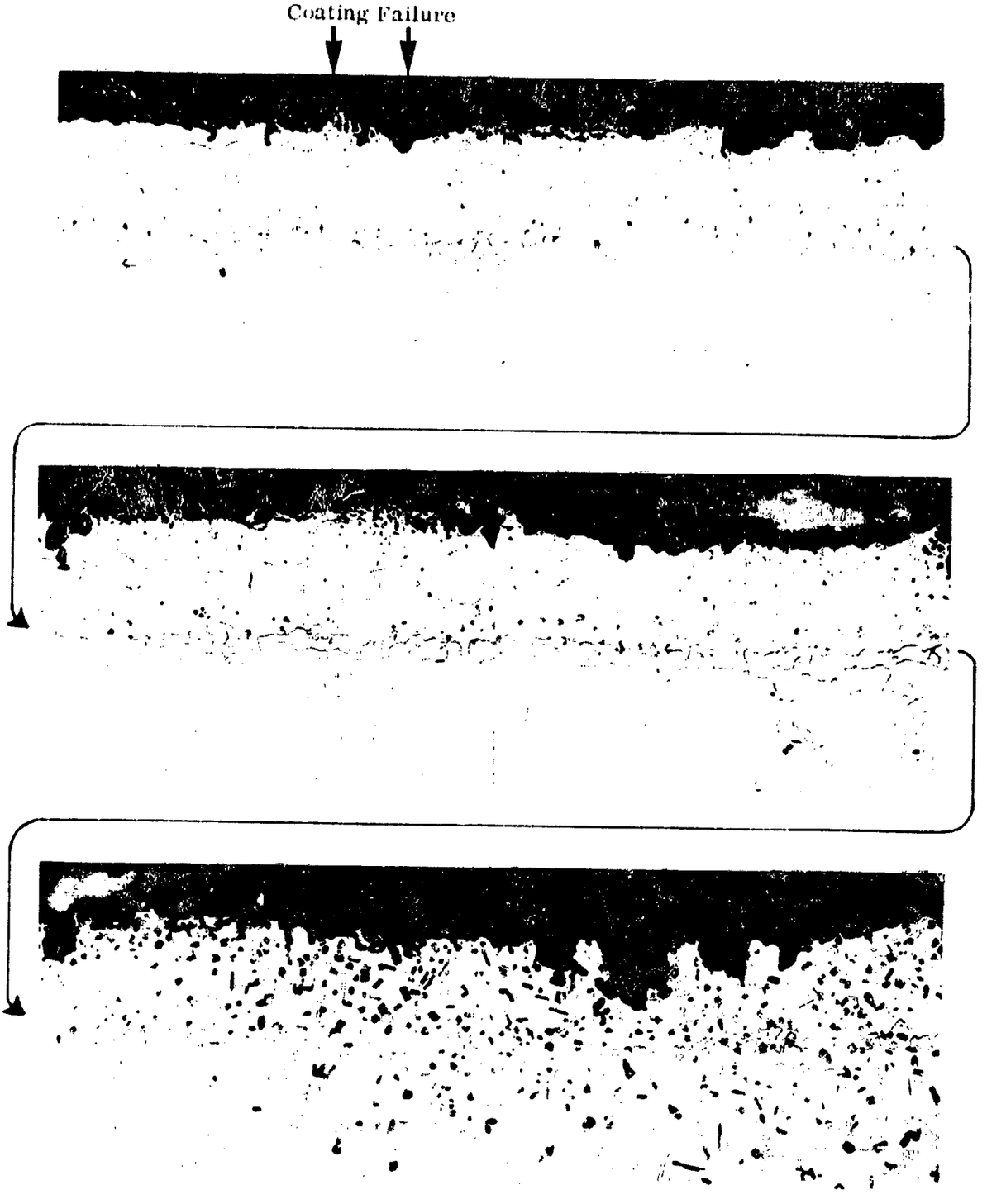

Magnification: 750X (reduced 10%) Etchant: Oxalic Acid-Electrolytic

FIGURE 64. REPRESENTATIVE COATING DEGRADATION OF COBALT-BASE ALLOYS
Note: Total Length of Blade Covered by These Photomicrographs Equivalent to 0.027 Inch (X-40 Alloy).

J Coating on X-40 Alloy

It was shown in Reference 1 that the J coating was the most uniform coating on X-40 alloy in terms of thickness and structure and was also the best performer in the high-temperature 100-hour tests. In this series of tests, the J coating was confirmed as the best performer on X-40 alloy.

Figures 65 to 67 show leading and trailing edge sections of specimens from Series 1, 2 and 3 tests. The coating had been consumed and substrate attack initiated after 1580 hours at 1845° F (Series 1 test). Thermogravimetric data (Sec. 4.1) did not indicate failure after this exposure based on an arbitrary weight loss criterion. Severe substrate attack had occurred at the trailing edge of Series 2 test specimen (Fig. 66) after an exposure of 985 hours at 1950° F. Above about 1800° F, coating failure was followed by rapid substrate oxidation. The Series 3 test also showed fairly extensive substrate attack at the trailing edge (Fig. 67), but failure was not indicated by the thermogravimetric data.

The microprobe data for specimen J28 are presented in Figure 68. The majority of the microprobe analyses were performed at the same location on the blade cross section, i.e., midway between leading and trailing edges on the concave side. The temperature corresponding to the location on specimen J28 was 1740°F and, as shown in Figure 68, the coating was still providing full protection to the substrate after the 1580 hours exposure, having lost only about 20 percent of its original thickness. The analysis in the oxide (Point 1) showed the presence of appreciable amounts of both aluminum and cobalt, indicating the presence of both Al_2O_3 and Co_3O_4 spinel, which was determined by surface X-ray diffraction studies on the 100-hour test specimens (Ref. 1). The aluminum level in the βMAl (Points 2 and 3) was about 22.6 weight percent (37 atomic percent) which, on the binary Co-Al diagram at 1700°F, would be just inside the β phase field. At lower temperatures the composition corresponded to the $\alpha + \beta$ two-phase region and, therefore, β of this composition is metastable. The data indicated, therefore, that the aluminum level was depleted almost to the point where the non-protective αCo would be formed within the coating (in addition to the very thin layer at the surface). Figure A-6 in Appendix A shows the probe data for specimen J44 (Series 2 test). After 994 hours at 1785°F the aluminum level in the βMAl was shown to be about 30 weight percent (48 atomic percent). The equilibrium solubility of chromium at this temperature in the βMAl was indicated to be about 8.0 weight percent.

Probe area 4 in Figure 68 was in the continuous chromium-rich interface phase which formed with all of the coatings on X-40 alloy. This phase was frequently noted to be continuous with the large $M_{23}C_6$ carbides in the matrix. (See Fig. A-6 in Appendix A.) Assuming the Co and Al values to be mostly background interference, the analysis of Point 4, 69.2Cr, 15.5W, 10.0Co, 2.0Al, 2.0Ni is in agreement with a Cr_{21} (Mo, W)$_2C_6$ composition which, in the absence of Mo, would be 71Cr, 24W, 5C. Additionally, qualitative scans for carbon and chromium indicated that the matrix $M_{23}C_6$ phase and the interface phase were identical. Because of low refractory metal

Leading Edge

Trailing Edge

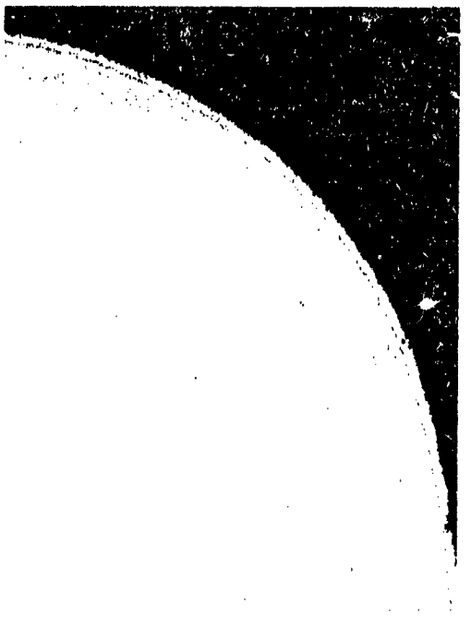

Specimen J28

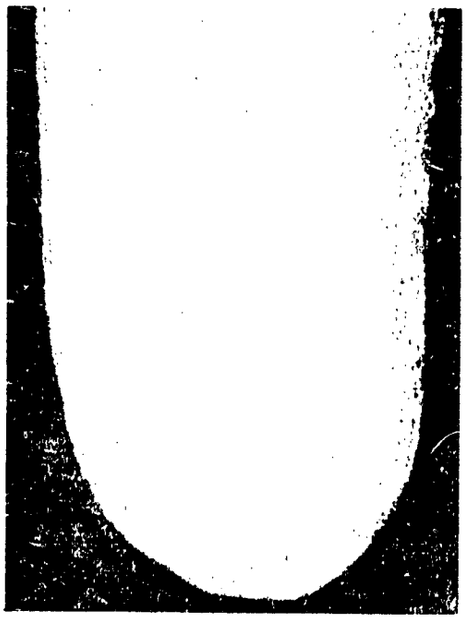

Local Temperature: 1625° F

Local Temperature: 1845° F

FIGURE 65. J COATING ON X-40 ALLOY AFTER 1580 HOURS; Series 1 Test

Etchant: Oxalic Acid-Electrolytic Magnification: 40X

Leading Edge

Trailing Edge

Specimen J44

Local Temperature: 1725° F

Local Temperature: 1950° F

FIGURE 66. J COATING ON X-40 ALLOY AFTER 985 HOURS; Series 2 Test

Leading Edge

Local Temperature: 1740° F

Specimen J21

Etchant: Oxalic Acid-Electrolytic

Magnification: 40X

Trailing Edge

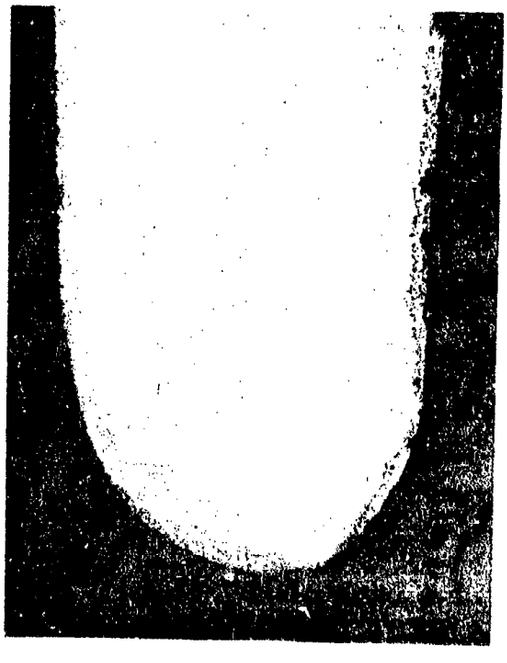

Local Temperature: 2050° F

FIGURE 67. COATING J AFTER 250 HOURS EXPOSURE IN SERIES 3 TEST

Specimen No. J28

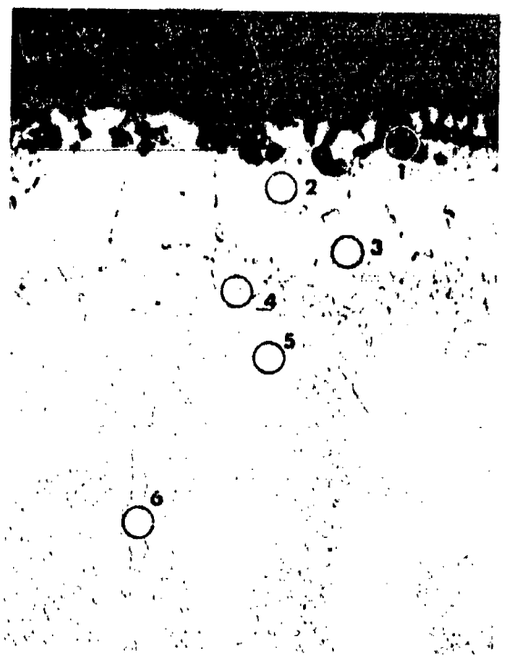

Test No. 36

Etchant: Oxalic Acid-Electrolytic

Magnification: 750X

Local Temperature: 1740°F

	Composition (wt %)						
	Al	Co	Cr	Ni	Si	W	Total
1	30.00	35.5	9.3	12.5	0.40	2.0	89.7
2	22.10	54.6	7.9	14.4	0.63	2.0	101.6
3	22.30	53.7	8.0	14.6	0.60	2.1	101.3
4	2.10	10.2	69.2	2.1	0.27	15.5	99.4
5	1.50	60.8	24.0	8.7	1.00	6.3	102.3
6	0.43	55.4	29.8	7.1	0.95	7.0	100.7
℄ 7	0.25	57.7	26.0	11.3	0.83	7.0	103.1

FIGURE 68. ELECTRON MICROPROBE ANALYSIS OF J COATING ON X-40 ALLOY AFTER 1580 HOURS; Series 1 Test (T_{max} 1845° F)

content, only the $M_{23}C_6$ carbide is formed in X-40 to any appreciable extent. In the as-coated condition, Cr_2Al was identified as a dispersed phase within the coating but, as shown in the short term tests, this phase was not stable during thermal exposures. Apparently the aluminum entered the βMAl and the chromium migrated to the $M_{23}C_6$ interface phase. From the current work, the presence of the interface carbide is believed to be a significant factor in the performance of coatings on cobalt alloys. Probe location 5 showed very low aluminum level in the substrate immediately below the coating, which is in contrast to the observations on nickel-base alloys where interdiffusion across the coating-matrix interface was apparently a significant factor in coating degradation. The data suggest that the $M_{23}C_6$ diffusion barrier restricted coating degradation due to aluminum depletion by oxide formation and spalling, which would explain why the relatively thin coatings on cobalt alloys performed relatively well compared to the much thicker coatings on nickel-base alloys. Analysis of Point 6 apparently yielded an average value of the matrix and carbide. Points 5 and 7 (Fig. A-6, App. A) provide more realistic values for the carbide phase.

K Coating on X-40 Alloy

The K coating was subject to significant thickness variations from specimen-to-specimen and from side-to-side (concave-to-convex) on individual specimens. This thickness variation was reflected in the oxidation-erosion tests where considerable variation in performance between pairs of specimens was noted. Table XV of Reference 1* reports a 2:1 thickness variation between convex and concave sides of as-coated specimens.

Figure 69 shows the leading and trailing edge locations of the specimen from the Series 1 test after 580 hours. This specimen had not failed according to the thermogravimetric data. The photomicrographs show the retention of a continuous aluminide layer at the hottest location; thus failure, as defined by the metallographic criterion, had also not occurred. The coating thickness variation is evident from the low magnification photograph of the trailing edge. Except for the absence of a dispersed Cr_2Al phase at the leading edge location, the coating was virtually unaltered (structurally) from the as-coated condition. At the trailing edge section, three phases were evident: an outer αCo layer, a continuous βMAl layer and a continuous $M_{23}C_6$ interface layer. As judged from the growth of the α layer, the coating was close to failure.

The structure at the center line and corresponding microprobe analyses are shown in Figure 70. Except for a thinner interface carbide zone, the structure and composition were similar to the J coating on X-40 following oxidation-erosion rig tests.

* Note: In Table XV of Reference 1 the reported thickness values for convex and concave sides should be reversed; i.e., the concave side had the thickest coating.

Leading Edge

Trailing Edge

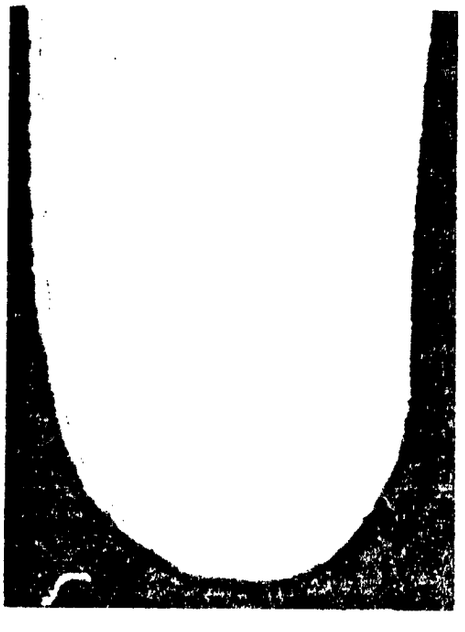

Specimen K32

Magnification:
40X

Local Temperature: 1625°F

Local Temperature: 1845°F

Etchant: Oxalic Acid-Electrolytic

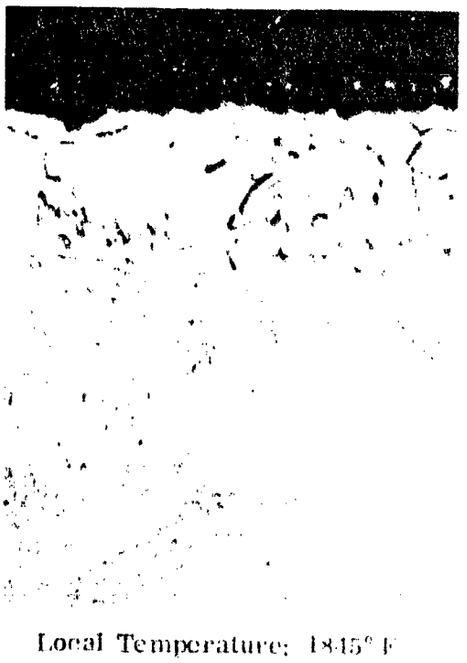

Specimen K32

Magnification:
750X

Local Temperature: 1625° F

Local Temperature: 1845° F

FIGURE 69. MICROSTRUCTURE AFTER 580 HOURS IN SERIES I TEST; K Coating on X-40 Alloy

Specimen No. K32

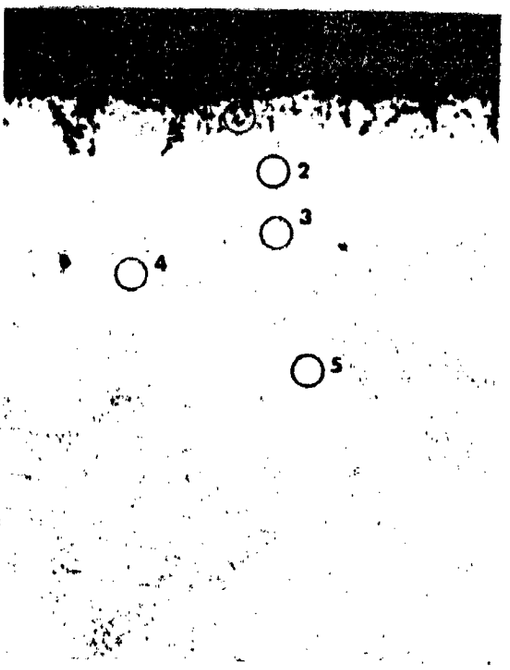

Test No. 36

Etchant: Oxalic Acid-Electrolytic

Magnification: 750X

Local Temperature: 1740°F

	Composition (wt %)						
	Al	Co	Cr	Ni	Si	W	Total
1	32.00	35.5	9.7	8.4	0.72	0 19	86.5
2	25.90	53.2	9.1	11.1	0.80	1.80	101.9
3	5.50	21.2	55.7	2.9	0.60	10.80	96.7
4	0.46	58.6	29.3	8.1	1.00	4.70	102.2
5	-	56.3	26.4	8.9	1.00	4.60	97.2
6	0.30	56.7	28.6	8.1	0.62	4.90	99.2

FIGURE 70. ELECTRON MICROPROBE ANALYSIS OF K COATING ON X-40 ALLOY AFTER 580 HOURS; Series I Test (T_{max} 1845° F)

The slightly higher aluminum level in the MAl phase of the K coating was in accord with the shorter exposure.

L Coating on X-40 Alloy

The L coating was shown (Ref. 1) to have the lowest average thickness of the coatings applied to X-40 alloy but structurally was very similar to the J and K coatings. No significant structural or chemical differences having practical significance in terms of coating life were identified in the present work.

The appearance of leading and trailing edge sections and the coating appearance at the failure location of specimen L48 (1480-hour exposure, Series 1 test) are shown in Figure 71. At the trailing edge concave side, complete coating consumption and extensive substrate attack had occurred. The temperature corresponding to the 1480-hour failure location was about 1800°F on the concave side (about 0.25 inch from the trailing edge tip).

Microprobe analysis for the Series 2 test specimen exposed for 520 hours is shown in Figure 72. The temperature during test at this centerline location was 1785°F. A high aluminum value (.50 weight percent was determined in the aluminide phase with a correspondingly lower chromium level (5 weight percent). The nickel level was about the same as found in J and K coatings; (i.e., equivalent to the substrate level). The interface phase (Point 3) had the same composition and was continuous with the massive $M_{23}C_6$ phase in the substrate (Point 4), and was therefore identified as the carbide. A very low Al level in the substrate was shown by Points 5 and 6. The silicon values are suspect because of anomalously high readings in the substrate.

N Coating on WI-52

The major carbide phases in WI-52 have been identified as the script type MC and the $M_6C + M_{23}C_6$ eutectic. The high refractory metal content MC carbide (Cb, W)C did not go into solution within the βMAl phase as readily as the $M_{23}C_6$ carbide in coatings on X-40 alloy and was present in the diffusion zone in all of the coatings on WI-52. This phase was recently shown (Ref. 8) to oxidize very rapidly in exposed, uncoated WI-52, forming $CoCb_2O_6$.

The as-received N coating was intermediate in thickness between the O and P coatings but had a low aluminum content in the outer layer which may have been an indication of decreasing Al activity during the coating process. The N coating was shown to be the worst performer on WI-52 alloy and very little testing was carried out on this coating in the present evaluation.

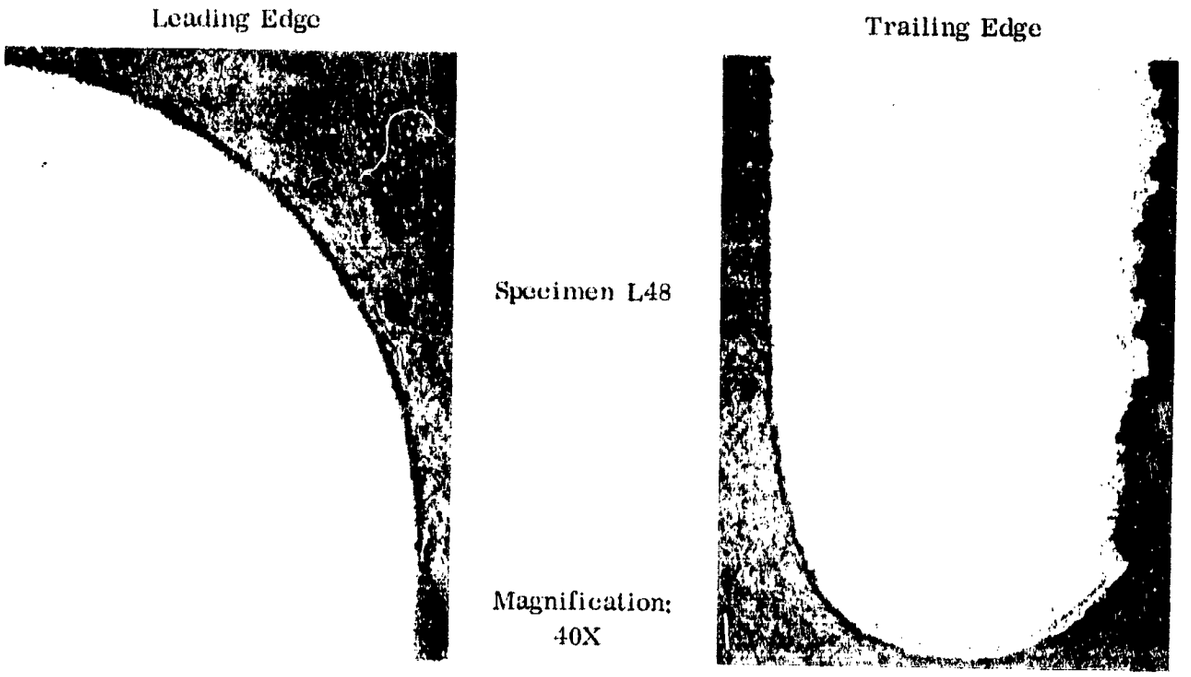

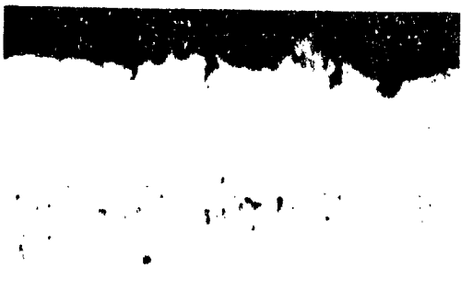

Magnification: 750X

Local Temperature: 1800° F

FIGURE 71. MICROSTRUCTURE AFTER 1480 HOURS IN SERIES I TEST; L-Coating on X-40 Alloy

Specimen No. L43

Test No. 33
Series 2 Test
Exposure: 520 Hours

Etchant: Oxalic Acid-Electrolytic

Magnification: 750X

Local Temperature: 1785° F

	Composition (wt %)						
	Al	Co	Cr	Ni	Si	W	Total
1	31.9	53.6	5.3	12.3	1.60	2.3	107.0
2	36.0	54.8	5.5	12.7	1.60	2.1	112.7
3	1.9	15.9	58.4	5.8	-	12.9	94.9
4	1.1	18.2	56.2	2.1	0.24	13.7	91.5
5	3.3	60.7	19.6	9.7	2.40	6.9	102.6
6	1.7	58.6	21.1	10.9	2.10	7.3	101.7
7	0.9	59.3	22.5	11.1	1.50	7.7	103.0

FIGURE 72. ELECTRON MICROPROBE ANALYSIS OF L COATING ON X-40 ALLOY AFTER 520 HOURS; Series 2 Test (T_{max} 1950° F)

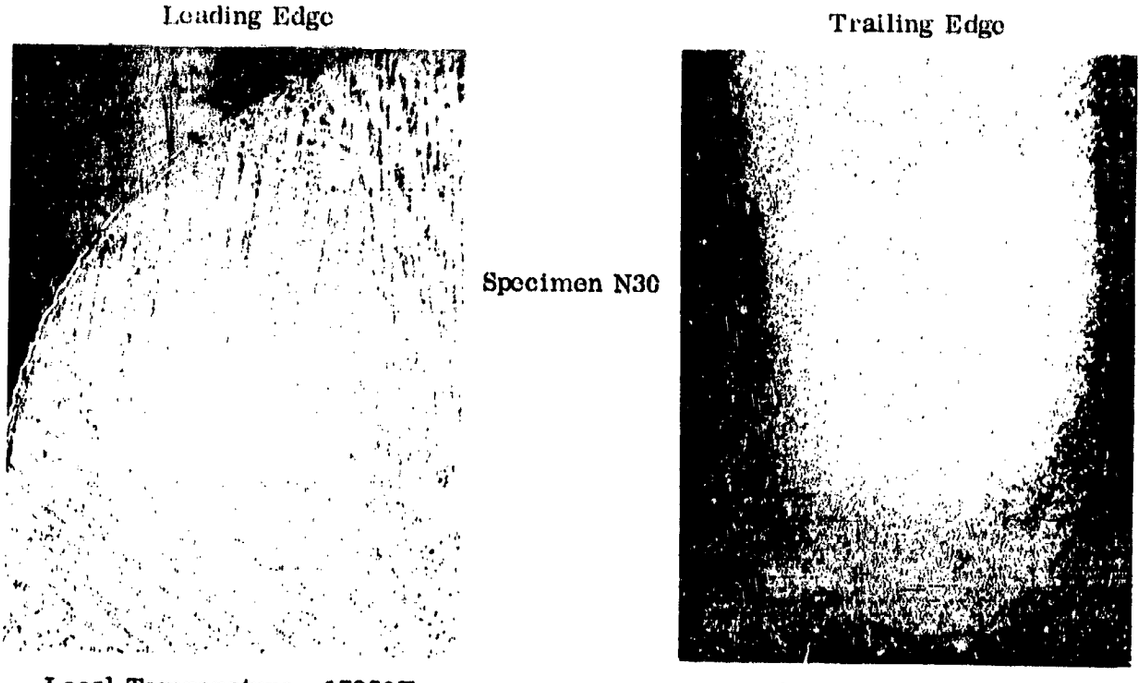

Magnification: 40X

Etchant: Oxalic Acid-Electrolytic

FIGURE 73. N COATING ON WI-52 ALLOY AFTER 160 HOURS EXPOSURE IN SERIES 2 TEST

Figure 73 shows leading and trailing edge sections (1725 and 1950°F locations) of N30 after 160 hours exposure in the Series 2 test. Failure of the coating and extensive substrate attack had occurred at the trailing edge.

Microprobe data and high magnification metallography for the same specimen are shown in Figure 74. More than 50 percent of the original βMAl was consumed at this centerline location (1785°F) so that only a thin layer (0.0005 inch) remained. The outer layer (Point 1) was α solid solution, containing only about 5 weight percent Al, with large oxide globules. A high aluminum level was obtained for the remaining MAl layer. Immediately below the coating (Points 3 and 4) was a complex region consisting of different carbide phases and internal oxidation products in the α matrix. The stability of the microprobe beam was a problem on poorly conducting phases. Point 6 evidently produced emissions from the mixed carbide phase and the matrix. Internal oxidation of the carbide phases at the coating/metal interface was responsible for coating spalling once the βMAl layer was penetrated. Minor internal oxidation below the coating was evident in all of the as-coated WI-52 specimens.

Specimen No. N30

Test No. 35

Etchant: Oxalic Acid-Electrolytic

Magnification: 750X

Local Temperature: 1785°F

	Composition (wt %)					
	Al	Co	Cr	Fe	W	Total
1	4.80	68.2	25.9	2.0	1.8	102.7
2	32.70	69.4	14.6	1.5	5.5	123.7
3	9.90	71.2	26.7	2.0	8.9	118.7
4	4.00	19.3	62.3	-	26.4	112.0
5	3.20	71.5	30.0	1.9	8.4	115.0
6	1.20	35.3	55.4	-	30.0	121.9
7	0.96	62.2	27.7	1.3	13.4	105.6

FIGURE 74. ELECTRON MICROPROBE ANALYSIS OF N COATING ON WI-52 ALLOY AFTER 160 HOURS; Series 2 Test (T_{max} 1950° F)

O Coating on WI-52 Alloy

The O coating was the thinnest coating applied to WI-52. A high aluminum level, however, was determined in the as-coated condition and the aluminum level was highest in the outer layers in contrast to the N coating, which showed a decreasing aluminum gradient toward the surface.

Specimen O42 survived 1000 hours in the Series 1 test before failure occurred as indicated by weight loss data. The leading and trailing edge sections (local temperatures were 1625°F and 1845°F) are shown in Figure 75. Substantial substrate attack had occurred at the trailing edge but the coating was still intact at the leading edge.

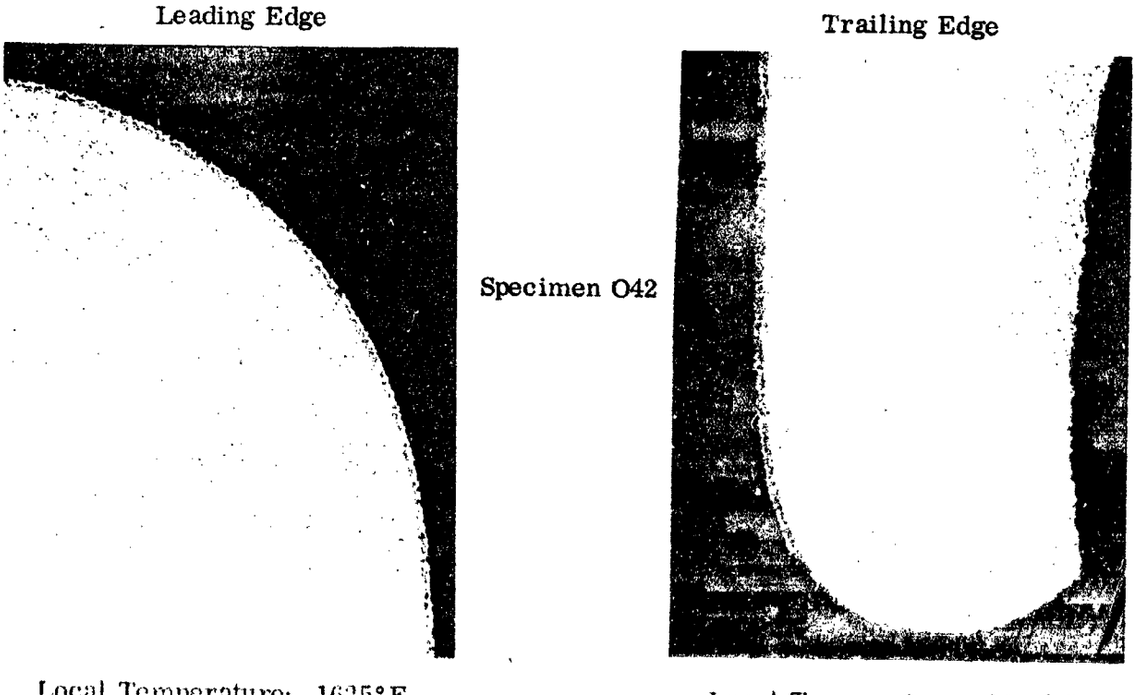

Magnification: 40X

Etchant: Oxalic Acid-Electrolytic

FIGURE 75. O COATING ON WI-52 ALLOY AFTER 1000 HOURS EXPOSURE IN SERIES 1 TEST

The structure at the center location (1740°F) and corresponding microprobe analysis are shown in Figure 76. The βMAl was still present as a continuous layer at this location but the determined Al composition (Points 1 and 2) was low (about 20 weight percent). In the binary phase diagram this aluminum composition is just on the $\beta/\alpha+\beta$

boundary at 1740°F. The coating failure location was defined at a region very close to that shown in Figure 76. Point 3 was in an area of carbides and internal oxides. The oxides exhibited a fluorescence under the electron beam, characteristic of Al_2O_3. Analyses 4 and 5 were typical substrate compositions. Iron was found to be distributed uniformly throughout the coating and substrate.

P Coating on WI-52

The P coating was found in previous work (Ref. 1) to be the best overall performer on the WI-52 alloy. It was shown to be the thickest and most uniform coating on WI-52 in terms of structure and aluminum distribution. The superior performance of this coating on WI-52 was confirmed in these longer term tests.

Figure 77 shows the low magnification photomicrographs of specimens tested in the Series 1 and Series 3 tests. Neither specimen had failed according to the thermogravimetric data and no gross substrate attack could be observed at the trailing edge locations after 1580 hours at 1845° F and after 220 hours at 2050° F. This coating was the only one on cobalt-base alloys which offered more than 100 hours protection at temperatures above 2000° F based on the Series 3 tests and is in conflict with the data presented in Volume I (Ref. 1) which showed coating J (X-40 alloy) to have superior oxidation resistance at 2000° F and above. Differences cannot be positively accounted for in this investigation, but microstructures in Figures 67 and 77 definitely support the superior performance of the P coating over the J coating.

More detailed metallography of Specimen P49 (1580 hours, Series 1 test) at the trailing edge is shown in Figure 78. The coating had failed at a location corresponding to an exposure temperature of 1845° F. (Fig. 78A) and oxidation of the MC carbides and α substrate at the interface was evident. Figure 78B was at a slightly cooler location about 1/8 inch along the blade from 78A. Although the coating was fully adequate for continued protection at this location, significant internal oxidation at the interface had occurred due to oxygen penetration from the failed region.

The structure and microprobe analysis of the same specimen at the centerline 1740° F location is shown in Figure 79. Virtually no change in thickness from the as-coated condition was found at this location, and the dendritic or script-type MC carbides in the lower half of the coating were also apparently unchanged. The major coating phase (Points 1 and 2) was essentially CoAl containing 7 to 8 weight percent chromium. Area 1 in atomic percent, yielded 41.2Al, 48.0Co, 6.5Cr, 0.8W, 1.3Fe and 2.3Si. The chromium-rich phase (Point 3) was similar in appearance to the $M_{23}C_6$ phase and Point 4 was a region of MC carbides, βMAl and chromium-rich phase. Points 5 and 6 were very similar to the centerline matrix value (Point 7) except for 1.7 weight percent Al in Point 5 at the coating/matrix interface. Again, surprisingly low aluminum values were obtained just below the coating. Iron and silicon appeared to be present to equivalent amounts in the MAl and WI-52 matrix.

Specimen No. O42

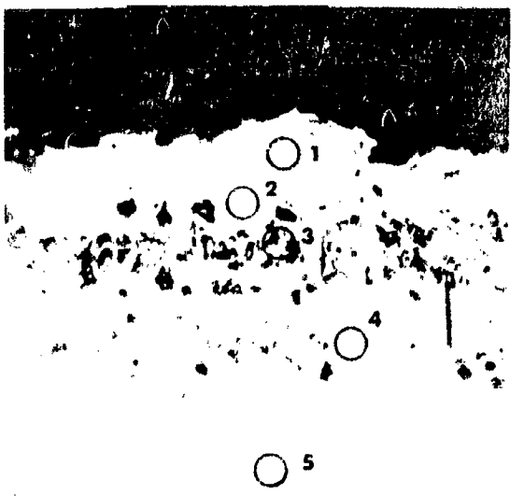

Test No. 36

Etchant: Oxalic Acid-Electrolytic

Magnification: 750X

Local Temperature: 1740°F

	Composition (wt %)						
	Al	Co	Cr	Fe	Si	W	Total
1	20.10	64.0	10.0	2.4	1.20	4.65	102.4
2	19.70	63.0	10.0	2.4	0.99	5.00	101.1
3	20.30	25.9	27.3	0.4	0.49	15.30	89.7
4	2.20	64.7	22.5	2.3	0.90	10.90	103.5
5	0.77	63.0	24.0	2.3	0.94	11.40	103.3
℄ 6	0.11	66.1	25.4	2.4	0.95	8.40	103.4

FIGURE 76. ELECTRON MICROPROBE ANALYSIS OF O COATING ON WI-52 ALLOY AFTER 1000 HOURS; Series 1 Test (T_{max} 1845° F)

Leading Edge

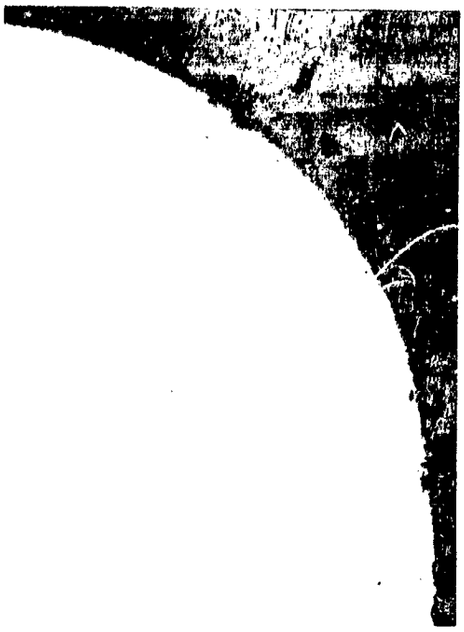

Local Temperature: 1625°F

Specimen P49

1580 Hours Exposure

Series 1 Test

Magnification: 40X

Trailing Edge

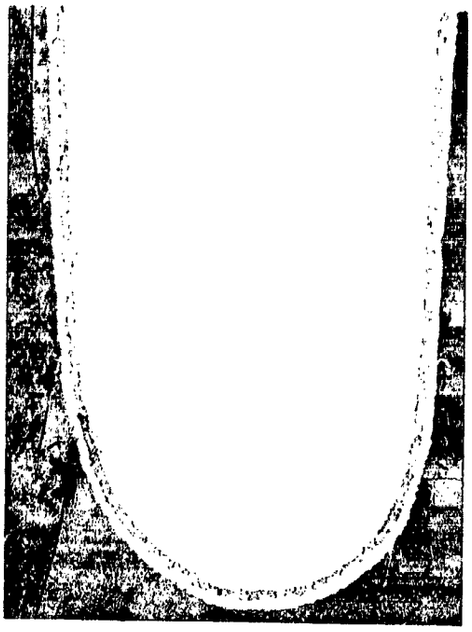

Local Temperature: 1845°F

Etchant: Oxalic Acid-Electrolytic

Local Temperature: 1740°F

Specimen P50

220 Hours Exposure

Series 3 Test

Magnification: 40X

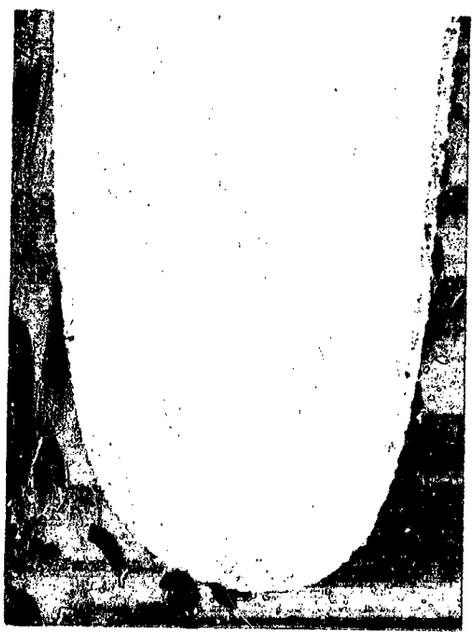

Local Temperature: 2050°F

FIGURE 77. P COATING ON WI-52 AFTER OXIDATION-EROSION RIG EXPOSURES

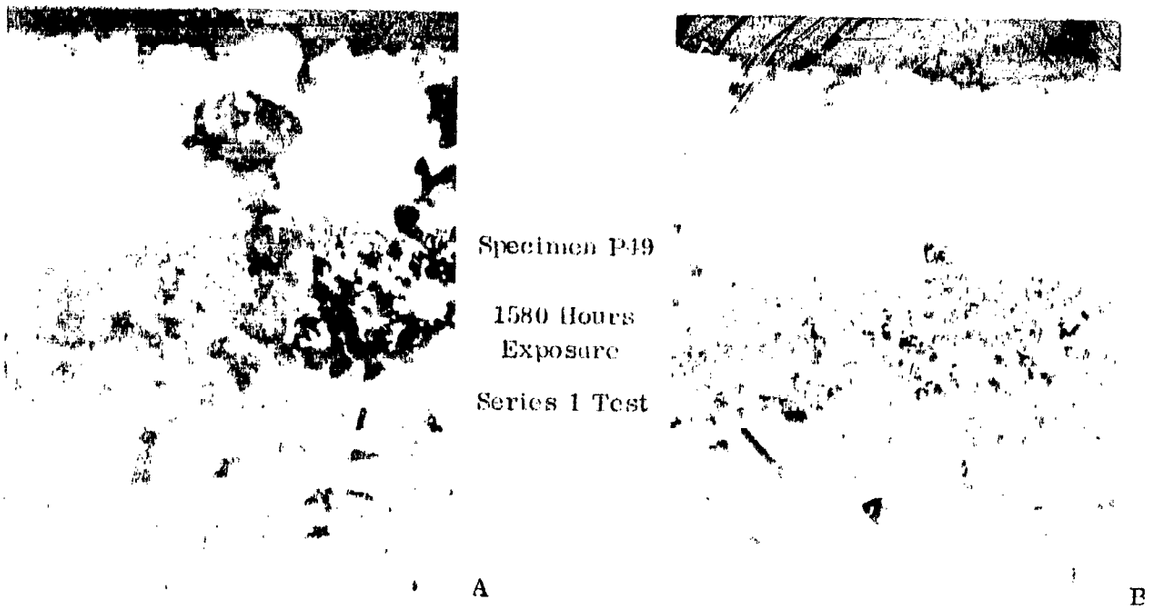

Local Temperature: 1845°F Local Temperature: 1825°F

Magnification: 750X

Etchant: Oxalic Acid-Electrolytic

FIGURE 78. COATING FAILURE AND INTERFACE OXIDATION ON P-COATED WI-52 (T_{max} 1845° F)

4.2.3 Comparison of Cobalt-Base Alloy Coatings (see page 66 for Nickel-Base Alloys)

The known temperature gradients along the airfoils during the three series of tests were used to correlate coating failure (defined metallographically, e.g., Fig. 64 and 78) with exposure temperature and time. Figure 80 shows the available data on a temperature/log time plot for X-40 and WI-52 alloys.

The J coating had the highest temperature capability, over the entire temperature range, of the three coatings on X-40 alloy. The extrapolated temperature for 3000-hour life was about 1800° F. Considerable scatter in the data points for the K coating was no doubt related to the considerable thickness variations. On WI-52 alloy, the P coating showed distinctly better performance than N or O. A 3000-hour life at 1800° F was indicated, which compared to the J coating life on X-40, but a higher temperature advantage (2000° F) in the short-term 100-hour tests was observed. On an overall basis the P coating was the best coating on cobalt-base alloys. (See qualification, paragraph 3, page 98.)

Thickness of the aluminide layer appeared to be the most significant parameter related to coating life for the cobalt-base alloy coatings. Compositional differences

Specimen No. P49

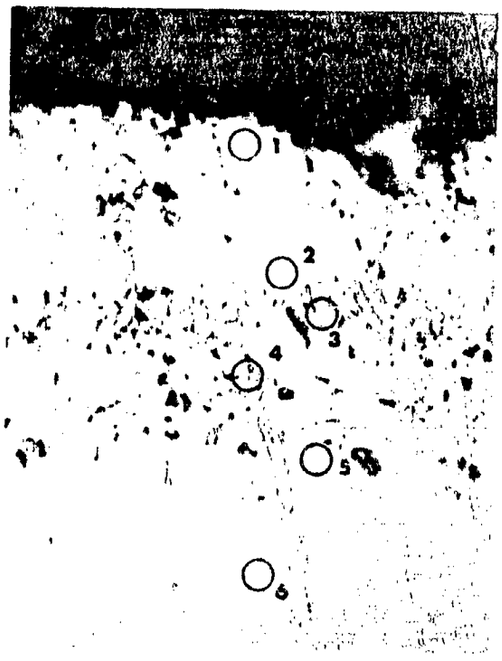

Test No. 36

Etchant: Oxalic Acid-Electrolytic

Magnification: 750X

Local Temperature: 1740°F

	Composition (wt %)						
	Al	Co	Cr	Fe	Si	W	Total
1	26.40	67.0	8.0	1.70	1.50	3.5	108.1
2	26.40	68.9	7.2	1.60	1.50	2.4	108.0
3	3.30	17.5	61.6	0.39	0.20	14.4	97.7
4	9.90	28.5	23.2	0.20	0.96	15.5	78.3
5	1.70	68.6	24.6	2.40	1.60	5.9	104.8
6	0.65	67.0	25.7	2.00	1.40	7.6	104.4
7	0.17	59.6	25.7	2.00	0.91	7.4	95.8

FIGURE 79. ELECTRON MICROPROBE ANALYSIS OF P COATING ON WI-52 ALLOY AFTER 1580 HOURS; Series 1 Test (T_{max} 1845° F)

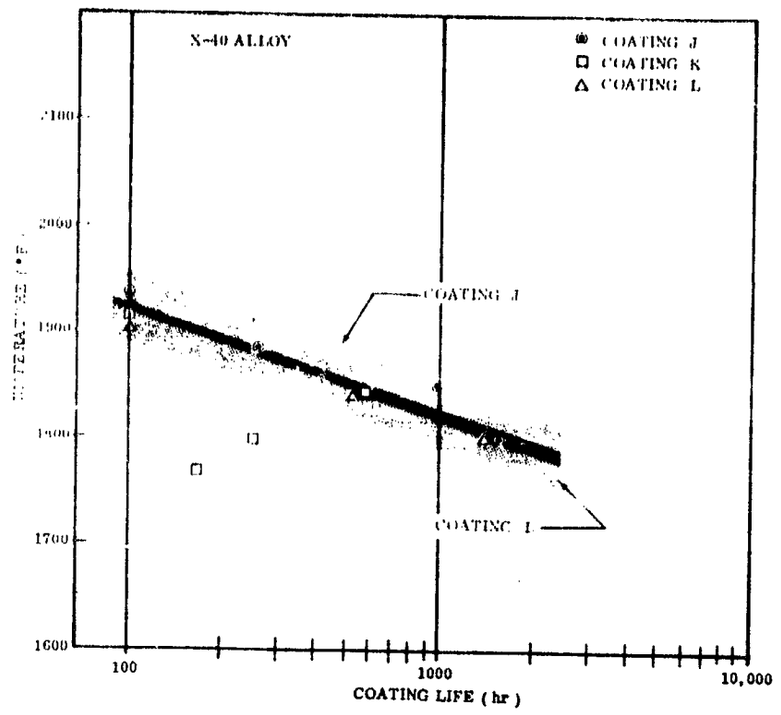

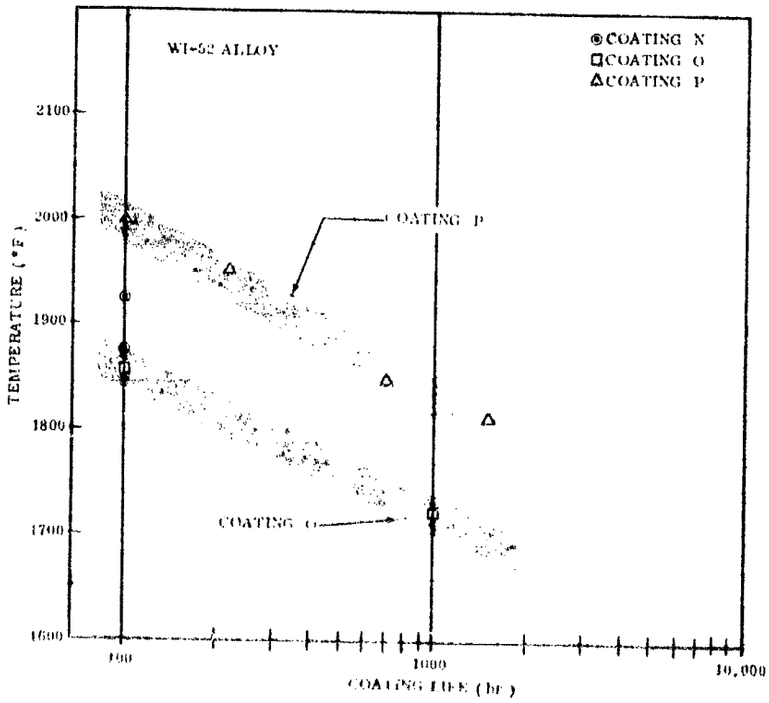

FIGURE 80. LIFE OF COATINGS ON COBALT-BASE ALLOYS

between the coatings were not found to be very great and the effects were largely overshadowed by coating thickness variations. There were, however, interesting structural differences between the coatings on X-40 and WI-52 alloys which were related to performance.

The X-40 alloy is slightly higher in chromium and carbon than the WI-52 alloy and does not contain MC carbide-forming elements such as columbium and tantalum. The major carbide phase in X-40 is $M_{23}C_6$. During coating deposition, $M_{23}C_6$ from the matrix was dissolved in the MAl phase and formed Cr_2Al as dispersed particles. During subsequent thermal exposures the chromium was rejected from the βMAl layer forming a continuous $M_{23}C_6$ phase at the coating/matrix interface. This interface zone was very stable and it is hypothesized that it acted as a diffusion barrier and prevented Al diffusion into the substrate alloy and Co diffusion into the coating. However, the equilibrium solubility of aluminum in a Co-Cr-W alloy is probably low so that the equilibrium concentration gradient would be small and the diffusivity of Al would be low.

The thickness of the interface zone was related directly to the thickness of the coating. Compared to the MC carbides in WI-52, the $M_{23}C_6$ phase had good oxidation resistance minimizing the contribution of oxidation along the interface to coating failure in coated X-40 specimens. In general, the coatings on X-40 contained fewer second phase particles within βMAl and were structurally more homogeneous.

The WI-52 alloy is more complex than X-40. Several carbide compositions and morphologies are normally present which could become part of the coating layer. The monocarbide (Cb, W)C was prevalent in the lower layers of the coatings on this alloy and did not go into solution after the longest test exposures. This phase formed interdendritically in the cast alloy and during the coating process the aluminide formed around it so that its original grain boundary location could be recognized relative to grain boundaries in the substrate. Minor internal oxidation occurred at the substrate alloy interface during the coating process. The recent data of Lowell (Ref. 8) showed that the grain boundary CbC was oxidized first during elevated temperature exposures of WI-52 in air, and the observed internal oxidation of as-coated WI-52 appeared to be related to this phase. It was found in the present work that rapid oxidation along the interface MC carbides occurred when the aluminide layer had failed, and thus contributed to accelerated spalling. Very low aluminum levels were invariably found in the substrate alloy and although a very thin layer of $M_{23}C_6$ was tentatively identified at the interface, it did not appear to be continuous. Therefore, the diffusion inward of aluminum was probably restricted by the low solubility in a Co-Cr-W solid solution rather than by a diffusion barrier mechanism.

Major differences between the coatings on the cobalt alloys were related to differences in the substrate alloy compositions. Variations which could be related to the coating processes were less apparent than with the coatings on nickel-base alloys.

For instance, the evaluations did not identify any duplex coating processes or unambiguously establish the presence of intentionally added elements in the coatings. A high aluminum level in the initial MAl phase was shown to be desirable (compare the performance of N and O coatings), as would be expected. The thick interface layers (15 to 20 μ m) noted on the J coating (X-40 alloy) and the P coating (WI-52 alloy) as-coated specimens (Ref. 1, Fig. 84 and 89) indicated that these coatings were applied at a sufficiently slow rate to permit significant diffusion of Co outward and Cr inward. A high-temperature process, with a moderately high aluminum activity is indicated, but which has a relatively low-deposition rate. Analyses on the P coating possibly indicated silicon additions, but the superior performance of this coating was apparently due largely to its thickness (Al reservoir).

Because of the brittle nature of aluminide coatings on cobalt alloys in the as-coated condition, it is difficult to produce coatings of thickness equivalent to those on nickel alloys and avoid spalling problems. Following thermal exposures, the coatings appeared to become considerably more ductile, indicating that initial supersaturation with elements from the substrate (Cr, C) may have been responsible for the as-coated cracking tendency.

It would be of considerable interest to conduct coating evaluation studies on one or two selected coatings applied to several different cobalt-base alloys in order to more clearly define the effects of substrate composition on coating thickness (or rate of formation), structure, and composition.

5
CONCLUSIONS

- Thicker coatings are more readily applied to nickel-base than cobalt-base alloys, but the life per 0.001 inch of coating is not significantly different between better coatings on the two alloy systems.

- Protection afforded the substrate above 2000° F was significantly longer for coated nickel-base than cobalt-base alloys. However, the test data when extrapolated out to 10,000 hours showed that the better coatings on X-40 (J and L) and on B1900 (F and H) are approximately equivalent, providing protection to approximately 1750 $\pm$ 50° F. Other coatings showing long-term protection, for example P on WI-52, B and C on IN-100, and G and H on B1900, indicated an extrapolated 10,000-hour operating temperature, 100° F lower, i.e., approximately 1700° F.

- Diffusion of aluminum into X-40 and WI-52 cobalt-base alloys was less pronounced than into IN-100 and B1900 nickel-base alloys, even though the concentration gradient $\frac{dc}{dx}$ was greater in the cobalt-base alloys. High concentrations of carbides and refractory metals rejected by the monoaluminides appeared to act as effective diffusion barriers for the diffusion of aluminum.

- High percentage chromium, aluminide coatings on nickel-base alloys (usually applied in two cycles), e.g., D on IN-100 and G on B1900, afforded longer protection above 2000° F than coatings low in chromium. However, because of hardness, spalling tendency and internal oxidation. life was less at lower temperatures compared to the better, low-chromium, aluminide coatings, e.g., C on IN-100 and F and H on B1900.

- Positive identification of additives to cobalt-base alloy coatings in addition to aluminum was not possible. The approximately 0.0005 inch thick $M_{23}C_6$ interface layer of the J coating on X-40 (Ref. 1, Fig. 78 and 84) indicated the possible application of chromium prior to aluminizing. But the high chromium content of X-40 alloy (25.5%) and low solubility of chromium in β-CoAl could be responsible for this interface layer. Very slow deposition of aluminum at high temperature may have produced the chromium-rich interface layer by rejection of chromium from the β-CoAl.

aluminide. The presence of this thick carbide layer must have contributed to the retention of the β-CoAl surface layer and the long life of the coating at intermediate temperatures, e.g., providing a 10,000-hour life at 1800° F.

- Coated X-40 specimens were less susceptible to intergranular and interface oxidation than coated WI-52 specimens. With X-40, the interface and intergranular carbides were primarily $M_{23}C_6$ which appeared to be quite oxidation resistant. The $M_{23}C_6$ carbides from the substrates were initially dissolved in the β-CoAl during coating formation. Following cyclic thermal exposures, an interface carbide layer was formed by rejection of chromium and carbon from the CoAl. The WI-52 alloy forms both $M_{23}C_6$ and CbC carbides. The latter carbide predominated and had extremely poor oxidation resistance. It was also essentially insoluble in the MAl coating. The CbC carbides were oxidized during both the coating process and testing.

- Within the β-NiAl or β-CoAl binary field the aluminum content should be as high as possible for maximum life at a given thickness, i.e., the aluminum reservoir should be large.

- For aluminide coatings on nickel-base alloys, coating life was directly related to thickness up to 0.004 inch. Above this thickness, excessive spalling could occur based on the limited test data with the D coating on IN-100.

- β-CoAl and β-NiAl coatings appeared to be saturated in chromium since during thermal exposures, chromium was rejected from the coatings until an equilibrium level was reached.

- The rejection of Cr, W, C, etc. from the β-CoAl coatings upon long-term exposure markedly decreased the sensitivity of the coating to delamination and cracking. β-NiAl coatings, probably because of the low chromium and carbon content of the nickel-base alloy substrates, were less sensitive to mechanical damage, as applied.

- Sigma phase or other TCP* phases appeared at the interface of all coated nickel-base alloys upon extended high-temperature exposure. These phases did not appear to promote thermal fatigue cracking. The influence of these phases on mechanical properties was not determined.

---

*Topologically close-packed phases

- Additives of elements other than aluminum to coatings was observed on the nickel-base alloys. Chromium and silicon were the most common. Chromium, as previously noted, improved performance above 2000° F but not at lower temperatures. Silicon in the C and F coatings improved the life as compared to a simple aluminide, probably by decreasing the spalling of aluminum oxide. A titanium oxide wash-coat was probably applied before aluminum application in the B coating. This very thin oxide layer was retained throughout oxidation testing. Interdiffusion with the substrate was not notably decreased nor performance of the coating improved by the presence of the oxide layer.

- The presence of a high chromium content promoted equilibrium between β-NiAl and γ instead of β-NiAl and γ' above a temperature of about 1850° F.

- Two properties not covered in this volume, but reported in detail in Volume I, are the change in surface roughness and specimen warpage as a result of the coating process. Conclusions in these two areas are noted below:

    - Surface roughness was found to be increased slightly for five of the six coatings on cobalt-base alloys and four of the six coatings on nickel-base alloys (see Table VI, Ref. 1). No correlation was found to associate surface roughness with coating spallation or other performance effects.

    - Dimensional control was measured using a contoured transcriber before and after coating the standard paddle specimens. None of the 12 coating combinations exhibited evidence of significant distortion. Of 641 paddles measured, the maximum bow after coating was 0.005 inch (0.00012 meter) and the maximum twist was zero degrees, 12 minutes of arc (0.0035 r).

REFERENCES

1. Moore, V. S., Brentnall, W. D., and Stetson, A. R., "Evaluation of Coatings for Cobalt- and Nickel-Base Superalloys", Contract NAS3-9401, Vol. I, NASA CR-72359 (January 1969).

2. Guard, R. W., and Smith, E. A., "Constitution of Nickel-Base Ternary Alloys", J. Inst. Metals, Vol. 88 (1959-1960), pp. 88, 369.

3. Kaufman, M., "Hot Corrosion Reactions in Nickel, Cobalt and Nickel-Aluminide-Base Alloys", Trans. Quarterly ASM, Vol. 62, No. 3 (1969), pp. 590-605.

4. Taylor, A., and Floyd, R. W., "The Constitution of Nickel-Rich Alloys of the Nickel-Chromium-Aluminum System", J. Inst. Metals, Vol. 81 (1952-1953), pp. 451-464.

5. Redden, T. K., "Ni-Al Coating-Base Metal Interactions in Several Nickel-Base Alloys", Trans. of the Metallurgical Society of AIME, Vol. 242 (August 1968), pp. 1695-1702.

6. Collins, H. E., "Relative Long-Time Stability of Carbide and Intermetallic Phases in Nickel-Base Superalloys", Trans. Quarterly, ASM Vol. 62, No. 1 (March 1969), pp. 82-104.

7. Havalda, A., "Influence of Tungsten on the γ' to η Transformation and Carbide Reactions in Nickel-Base Superalloys", Trans. Quarterly, ASM Vol. 62 (1969) pp. 581-587.

8. Lowell, C. E., "Oxidation of WI-52", Aerospace Structural Materials Conference, NASA-Lewis Research Center (November 18, 1969).

9. Colby, J.W., "Magic - A Computer Program for Quantitative Electron Microprobe Analysis", Bell Telephone Laboratories, Inc., Allentown, Pa.

30

APPENDIX A

ADDITIONAL MICROPROBE DATA

Specimen No. B35

Test No. 32

Etchant: Oxalic Acid-Electrolytic

Magnification: 750X

Local Temperature: 1705°F

	Composition (wt %)						
	Al	Co	Cr	Ni	Si	Ti	Total
1	31.50	0.49	0.34	3.60	-	1.80	37.7
2	17.50	15.50	2.70	70.20	2.2	6.60	114.7
3	29.30	14.40	3.90	62.40	1.5	4.10	115.6
4	14.80	6.00	1.60	22.50	2.1	38.80	85.8
5	15.60	15.30	2.80	68.90	2.2	6.90	111.7
6	6.50	6.60	52.10	38.50	1.9	3.10	108.7
7	4.40	7.70	67.00	32.90	2.2	5.20	99.4
8	12.40	13.70	13.10	63.50	3.4	6.80	112.9
9	11.70	16.50	8.10	61.70	1.6	5.70	105.3
10	12.60	17.00	9.20	60.60	1.8	6.50	107.7

FIGURE A-1. ELECTRON MICROPROBE ANALYSIS OF B COATING ON IN-100 ALLOY AFTER 2160 HOURS; Series 1 Test (T_{max} 1870° F)

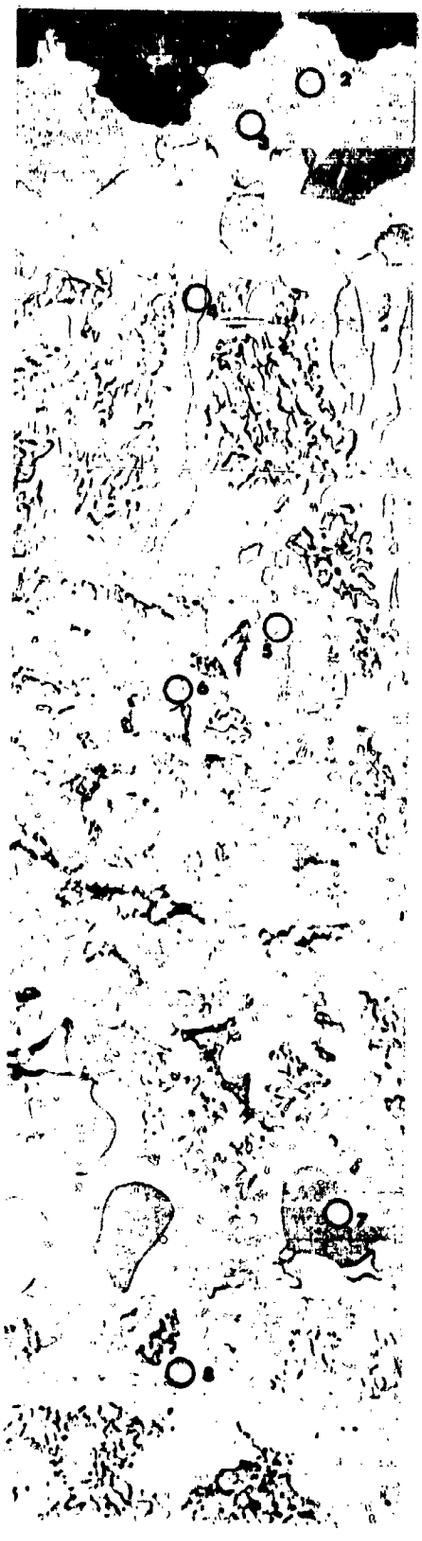

Specimen No. C52

	Composition (wt %)						
	Al	Co	Cr	Mo	Ni	Si	Total
1	22.1	0.72	0.75	-	6.3	0.18	30.0
2	31.1	14.70	5.25	-	60.1	3.90	115.0
3	17.1	14.40	3.50	0.18	67.3	3.01	105.5
4	3.5	25.90	37.50	8.90	22.7	4.50	103.0
5	13.8	14.70	4.50	2.20	65.4	4.10	104.7
6	5.5	12.60	18.70	2.20	30.7	2.00	71.7
7	29.7	15.90	5.50	-	60.0	3.50	115.0
8	6.3	13.00	13.20	13.10	44.6	6.60	96.8
9	11.9	21.10	7.50	1.60	58.5	2.30	102.9
10	11.9	17.90	8.40	2.10	61.5	1.70	103.5

Test No. 32

Etchant: Oxalic Acid-Electrolytic

Magnification: 750X (reduced 17%)

Local Temperature: Approx. 1870°F

FIGURE A-2. ELECTRON MICROPROBE ANALYSIS OF C COATING ON IN-100 ALLOY AFTER 2560 HOURS; Series 1 Test (Section Through Region of Incipient Melting)

Specimen No. C63

Test No. 35

Etchant: Oxalic Acid-Electrolytic

Magnification: 750X

Local Temperature: 1785°F

	Composition (wt %)						
	Al	Co	Cr	Mo	Ni	Si	Total
1	31.6	0.10	0.20	-	0.80	-	32.7
2	15.5	16.80	0.30	-	70.90	0.30	103.8
3	29.9	17.30	0.40	-	66.00	-	113.6
4	2.0	14.20	2.30	16.60	34.70	5.30	75.1
5	15.3	17.70	0.50	-	69.90	0.10	103.5
6	8.3	26.20	3.20	1.60	56.70	0.20	96.2
7	8.8	18.00	5.20	0.90	63.40	-	96.3

FIGURE A-3. ELECTRON MICROPROBE ANALYSIS OF C COATING ON IN-100 ALLOY AFTER 2000 HOURS; Series 2 Test (T_{max} 1950° F)

Specimen No. D28

Local Temperature: 1785°F

	Composition (wt %)						
	Al	Co	Cr	Fe	Ni	Si	Total
1	5.6	4.7	68.5	15.70	4.2	0.45	99.1
2	4.2	4.8	71.0	14.50	2.9	0.81	98.2
3	17.7	4.0	44.6	7.40	39.9	0.82	114.4
4	35.1	9.5	8.4	5.50	54.5	0.84	113.8
5	37.1	10.3	5.3	3.50	52.3	0.65	109.1
6	8.3	3.7	59.5	1.30	10.3	1.40	84.5
7	29.9	13.0	7.6	1.70	53.6	0.81	106.6
8	5.3	6.3	4.4	0.90	23.3	0.53	40.7
9	12.5	14.1	11.0	1.20	57.4	1.10	97.3
10	11.7	10.7	6.1	0.05	67.5	0.80	96.9

Test No. 33

Etchant: Oxalic Acid-Electrolytic

Magnification: 750X

FIGURE A-4. ELECTRON MICROPROBE ANALYSIS OF D COATING ON IN-100 ALLOY AFTER 440 HOURS; Series 2 Test (T_{max} 1950° F)

Specimen No. G42

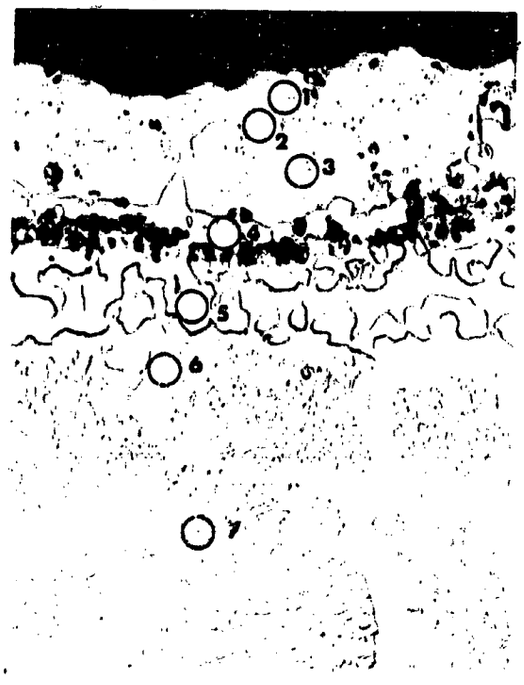

Test No. 35

Etchant: Oxalic Acid-Electrolytic

Magnification: 750X

Local Temperature: 1785°F

	Composition (wt %)						
	Al	Co	Cr	Mo	Ni	Ta	Total
1	29.7	7.6	6.1	-	66.6	-	110.0
2	16.1	8.7	6.7	0.50	69.4	0.40	101.8
3	30.2	7.7	6.4	-	66.5	-	110.8
4	0.4	1.5	85.6	5.10	3.6	-	96.2
5	0.4	1.9	80.4	12.60	3.9	-	99.2
6	14.4	8.8	16.8	0.90	67.3	4.40	112.6
7	12.6	10.1	10.1	1.60	63.2	3.70	101.3
8	8.7	9.9	10.1	4.70	64.6	4.10	102.1

FIGURE A-5. ELECTRON MICROPROBE ANALYSIS OF G COATING ON B1900 ALLOY AFTER 1360 HOURS; Series 2 Test (T_{max} 1950° F)

Specimen No. J44

Test No. 33

Etchant: Oxalic Acid–Electrolytic

Magnification: 750X

Local Temperature: 1785°F

	Composition (wt %)					
	Al	Co	Cr	Ni	W	Total
1	24.1	8.1	16.9	2.6	1.8	53.5
2	30.5	51.9	7.1	15.5	1.6	106.6
3	2.4	12.7	70.9	1.1	12.9	100.0
4	4.0	61.4	21.2	8.8	6.1	101.5
5	2.7	13.9	77.6	1.7	4.2	100.1
6	5.1	58.6	25.1	11.6	2.2	102.6
7	1.0	17.4	70.6	2.4	14.4	105.8
8	1.2	61.4	24.8	11.2	6.7	105.3

FIGURE A-6. ELECTRON MICROPROBE ANALYSIS OF J COATING ON X-40 ALLOY AFTER 994 HOURS; Series 2 Test (T_{max} 1950° F)

Specimen No. K25

Test No. 35

Etchant: Oxalic Acid-Electrolytic

Magnification: 750X

Local Temperature: 1785°F

	Composition (wt %)					
	Al	Co	Cr	Ni	W	Total
1	7.00	55.1	12.5	10.6	4.9	90.1
2	26.80	45.8	4.3	21.7	1.5	100.1
3	7.10	56.9	14.4	10.4	4.9	93.7
4	2.60	41.1	24.5	5.7	12.2	86.1
5	1.70	29.8	56.8	4.7	12.4	105.4
6	4.10	58.0	17.4	10.9	5.9	96.3
7	1.05	16.6	64.4	2.2	13.9	107.6
8	1.05	59.3	18.9	11.1	6.5	96.9

FIGURE A-7. ELECTRON MICROPROBE ANALYSIS OF K COATING ON X-40 ALLOY AFTER 170 HOURS; Series 2 Test (T_{max} 1950° F)

Specimen No. L48

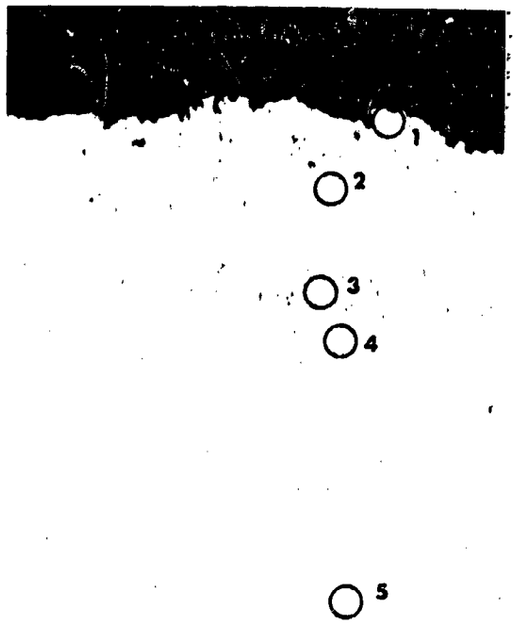

Test No. 36

Etchant: Oxalic Acid-Electrolytic

Magnification: 750X

Local Temperature: 1740°F

	Composition (wt %)						
	Al	Co	Cr	Ni	Si	W	Total
1	15.80	58.0	6.4	14.5	2.10	3.3	100.1
2	21.19	57.9	8.9	13.1	1.03	2.4	104.5
3	4.04	21.7	72.9	2.5	0.60	13.1	114.8
4	0.87	22.0	46.2	9.2	0.61	13.6	92.5
5	0.40	17.7	63.8	1.9	0.46	7.4	91.7
6	0.26	56.7	22.5	12.1	0.62	7.8	100.0

FIGURE A-8. ELECTRON MICROPROBE ANALYSIS OF L COATING ON X-40 ALLOY AFTER 1480 HOURS; Series 1 Test (T_{max} 1845° F)

Specimen No. N42

Test No. 36

Etchant: Oxalic Acid-Electrolytic

Magnification: 750X

Local Temperature: 1740° F

	Composition (wt %)						
	Al	Co	Cr	Fe	Si	W	Total
1	29.60	36.5	9.3	1.0	1.60	1.4	79.4
2	26.00	66.7	8.1	2.0	2.10	2.1	107.0
3	9.80	35.3	27.0	1.4	0.75	16.8	91.0
4	2.20	59.7	26.0	3.2	1.90	11.5	104.5
5	0.23	66.0	27.6	2.3	1.20	12.4	109.7
6	0.16	40.2	32.6	1.7	0.90	31.7	107.3
7	0.04	66.0	27.2	2.4	1.50	12.0	109.1

FIGURE A-9. ELECTRON MICROPROBE ANALYSIS OF N COATING ON WI-52 ALLOY AFTER 100 HOURS; Series 1 Test (T_{max} 1845° F)

Specimen No. O45

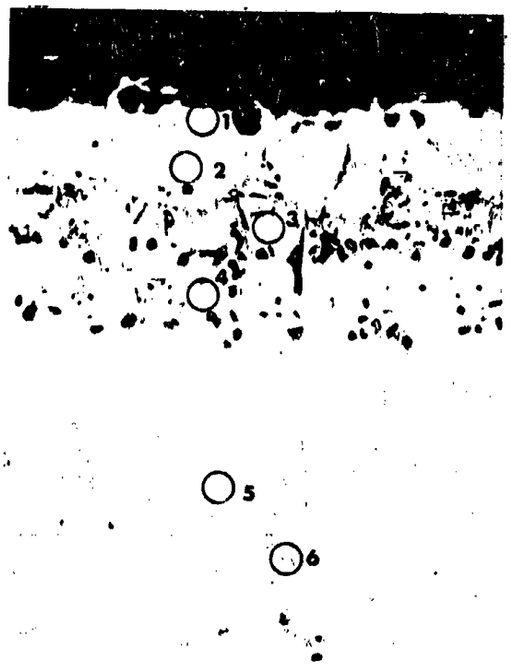

Test No. 33

Etchant: Oxalic Acid-Electrolytic

Magnification: 750X

Local Temperature: 1785° F

	Composition (wt %)					
	Al	Co	Cr	Fe	W	Total
1	6.40	69.9	17.3	3.3	4.9	101.8
2	30.30	66.6	7.8	2.9	4.2	111.8
3	6.20	66.7	18.3	3.1	5.7	100.0
4	4.20	67.4	19.4	3.4	10.4	104.8
5	1.00	70.0	20.7	3.5	7.6	102.8
6	0.92	35.2	12.0	1.7	13.5	63.3
℄ 7	0.78	58.6	19.0	2.7	10.3	91.4

FIGURE A-10. ELECTRON MICROPROBE ANALYSIS OF O COATING ON WI-52 ALLOY AFTER 520 HOURS; Series 2 Test (T_{max} 1950° F)

Specimen No. P29

Test No. 33

Etchant: Oxalic Acid-Electrolytic

Magnification: 750X

Local Temperature: 1785°F

	Composition (wt %)					
	Al	Co	Cr	Fe	Si	Total
1	33.00	70.0	10.4	1.6	2.8	117.8
2	33.10	69.8	10.9	1.6	2.7	118.1
3	2.90	23.8	60.3	0.4	1.0	88.4
4	27.10	57.3	11.5	1.5	2.5	99.9
5	2.20	69.0	25.9	2.1	3.0	102.2
6	1.50	72.6	24.8	2.3	3.0	104.2
7	1.70	46.1	18.8	1.1	3.5	71.2
℄ 8	0.73	73.0	25.6	2.1	2.6	104.0

FIGURE A-11. ELECTRON MICROPROBE ANALYSIS OF P COATING ON WI-52 ALLOY AFTER 694 HOURS; Series 2 Test (T_{max} 1950° F)

APPENDIX B

WEIGHT CHANGE TABLES

WEIGHT CHANGE DURING OXIDATION-EROSION TEST

TEST NUMBER 32, RIG NUMBER 2
1870° F MAXIMUM TEMPERATURE ALONG THE TRAILING EDGE

Exposure Time (Hours)	Cumulative Weight Change (mg)							
	Specimen Number							
	F3	B35	C52	H49	F34	B46	C53	H54
20	+1.0	+2.8	+3.5	+9.0	+1.1	+2.2	+0.4	+6.2
40	+1.8	+3.4	+3.8	+10.9	+1.5	+2.5	+0.3	+7.3
60	+2.5	+3.9	+4.3	+11.8	+2.0	+3.1	+0.5	+8.2
80	+3.2	+4.3	+4.9	+12.6	+2.5	+3.4	+0.9	+8.4
100	+3.4	+4.3	+4.9	+13.2	+2.5	+3.7	+0.9	+9.2
120	+4.1	+4.7	+5.1	+13.7	+2.6	+3.7	+0.5	+9.3
140	+4.6	+5.0	+5.9	+14.3	+3.3	+4.1	+0.7	+9.6
160	+4.8	+5.4	+5.4	+14.6	+3.2	+4.4	+0.8	+10.1
180	+5.0	+5.5	+5.5	+14.9	+3.1	+4.8	+0.5	+10.1
200	+6.1	+6.3	+6.5	+15.9	+3.9	+5.2	+1.9	+10.8
220	+6.0	+6.4	+6.7	+16.4	+4.1	+5.0	+1.5	+11.5
240	+5.2	+5.8	+5.5	+15.3	+3.2	+4.9	+0.4	+10.6
260	+5.7	+6.1	+6.0	+15.5	+3.6	+5.1	+0.8	+10.7
280	+6.3	+6.3	+6.1	+16.0	+4.1	+5.2	+1.2	+11.0
300	+6.9	+6.2	+6.4	+16.0	+4.3	+5.4	+1.1	+11.0
320	+6.9	+5.8	+5.4	+15.8	+3.6	+5.0	+0.3	+11.0
340	+7.8	+6.3	+5.8	+16.3	+4.0	+5.5	+0.3	+11.4
360	+7.7	+6.1	+5.2	+16.2	+3.6	+5.1	+0.1	+11.3
380	+7.6	+5.9	+4.5	+15.8	+3.3	+4.6	-0.5	+11.1
400	+7.5	+5.7	+4.7	+15.7	-12.9	+5.1	-0.1	+11.1
420	+8.5	+5.9	+4.8	+16.0	+3.2	+4.6	-0.6	+10.8
440	+9.2	+6.0	+4.8	+16.5	+3.3	+5.0	-0.5	+11.0
460	+9.7	+6.3	+4.8	+16.7	+3.5	+5.1	-0.4	+11.2
480	+9.5	+7.9	+4.7	+16.7	+3.6	+5.1	-0.6	+11.0
500	+10.4	+9.0	+5.0	+17.3	+4.3	+6.1	+0.4	+11.2
520	+10.1	+8.0	+4.8	+16.2	+3.5	+5.0	-0.2	+9.6
540	+10.6	+8.0	+4.8	+16.2	+3.6	+4.9	0.0	+9.4
560	+11.0	+8.1	+4.6	+16.1	+3.6	+5.0	-0.2	+9.4
580	+10.4	+7.6	+4.0	+15.7	+3.4	+4.6	-0.9	+9.2
600	+10.4	+7.9	+4.0	+16.2	+3.4	+5.0	-0.7	+9.2

WEIGHT CHANGE DURING OXIDATION-EROSION TEST

TEST NUMBER 32, RIG NUMBER 2
1870° F MAXIMUM TEMPERATURE ALONG THE TRAILING EDGE

Exposure Time (Hours)	Cumulative Weight Change (mg)							
	Specimen Number							
	F3	B35	C52	H49	F34	B46	C53	H54
620	+10.7	+7.5	+3.6	+15.9	+3.3	+5.0	-0.7	+9.2
640	+11.4	+7.6	+3.4	+15.6	+3.0	+4.6	-1.2	+9.1
660	+11.5	+7.5	+3.1	+15.7	+2.9	+4.2	-1.4	+8.8
680	+12.4	+8.7	+3.6	+15.9	+3.7	+5.9	-0.5	+8.3
700	+11.5	+8.0	+2.4	+14.8	+2.2	+4.0	-1.8	+7.2
720	+11.3	+7.0	+2.4	+14.5	+2.4	+3.7	-2.1	+6.0
740	+12.9	+7.5	+3.3	+15.2	+2.8	+4.7	-0.9	+6.3
760	+12.2	+7.0	+2.7	+14.5	+2.4	+4.1	-1.4	+5.9
780	+13.6	+7.0	+2.5	+14.7	+2.6	+3.9	-1.4	+6.2
800	+12.4	+6.6	+1.8	+14.3	+2.5	+3.6	-1.9	+5.6
820	+12.6	+5.8	+0.8	+13.2	+1.8	+2.8	-3.0	+4.7
840	+37.4	+6.6	+1.4	+14.2	+2.5	+3.8	-1.7	+5.2
860	+14.6	+6.4	+1.7	+14.5	+2.9	+4.1	-1.9	+5.8
880	+14.6	+6.1	+0.8	+13.8	+2.2	+3.3	-2.3	+4.9
900	+14.4	+4.4	+0.8	+12.2	+2.3	+2.0	-2.3	+3.0
920	+14.6	-0.1	-0.6	+11.2	+1.6	-1.7	-3.1	+1.8
940	+14.4	-1.7	-1.6	+10.4	+0.2	-3.1	-3.8	+1.3
960	+14.8	-1.3	-1.1	+11.2	+1.3	-2.1	-3.2	+2.0
980	+15.4	-1.1	-1.8	+10.7	+1.3	-2.4	-3.3	+2.1
1000	+15.4	-1.5	-1.7	+11.4	+1.7	-2.3	-3.5	+2.0
1020	+14.6	-1.9	-2.2	+10.4	+0.8	-2.7	-3.9	+1.8
1040	+14.6	-1.7	-1.7	+11.1	+1.2	-2.7	-3.8	+1.5
1060	+13.6	-2.7	-2.6	+10.7	+1.3	-3.2	-4.6	+1.2
1080	+14.2	-2.1	-3.0	+10.6	+1.0	-3.3	-4.6	+1.2
1100	+15.1	-1.5	-2.8	+11.0	+0.9	-2.8	-4.2	+0.2
1120	+14.9	-1.9	-3.5	+10.3	+0.7	-2.5	-4.6	-0.3
1140	+14.8	-1.8	-2.9	+10.3	+1.2	-2.5	-4.7	-0.1
1160	+14.1	-2.4	-4.1	+9.8	+0.6	-3.1	-5.4	-0.7
1180	+14.9	-3.3	-4.9	+9.5	+0.0	-4.1	-6.0	-1.1
1200	+16.4	-2.2	-4.4	+10.3	+0.8	-3.1	-5.4	-1.3

WEIGHT CHANGE DURING OXIDATION-EROSION TEST

TEST NUMBER 32, RIG NUMBER 2
1870° F MAXIMUM TEMPERATURE ALONG THE TRAILING EDGE

Exposure Time (Hours)	Cumulative Weight Change (mg)							
	Specimen Number							
	F3	B35	C52	H49	F34	B46	C53	H54
1220	+16.4	-2.9	-5.2	+8.7	+0.6	-3.2	-5.7	-1.7
1240	+21.4	-0.7	-3.4	+11.9	+2.4	-1.7	-4.1	-0.4
1260	+17.7	-1.8	-4.4	+11.9	+1.6	-1.8	-4.3	-0.4
1280	+17.8	-2.2	-4.4	+11.9	+2.0	-1.7	-4.5	-0.9
1300	+17.7	-2.9	-5.4	+11.3	+1.3	-2.9	-5.5	-1.4
1320	+17.9	-2.7	-5.7	+11.1	+1.3	-2.7	-5.8	-1.3
1340	+17.9	-2.4	-6.4	+11.4	+0.8	-3.1	-6.9	-1.8
1360	+18.7	-3.2	-6.4	+11.0	+1.1	-3.1	-6.7	-1.7
1380	+18.8	-3.8	-7.0	+10.4	+0.5	-5.1	-7.5	-2.2
1400	+20.7	-2.8	-5.7	+11.6	+1.7	-2.5	-6.2	-1.2
1420	+20.3	-3.8	-7.4	+10.3	+0.7	-3.8	-7.9	-2.5
1440	+20.7	-3.4	-7.1	+11.0	+0.8	-3.2	-7.5	-2.2
1460	+21.4	-3.7	-7.0	+11.1	+1.3	-2.8	-7.1	-1.7
1480	+21.2	-3.7	-7.3	+11.6	+1.6	-2.9	-7.1	-1.8
1505	+22.8	-3.4	-6.4	+11.6	+1.8	-2.7	-7.0	-1.4
1520	+22.0	-3.7	-7.0	+11.4	+1.4	-2.9	-7.4	-1.9
1540	+21.1	-4.2	-7.4	+11.2	+1.3	-3.2	-7.7	-2.5
1560	+21.7	-4.1	-7.1	+11.5	+1.6	-2.9	-7.3	-2.4
1580	(1)	-4.0	-6.8	+10.8	+1.4	-3.5	-8.3	-3.3
1600		-4.5	-7.2	+11.1	+2.0	-3.3	-7.7	-3.1
1620		-5.3	-7.9	+10.4	+1.6	-4.2	-8.3	-3.6
1640		-4.4	-7.2	+11.1	+2.4	-3.8	-8.1	-3.1
1660		-5.3	-7.9	+10.4	+1.8	-4.7	-8.7	-3.7
1680		-5.5	-8.1	+10.0	+2.0	-4.6	-8.7	-3.6
1700		-6.5	-9.0	+9.2	+1.1	-5.9	-9.9	-4.8
1720		-7.2	-9.6	+9.5	+1.0	-6.2	-10.3	-5.6
1740		-5.9	-8.1	+9.9	+2.6	-4.8	-9.0	-4.8
1760		-4.0	-6.0	+12.2	+5.1	-2.8	-7.1	-2.1
1780		-2.7	-5.3	+12.0	+6.0	-2.4	-5.9	-1.9

Note (1): Data not accurate; piece of thermocouple broke off inside specimen.

WEIGHT CHANGE DURING OXIDATION-EROSION TEST

TEST NUMBER 32, RIG NUMBER 2
1870° F MAXIMUM TEMPERATURE ALONG THE TRAILING EDGE

Exposure Time (Hours)	Cumulative Weight Change (mg)							
	Specimen Number							
	F3	B35	C52	H49	F34	B46	C53	H54
1800	-	-3.4	-4.8	+12.4	+7.2	-1.5	-5.3	-1.8
1820	-	-3.5	-5.3	+11.9	+7.9	-4.1	-7.6	-1.8
1840	-	-4.7	-5.7	+11.4	+7.5	-4.4	-7.5	-2.6
1860	-	-6.0	-6.5	+10.8	+6.5	-4.5	-7.7	-3.3
1880	-	-7.2	-7.9	+9.1	+5.1	-5.9	-9.1	-4.8
1900	-	-7.8	-8.3	+8.8	+5.4	-6.3	-9.4	-4.8
1920	-	-9.5	-11.1	+7.7	+4.0	-8.0	-11.1	-5.9
1940	-	-6.0	-7.0	+10.9	+8.4	-3.7	-7.2	-3.8
1960	-	-8.4	-9.4	+8.3	+7.0	-6.7	-8.9	-6.4
1980	-	-11.9	-11.3	+7.1	+5.9	-8.0	-11.4	-8.0
2000	-	-13.9	-13.5	+5.8	+4.9	-10.7	-13.1	-9.0
2020	-	-15.7	-14.9	+4.3	+4.0	-12.5	-14.8	-10.5
2040	-	-16.2	-14.5	+4.9	+5.1	-12.3	-14.6	-10.0
2060	-	-16.6	-14.4	+5.0	+5.5	-12.7	-14.8	-10.9
2080	-	-18.0	-15.0	+4.4	+5.4	-14.0	-15.6	-11.7
2100	-	-16.2	-12.5	+7.3	+8.3	-11.8	-13.2	-8.9
2120	-	-20.5	-15.6	+4.1	+5.5	-15.2	-16.5	-11.9
2140	-	-20.7	-14.4	+5.2	+6.9	-14.8	-15.7	-11.2
2160	-	-23.5	-15.1	+4.0	+6.2	-16.8	-16.8	-12.4
	B35 and B46 Removed from test - Replaced with D2 and D52							
	F3	D2	C52	H49	F34	D52	C53	H54
2180	-	-	-14.9	+4.4	+6.2	-	-16.4	-12.4
20	-	+6.3	-	-	-	+3.5	-	-
2200	-	-	-15.5	+4.3	+5.6	-	-17.6	-13.1
40	-	+5.4	-	-	-	+1.5	-	-
2220	-		-14.7	+4.5	+6.8	-	-16.8	-11.9
60	-	+6.6	-	-	-	+2.8	-	-
2240	-	-	-14.2	+4.8	+7.6	-	-16.4	-11.8
80	-	+7.9	-	-	-	+3.2	-	-
2260		-	-14.4	+4.7	+7.3	-	-16.7	-12.4
100		+7.0	-	-	-	+2.6	-	-
2280	-	-	-13.5	+4.5	+8.4	-	-16.0	-11.4
120	-	+9.4	-	-	-	+4.4	-	-
2300	-	-	-14.1	+5.2	+8.1	-	-16.0	-11.8
140	-	+10.6	-	-	-	+5.0	-	-
2320	-	-	-14.4	+5.7	+8.5	-	-16.5	-11.4
160	-	+12.3	-	-	-	+6.6	-	-
2340	-	-	-14.6	+5.7	+8.5	-	-16.7	-11.7
180	-	+13.8	-	-	-	+7.1	-	-
2360	-	-	-16.9	+4.2	+8.0	-	-18.6	-13.1
200	-	+13.7	-	-	-	+7.1	-	-
2380	-	-	-16.9	+4.1	+8.0	-	-19.0	-13.4
220	-	+11.7	-	-	-	+8.2	-	-

WEIGHT CHANGE DURING OXIDATION-EROSION TEST

TEST NUMBER 32, RIG NUMBER 2
1870° F MAXIMUM TEMPERATURE ALONG THE TRAILING EDGE

Exposure Time (Hours)	Cumulative Weight Change (mg)							
	Specimen Number							
	F3	D2	C52	H49	F34	D52	C53	H54
2400			-16.6	+4.8	+5.6		-18.3	-12.3
240		+9.2				+9.3		
2420			-15.8	+5.1	+6.3		-18.0	-12.6
260		+8.4				+11.3		
2440			-16.5	+4.9	+6.0		-18.2	-12.9
280		+9.0				+10.8		
2460			-18.1	+4.2	+6.6		-20.1	-11.4
300		+8.6				+11.1		
2480			-16.2	+6.1	+7.7		-19.4	-11.8
320		+12.0				+13.5		
2500			-16.6	+4.5	+7.2		-19.8	-12.3
340		+12.0				+13.5		
2520			-17.7	+5.4	+7.1		-20.1	-12.8
360		+13.9				+14.4		
2540			-18.5	+4.6	+6.5		-20.7	-13.6
380		+15.5				+13.7		
2560			-19.5	+3.7	+5.7		-21.8	-14.6
400		+14.8				+13.1		
C52 and C53 removed from test. Replaced with J40 and J41.								
	F3	D2	J40	H49	F34	D52	J41	H54
2580				+5.0	+7.1			-13.4
420		+16.3				+14.4		
20			+9.8				+10.3	
2600				+6.7	+8.9			-11.8
440		+18.4				+16.0		
40			+13.2				+13.9	

WEIGHT CHANGE DURING OXIDATION-EROSION TEST

TEST NUMBER 32, RIG NUMBER 2
1870° F MAXIMUM TEMPERATURE ALONG THE TRAILING EDGE

Exposure Time (Hours)	Cumulative Weight Change (mg)							
	Specimen Number							
	F3	D2	J40	H49	F34	D52	J41	H54
2620				+4.7	+7.1			-13.7
460		+17.0				+14.3		
60			+12.9				+14.7	
2640				+5.7	+9.5			-14.0
480		+18.2				+15.4		
80			+14.3				+15.2	
2660				+3.7	+6.6			-15.7
500		+16.2				+11.5		
100			+14.0				+16.7	
2680				+3.7	+6.2			-16.5
520		+14.1				+6.8		
120			+14.9				+16.3	
2700				+2.9	+5.4			-17.2
540		+11.6				+0.9		
140			+14.8				+16.3	
2720				+3.4	+5.1			-18.2
560		+9.6				-13.8		
160			+15.8				+16.8	
2740				+3.5	+5.5			-18.2
580		-3.8				-21.9		
180			+16.1				+16.8	
2760				+0.9	+2.8			-21.0
600		-59.0				-33.5		
200			+13.3				+13.8	
D2 and D52 removed from test. Replaced with L36 and L40.								

WEIGHT CHANGE DURING OXIDATION-EROSION TEST

TEST NUMBER 32, RIG NUMBER 2
1870° F MAXIMUM TEMPERATURE ALONG THE TRAILING EDGE

Exposure Time (Hours)	Cumulative Weight Change (mg)							
	Specimen Number							
	F3	L36	J40	H49	F34	L40	J41	H54
2780				+2.0	+3.8			-20.2
220			+15.0				+15.2	
20		+6.4				+6.8		
2800				+1.7	+3.5			-20.3
240			+14.6				+14.5	
40		+8.2				+8.4		
2820				+2.9	+4.8			-18.8
260			+15.8				+16.1	
60		+11.6				+10.8		
2840				+2.3	+4.2			-19.8
280			+15.5				+15.4	
80		+10.6				+11.0		
2860				+1.7	+2.1			-19.9
300			+14.7				+14.3	
100		+10.4				+10.7		
2880				+1.0	-0.1			-21.2
320			+14.1				+13.7	
120		+10.4				+10.6		
2900				+1.3	-1.4			-20.9
340			+14.5				+14.1	
140		+11.0				+11.1		
2920				+1.5	-1.5			-21.1
360			+14.6				+14.2	
160		+10.0				+11.5		
2940				+1.8	-1.1			-20.3
380			+15.1				+14.5	
180		+12.0				+12.0		

WEIGHT CHANGE DURING OXIDATION-EROSION TEST

TEST NUMBER 32, RIG NUMBER 2
1870° F MAXIMUM TEMPERATURE ALONG THE TRAILING EDGE

Exposure Time (hours)	Cumulative Weight Change (mg)							
	Specimen Number							
	F3	L36	J40	H49	F34	L40	J41	H54
2960				+1.9	-1.4			-20.8
400			+15.1				+14.2	
200		+11.9				+12.3		
2980				+2.4	-0.9			-19.8
420			+15.6				+14.6	
220		+12.5				+13.0		
3000				+1.6	-1.8			-20.4
440			+14.8				+13.5	
240		+11.4				+12.4		
3020				+2.2	-1.7			-19.4
460			+15.8				+14.1	
260		+11.6				+12.8		
3040				+1.9	-2.2			-19.9
480			+15.2				+13.5	
280		+11.3				+12.1		
	Test terminated. Specimens badly oxidized during temperature-controller malfunction.							

WEIGHT CHANGE DURING OXIDATION-EROSION TEST
TEST NUMBER 33, RIG NUMBER 1
1950° F MAXIMUM TEMPERATURE ALONG TRAILING EDGE

Exposure Time (Hours)	Cumulative Weight Change (mg)									
	Specimen Number									
	L43	L45	O32	O45	D28	D45	G37	G42	G48	G54
20	+4.8	+4.8	+9.3	+9.1	+1.7	+4.2	+7.1	+6.6	+4.0	+10.0
40	+5.9	+5.3	+11.2	+11.9	+0.9	+3.2	+8.4	+8.8	+4.0	+12.5
60	+6.5	+5.8	+13.3	+13.7	-0.9	+0.6	+9.3	+9.8	+7.5	+16.6
80	+6.8	+6.4	+14.5	+15.1	-1.7	-0.6	+11.1	+11.3	+8.0	+17.7
100	+6.4	+5.9	+15.5	+15.8	-0.5	+0.8	+11.6	+11.9	+10.6	+18.1
120	+5.9	+5.8	+16.4	+16.7	+0.8	+1.2	+12.2	+12.3	+11.4	+19.0
140	+5.4	+5.3	+16.6	+17.1	+1.7	+2.2	+13.2	+13.0	+11.4	+18.8
160	+4.6	+4.8	+16.7	+17.6	+2.5	-2.2	+13.0	+13.7	+12.1	+19.0
180	+3.6	+3.3	+16.3	+17.0	+3.5	-1.4	+13.6	+13.8	+12.1	+19.0
200	+3.9	+3.8	+18.2	+18.6	+7.0	-1.2	+15.1	+14.6	+12.6	+19.8
220	+3.1	+2.5	+18.1	+18.7	+7.5	-0.4	+15.7	+15.9	+12.4	+19.9
240	+0.9	+0.3	+16.9	+17.5	+7.5	-0.7	+15.7	+15.9	+11.9	+20.2
260	+0.4	-0.1	+17.0	+19.1	+6.9	-0.2	+16.4	+16.7	+12.0	+20.4
280	+1.4	+1.1	+19.3	+19.6	+4.5	-1.2	+16.0	+16.1	+11.7	+20.8
300	-0.6	+0.7	+18.5	+19.0	+2.1	-3.1	+15.8	+16.4	+11.2	+21.1
320	-2.5	-2.8	+18.2	+18.2	-0.3	-9.2	+15.6	+15.8	---	---
340	-4.0	-5.2	+17.8	+17.1	-1.9	-12.4	+16.0	+16.5		
360	-8.3	-10.1	+14.6	+13.4	-5.5	-16.9	+16.2	+16.5		
380	-10.2	-12.1	+13.4	+12.4	-8.7	-24.4	+16.2	+16.6		
400	-12.0	-14.5	+9.7	+8.8	-12.5	-32.6	+13.0	+16.6		
420	-12.6	-15.7	+8.5	+7.8	-24.4	-54.1	+16.6	+16.8		
440	-16.0	-18.4	+6.2	+5.5	-37.9	-93.1	+16.5	+16.7		
460	-18.6	-20.9	+2.3	+1.9	---	---	---	---		
480	-19.5	-21.5	+1.7	-2.5						
500	-20.4	-27.3	-6.3	-12.1						
520	-22.4	-35.3	-18.8	-23.5						
540	---									

Exposure Time (Hours)	Cumulative Weight Change (mg)				Exposure Time (Hours)	Cumulative Weight Change (mg)			
	Specimen Number					Specimen Number			
	J2	J44	P27	P29		J2	J44	P27	P29
20	+9.0	+10.6	+6.0	+5.4	574	+17.9	+19.9	+2.5	-1.8
34	+11.3	+12.3	+6.0	+5.9	594	+17.6	+19.6	+2.7	-2.1
54	+13.9	+15.0	+7.7	+7.8	614	+16.6	+19.6	+2.9	-2.7
74	+15.6	+17.2	+8.8	+8.6	634	+16.4	+18.9	+1.7	-7.0
94	+17.5	+17.9	+9.9	+9.5	654	+15.4	+18.5	-0.3	-18.0
114	+18.5	+19.4	+10.4	+10.5	674	+14.9	+18.0	-3.6	-30.4
134	+18.6	+19.2	+10.6	+9.4	694	+14.2	+18.4	-8.5	-47.0
154	+19.2	+19.2	+10.4	+9.5	714	+12.7	+17.0	---	---
174	+19.6	+19.3	+10.5	+9.0	734	+11.5	+16.7		
194	+19.5	+19.2	+10.0	+8.8	754	+11.9	+17.1		
214	+19.3	+18.7	+9.4	+7.5	774	+10.5	+16.7		
234	+20.6	+20.9	+10.1	+8.4	794	+8.6	+15.8		
254	+20.9	+20.7	+10.0	+7.3	814	+7.0	+15.4		
274	+19.7	+19.2	+8.3	+5.6	834	+4.9	+13.8		
294	+19.7	+19.8	+8.1	+5.3	854	+1.5	+11.3		
314	+21.3	+21.5	+9.8	+6.5	874	-1.9	+8.7		
334	+20.0	+20.8	+7.8	+4.8	894	-5.3	+6.0		
354	+19.9	+20.4	+7.0	+3.7	914	-8.4	+2.4		
374	+19.2	+20.3	+5.8	+2.4	934	-12.7	-0.2		
394	+18.6	+19.3	+2.9	-0.6	954	-17.0	-2.0		
414	+18.6	+19.8	+2.3	-1.0	974	-22.0	-6.4		
434	+18.4	+19.3	+1.2	-2.8	994	-34.4	-16.3		
454	+18.9	+19.8	+1.7	-2.5					
474	+18.1	+19.6	+0.6	-3.4					
494	+17.7	+18.9	-0.1	-3.0					
514	+19.0	+20.0	+2.1	-1.6					
534	+18.8	+20.2	+1.8	-1.3					
554	+18.7	+20.3	+2.4	-1.6					

WEIGHT CHANGE DURING OXIDATION-EROSION TEST

TEST NUMBER 35, RIG NUMBER 1
1950° F MAXIMUM TEMPERATURE ALONG THE TRAILING EDGE

Exposure Time (Hours)	Cumulative Weight Change (mg)							
	Specimen Number							
	H3	B40	C56	F29	H59	B49	C63	F36
20	+9.2	+1.0	+0.0	+0.6	+9.6	-0.1	+0.5	-1.6
40	+11.0	+1.8	+0.8	+1.2	+11.7	+1.5	+1.3	-1.4
60	+11.0	+2.0	+1.2	+1.3	+12.4	+1.4	+1.4	-1.2
80	+12.4	+2.9	+1.9	+2.2	+14.1	+2.8	+2.7	-0.2
100	+13.2	+2.1	+1.0	+1.2	+13.3	+1.4	+2.5	-1.1
120	+13.6	+2.9	+1.8	+1.9	+14.6	+2.6	+3.1	-1.4
140	+15.5	+3.7	+2.7	+2.4	+17.2	+3.4	+3.8	+0.2
160	+17.5	+4.5	+2.4	+2.4	+18.4	+3.7	+3.9	+0.6
180	+17.4	+3.9	+2.0	+2.0	+18.4	+3.4	+3.2	+0.3
200	+19.0	+6.2	+3.8	+6.6	+20.7	+5.5	+6.4	+2.3
220	+20.2	+5.0	+2.3	+2.5	+22.7	+4.2	+4.4	+0.8
240	+21.1	+5.0	+2.5	+2.2	+25.2	+3.8	+4.3	+0.6
260	+21.3	+4.5	+1.3	+1.2	+24.7	+3.4	+3.6	+0.0
280	+22.5	+6.1	+3.3	+2.9	+26.2	+5.7	+4.9	+1.3
300	+22.0	+5.1	+2.1	+2.3	+25.6	+4.9	+4.9	+0.8
320	+21.6	+4.2	+0.8	+1.9	+25.2	+4.2	+4.0	+0.2
340	+22.0	+4.8	+1.0	+2.1	+25.3	+3.4	+4.2	+0.3
360	+23.4	+5.1	+0.6	+2.1	+25 5	+4.6	+4.2	+1.6
380	+25.3	+6.3	+1.8	+3.4	+26.8	+5.5	+5.3	+2.4
400	+24.4	+5.5	+1.1	+2.8	+26.5	+5.0	+5.2	+1.1
420	+24.3	+5.7	+0.9	+2.7	+26.2	+4.6	+4.6	+0.9
440	+23.9	+5.0	+0.3	+2.1	+25.5	+4.0	+3.9	+0.4
460	+24.2	+5.3	+0.6	+2.6	+26.1	+4.3	+4.6	+1.5
480	+24.7	+5.6	+0.9	+2.8	+26.1	+4.1	+4.3	+1.1
500	+23.1	+4.0	+1.0	+1.2	+24.5	+2.6	+2.2	+0.3
520	+24.9	+5.1	+0.2	+2.3	+25.2	+3.5	+3.2	+1.0
540	+24.3	+6.0	+1.8	+3.0	+25.6	+4.0	+4.4	+2.0
560	+23.6	+5.6	+1.8	+3.0	+24.4	+3.5	+5.3	+1.5
580	+22.6	+4.4	+0.8	+2.4	+23.3	+2.0	+4.0	+0.6

WEIGHT CHANGE DURING OXIDATION-EROSION TEST

TEST NUMBER 35, RIG NUMBER 1
1950° F MAXIMUM TEMPERATURE ALONG THE TRAILING EDGE

Exposure Time (Hours)	Cumulative Weight Change (mg)							
	Specimen Number							
	H3	B40	C56	F29	H59	B49	C63	F36
600	+23.4	+4.1	+0.3	+2.1	+22.7	+1.6	+3.4	+0.4
620	+23.7	+4.7	+0.7	+2.6	+23.1	+2.1	+3.8	+1.1
640	+21.2	+4.1	-0.2	+1.9	+22.0	+1.4	+2.9	-0.2
660	+21.0	+3.8	-1.0	+1.5	+21.4	+0.6	+2.0	-0.5
680	+20.6	+3.3	-1.7	+1.1	+21.2	+0.2	+1.2	-0.8
700	+20.9	+3.6	-1.7	+1.4	+21.3	+0.2	+1.4	-1.1
720	+21.1	+3.5	-2.1	+1.2	+21.0	+0.2	+0.9	-0.9
740	+20.7	+3.1	-2.8	+0.8	+20.2	-0.6	-0.2	-0.9
760	+20.5	+3.0	-2.9	+0.9	+19.9	-0.7	-0.2	-1.2
780	+21.1	+3.7	-2.2	+1.9	+20.6	+0.4	+0.8	-0.1
800	+21.8	+3.8	-2.7	+1.5	+19.5	-0.7	-1.2	-1.5
820	+18.4	+2.3	-4.0	+0.7	+17.8	-1.7	-1.5	-1.8
840	+17.7	+1.9	-4.6	+0.5	+17.3	-2.1	-1.6	-1.7
860	+17.9	+1.8	-4.9	+0.1	+16.5	-2.4	-2.4	-2.2
880	+17.0	+1.0	-5.7	-1.0	+15.5	-3.1	-3.5	-3.0
900	+16.7	+1.1	-6.2	-1.2	+14.6	-3.7	-4.1	-3.8
920	+19.8	+2.2	-5.2	+0.2	+15.9	-2.1	-2.8	-2.2
Specimens C56, F29, H59, B49 damaged in test. Replaced with specimens K25, K35, N30 and N32.								
940	+18.7	-0.2	---	---	---	---	+44.0 (1)	-0.8
960	+19.0	-0.8	---	---	---	---	+28.6	-4.3
980	+14.6	-1.4	---	---	---	---	+11.4	-5.2
1000	+15.6	-1.6	---	---	---	---	+10.5	-6.6
1020	+14.2	-1.7	---	---	---	---	+1.0	-7.5
1040	+9.1	-2.7	---	---	---	---	-1.9	-9.2
1060	+5.9	-5.0	---	---	---	---	-5.0	-10.8
1080	+4.4	-4.3	---	---	---	---	-5.2	-10.2
1100	+3.5	-4.8	---	---	---	---	-6.5	-11.3
1120	+3.0	-3.3	---	---	---	---	-7.1	-10.8
1140	+1.6	-4.7	---	---	---	---	-7.7	-11.4

Notes: (1) Weight gain due to metal deposited on surface of blade when adjacent specimen failed at 921 hours.

WEIGHT CHANGE DURING OXIDATION-EROSION TEST

TEST NUMBER 35, RIG NUMBER 1
1950° F MAXIMUM TEMPERATURE ALONG THE TRAILING EDGE

Exposure Time (Hours)	Cumulative Weight Change (mg)							
	Specimen Number							
	H3	B40	C56	F29	H59	B49	C63	F36
1160	+1.3	-6.8	---	---	---	---	-9.1	-12.5
1180	+2.1	-5.7	---	---	---	---	-7.6	-11.2
1200	+1.5	-6.2	---	---	---	---	-8.4	-11.9
1220	+0.6	-6.3	---	---	---	---	-7.2	-11.2
1240	0.0	-8.1	---	---	---	---	-8.6	-12.3
1260	+0.1	-8.9	---	---	---	---	-7.7	-11.9
1280	+0.9	-7.2	---	---	---	---	-7.5	-11.0
1300	+2.8	-9.3	---	---	---	---	-7.6	-11.0
1320	+1.3	-11.7	---	---	---	---	-9.2	-12.7
1340	+0.8	-15.0	---	---	---	---	-10.2	-13.5

WEIGHT CHANGE DURING OXIDATION-EROSION TEST

TEST NUMBER 35, RIG NUMBER 1
1950° F MAXIMUM TEMPERATURE ALONG THE TRAILING EDGE

Exposure Time (Hours)	Cumulative Weight Change (mg)							
	Specimen Number							
	H3	B40	C63	F36	G37	G42	G48	G54
1360	-0.7	-18.0	-11.5	-15.3				
720					+9.5	+17.3		
320							+8.0	+18.1
1380	-0.1	-18.3	-8.9	-12.7				
740					+10.2	+19.9		
340							+9.5	+22.1
1400	-0.2	-23.6	-10.6	-14.1				
760					+8.2	+18.8		
360							+7.0	+21.4
	Specimen B40 removed from test. Replaced with D34.							
	H3	D34	C63	F36	G37	G42	G48	G54
1420	-0.4		-11.2	-15.0				
780					+6.6	+18.6		
380							+5.5	+21.6
20		+0.2						
1440	+0.0		-11.0	-14.0				
800					+5.4	+19.5		
400							+4.1	+23.5
40		-2.1						
1460	-0.1		-10.9	-13.8				
820					+4.2	+21.1		
420							+3.9	+24.8
60		-0.5						
1480	-0.5		-10.9	-14.1				
840					+0.3	+20.1		
440							+2.3	+25.0
80		-0.8						

WEIGHT CHANGE DURING OXIDATION-EROSION TEST

TEST NUMBER 35, RIG NUMBER 1
1950° F MAXIMUM TEMPERATURE ALONG THE TRAILING EDGE

Exposure Time (Hours)	Cumulative Weight Change (mg)							
	Specimen Number							
	H3	D34	C63	F36	G37	G42	G48	G54
1500	-7.0		-12.7	-15.9				
860					-2.6	+20.4		
460							+0.5	+24.5
100		-1.1						
1520	-5.4		-10.5	-12.8				
880					-1.4	+23.9		
480							+1.3	+25.9
120		+2.3						
1540	-4.2		-9.1	-11.1				
900					-8.8	+25.4		
500							+0.3	+24.6
140		+8.0						
1560	-2.7		-6.6	-7.8				
920					-9.6	+28.4		
520							+1.8	+26.0
160		+10.4						
1580	-3.9		-9.9	-9.0				
940					-12.8	+27.9		
540							+3.3	+20.0
180		+10.3						
1600	-3.9		-7.6	-7.7				
960					-15.5	+28.7		
560							-1.7	+23.0
200		+10.5						
1620	-5.7		-8.1	-8.7				
980					-32.5	+24.1		
580							-6.3	+17.3
220		+4.7						

WEIGHT CHANGE DURING OXIDATION-EROSION TEST

TEST NUMBER 35, RIG NUMBER 1
1950° F MAXIMUM TEMPERATURE ALONG THE TRAILING EDGE

Exposure Time (Hours)	Cumulative Weight Change (mg)							
	Specimen Number							
	H3	D34	C63	F36	G37	G42	G48	G54
1640	-10.1		- 9.0	- 9.7				
1000					-37.9	+18.4		
600							- 8.2	+15.2
240		- 1.3						
1660	- 9.5		- 8.3	- 8.1				
1020					-38.8	+16.5		
620							- 7.9	+15.7
260		- 4.9						
1680	-11.0		-10.1	- 8.7				
1040					-40.7	+ 9.6		
640							-10.5	+10.7
280		-13.8						
	G37 removed from test - replaced with D63							
	H3	D34	C63	F36	D63	G42	G48	G54
1700	- 9.5		- 9.2	- 6.7				
1060						+ 7.4		
660							-10.8	+ 9.0
300		-20.8						
20					+ 2.8			
1720	-10.6		-10.7	- 6.8				
1080						+ 4.0		
680							-12.6	+ 6.5
320		-28.9						
40					+ 0.7			
1740	-11.0		- 7.9	- 3.1				
1100						+ 3.8		
700							-11.1	+ 7.5
340		-35.3						
60					+ 0.2			
D34 removed from test - replaced with A45								

WEIGHT CHANGE DURING OXIDATION-EROSION TEST

TEST NUMBER 35, RIG NUMBER 1
1950° F MAXIMUM TEMPERATURE ALONG THE TRAILING EDGE

Exposure Time (Hours)	Cumulative Weight Change (mg)							
	Specimen Number							
	H3	A45	C63	F36	D63	G42	G48	G54
1760	-13.3		- 7.9	- 1.7				
1120						+ 2.5		
720							-11.5	+ 7.1
80					+ 0.2			
20		+ 1.5						
1780	-10.8		- 5.6	+ 0.6				
1140						+ 3.7		
740							- 9.7	+ 8.6
100					+ 4.0			
40		+ 5.6						
1800	-12.7		- 7.2	- 0.7				
1160						+ 0.9		
760							-12.5	+ 4.4
120					+ 3.7			
60		0.0						
1820	-12.5		- 6.5	+ 0.4				
1180						- 1.1		
780							-13.7	- 6.6
140					+ 5.9			
80		- 4.5						
1840	-13.2		- 7.6	- 0.3				
1200						-2.8		
800							-15.7	-15.3
160					+ 6.7			
100		- 9.5						

WEIGHT CHANGE DURING OXIDATION-EROSION TEST

TEST NUMBER 35, RIG NUMBER 1
1950° F MAXIMUM TEMPERATURE ALONG THE TRAILING EDGE

Exposure Time (Hours)	Cumulative Weight Change (mg)							
	Specimen Number							
	H3	A45	C63	F36	D63	G42	G48	G54
1860	-13.5		-9.0	-0.7				
1220						-4.6		
820							-17.4	-24.3
180					+8.3			
120		-20.1						
1880	-13.7		-9.4	-0.4				
1240						-5.9		
840							-18.7	-32.3
200					+9.3			
140		-24.6						
1900	-13.6		-9.3	-0.2				
1260						-7.6		
860							-20.7	-49.7
220					+6.9			
160		-32.6						
1920	-14.3		-10.6	-0.4				
1280						-10.1		
880							-23.3	-65.6
240					+6.9			
180		-40.3						
1940	-14.2		-10.6	+0.5				
1300						-11.1		
900							-24.6	-76.6
260					+8.8			
200		-47.9						
1960	-15.3		-11.1	+0.8				
1320						-12.4		
920							-26.3	-84.8
280					+8.8			
220		-57.0						

WEIGHT CHANGE DURING OXIDATION-EROSION TEST

TEST NUMBER 35, RIG NUMBER 1
1950° F MAXIMUM TEMPERATURE ALONG THE TRAILING EDGE

Exposure Time (Hours)	Cumulative Weight Change (mg)							
	Specimen Number							
	H3	A45	C63	F36	D63	G42	G48	G54
1980	-15.3		-11.0	+1.2				
1340						-14.9		
940							-29.3	-99.3
300					+10.6			
240		-75.4						
2000	-15.3		-12.5	+1.2				
1360						-19.3		
960							-34.7	-122.6
320					+9.8			
260		-98.6						

WEIGHT CHANGE DURING OXIDATION-EROSION TEST

TEST NUMBER 36, RIG NUMBER 2

1845° F MAXIMUM TEMPERATURE ALONG THE TRAILING EDGE

Exposure Time (Hours)	Cumulative Weight Change (mg)							
	Specimen Number							
	C4	J29	L47	P48	O42	J28	L48	P49
20	+6.1	+11.0	+4.8	+5.9	+9.8	+10.1	+4.9	+5.7
40	+10.2	+14.3	+6.5	+7.9	+13.7	+13.2	+6.6	+7.5
60	+10.2	+14.8	+5.8	+6.6	+12.8	+12.3	+5.6	+6.4
80	+11.6	+14.7	+7.2	+8.5	+13.2	+14.4	+5.9	+7.0
100	+13.0	+16.0	+7.8	+8.5	+14.5	+16.1	+7.0	+7.6
120	+15.9	+18.6	+9.1	+9.8	+18.9	+16.8	+8.5	+9.9
140	+16.5	+18.8	+8.8	+9.6	+19.1	+16.9	+8.1	+9.7
160	+16.9	+18.7	+8.9	+9.6	+19.0	+16.7	+8.3	+9.9
180	+17.5	+19.2	+9.5	+10.1	+20.1	+17.4	+9.0	+10.7
200	+16.3	+18.8	+9.2	+9.6	+19.2	+16.9	+8.4	+10.2
220	+15.3	+18.2	+8.5	+8.9	+18.8	+16.4	+7.9	+9.8
240	+16.7	+19.3	+9.6	+12.4	+16.1	+16.3	+7.6	+9.6
260	+16.5	+19.3	+9.4	+10.2	+20.7	+17.7	+9.0	+10.8
280	+15.9	+18.9	+9.1	+10.7	+20.2	+17.2	+8.4	+10.2
300	+15.0	+18.8	+9.8	+9.8	+20.4	+17.2	+8.4	+10.3
320	+14.4	+18.1	+7.9	+8.8	+19.8	+16.4	+7.5	+10.3
340	+15.4	+18.5	+8.2	+9.3	+20.3	+16.8	+7.6	+10.0
360	+15.9	+18.2	+8.2	+9.2	+20.3	+16.5	+7.4	+10.2
380	+16.6	+18.6	+8.7	+9.4	+20.9	+17.0	+7.8	+10.5
400	+16.4	+18.4	+8.5	+9.4	+21.3	+17.0	+7.7	+10.5
420	+17.0	+18.1	+7.8	+9.3	+21.8	+17.0	+7.1	+10.6
440	+16.8	+18.0	+7.6	+9.4	+22.0	+16.8	+7.0	+10.4
460	+16.9	+17.4	+7.1	+8.9	+21.6	+16.4	+6.5	+10.3
480	+17.8	+18.2	+7.6	+9.4	+22.3	+16.8	+7.7	+10.7
500	+15.0	+15.6	+4.5	+6.7	+22.3	+16.7	+6.4	+10.4
520	+16.9	+17.4	+6.5	+8.9	+21.9	+16.5	+5.9	+10.1
540	+16.0	+16.4	+7.3	+8.3	+21.7	+15.9	+5.1	+9.6
560	+19.4	+19.2	+7.9	+10.9	+24.2	+18.4	+7.5	+11.9
580	+17.9	+18.5	+7.1	+9.9	+22.7	+17.3	+6.4	+11.2

Notes: + denotes weight gain

WEIGHT CHANGE DURING OXIDATION-EROSION TEST
TEST NUMBER 36, RIG NUMBER 2

1845° F MAXIMUM TEMPERATURE ALONG THE TRAILING EDGE

Exposure Time (Hours)	Cumulative Weight Change (mg)							
	Specimen Number							
	C4	J29	L47	P48	O42	J28	L48	P49
600	+18.5	+19.1	+7.7	+11.0	+23.7	+18.4	+7.2	+12.1
620	+17.7	+18.5	+6.8	+10.5	+22.6	+19.8	+6.4	+11.7
640	+18.9	+18.1	+6.1	+10.0	+21.4	+17.2	+5.7	+11.1
660	+19.2	+19.0	+7.0	+11.0	+22.5	+18.5	+6.6	+12.1
680	+16.4	+18.8	+6.6	+10.8	+21.9	+18.2	+6.3	+12.8
700	+17.9	+18.4	+5.7	+10.4	+20.9	+17.5	+5.4	+11.9
720	+16.5	+17.8	+5.0	+9.6	+19.9	+17.2	+5.0	+11.6
740	+15.9	+17.1	+4.2	+8.9	+19.0	+16.5	+4.5	+10.3
760	+11.2	+17.9	+5.0	+10.2	+19.5	+17.6	+5.2	+12.0
780	+11.6	+17.8	+4.7	+10.2	+19.0	+17.7	+5.1	+12.0
800	+9.7	+17.9	+4.7	+10.4	+18.5	+17.9	+5.1	+12.2
820	+9.3	+18.4	+5.0	+11.0	+18.5	+18.3	+5.4	+12.2
840	+9.8	+18.2	+4.1	+10.7	+17.5	+18.1	+4.5	+12.3
860	+9.3	+18.3	+3.7	+10.4	+16.2	+18.3	+4.5	+12.7
880	+9.5	+18.4	+4.0	+10.6	+16.3	+18.2	+4.8	+12.5
900	+7.8	+19.8	+4.7	+12.1	+11.4	+19.6	+5.2	+13.8

Note: + denotes weight gain

WEIGHT CHANGE DURING OXIDATION-EROSION TEST
TEST NUMBER 36, RIG NUMBER 2

1845° F MAXIMUM TEMPERATURE ALONG THE TRAILING EDGE

Exposure Time (Hours)	Cumulative Weight Change (mg)							
	Specimen Number							
	C4	J29	L47	P48	O42	J28	L48	P49
920	+6.1	+19.2	+3.8	+11.6	+7.7	+19.1	+4.8	+13.3
940	+5.6	+18.5	+2.8	+10.8	+2.8	+18.9	+4.3	+13.2
960	+7.7	+19.4	+2.9	+11.6	-0.8	+19.6	+4.4	+13.7
980	+6.0	+18.9	+1.6	+10.9	-8.6	+18.5	+3.8	+12.7
1000	+6.6	+19.2	+1.5	+11.5	-15.0	+19.5	+3.3	+13.6
	C4 and O42 removed from test at 1000 hours - D3 and K32 into test.							
	D3	J29	L47	P48	K32	J28	L48	P49
1020	—	+19.6	+1.3	+12.0	—	+19.4	+3.1	+13.7
20	+4.4	—	—	—	+4.9	—	—	—
1040	—	+19.2	+0.3	+11.5	—	+19.0	+2.3	+13.4
40	+7.7	—	—	—	+6.4	—	—	—
1060	—	+19.4	+0.1	+11.6	—	+19.3	+2.7	+13.8
60	+8.4	—	—	—	+7.2	—	—	—
1080	—	+20.6	+0.9	+12.7	—	+19.7	+3.1	+14.1
80	+9.9	—	—	—	+7.9	—	—	—
1100	—	+18.6	-1.8	+10.8	—	+18.2	+1.4	+12.6
100	+8.3	—	—	—	+6.3	—	—	—
1120	—	+20.3	-0.6	+13.0	—	+20.0	+3.8	+14.1
120	+10.1	—	—	—	+8.1	—	—	—
1140	—	+18.6	-3.5	+11.5	—	+18.4	+1.1	+13.2
140	+9.8	—	—	—	+7.4	—	—	—
1160	—	+19.5	-2.5	+12.6	—	+19.0	+1.5	+13.8
160	+11.4	—	—	—	+7.9	—	—	—
1180	—	+19.8	-3.0	+13.4	—	+19.5	+1.8	+13.9
180	+12.3	—	—	—	+8.6	—	—	—
1200	—	+20.2	-3.2	+14.3	—	+19.9	+1.9	+14.4
200	+14.1	—	—	—	+9.2	—	—	—
1220	—	+19.9	-4.1	+14.2	—	+19.6	+1.4	+14.4
220	+14.6	—	—	—	+9.1	—	—	—
1240	—	+19.8	-5.0	+14.4	—	+19.6	+1.1	+14.2
240	+14.9	—	—	—	+9.3	—	—	—
1260	—	+18.2	-6.2	+13.3	—	+18.8	+0.9	+12.6
260	+13.7	—	—	—	+7.8	—	—	—

WEIGHT CHANGE DURING OXIDATION-EROSION TEST

TEST NUMBER 36, RIG NUMBER 2
1845° F MAXIMUM TEMPERATURE ALONG THE TRAILING EDGE

Exposure Time (hours)		Cumulative Weight Change (mg)						
		Specimen Number						
	D3	J29	L47	P48	K32	J28	L48	P49
1280		+19.7	-6.4	+15.3		+19.2	+0.3	+14.2
280	+15.5				+9.4			
1300		+19.4	-7.7	+15.2		+19.2	±0.0	+14.4
300	+16.3				+9.6			
1320		+19.4	-8.6	+15.4		+19.6	+0.1	+14.7
320	+17.0				+9.6			
1340		+18.7	-10.1	+15.2		+18.0	-1.7	+13.7
340	+16.9				+8.9			
1360		+19.7	-10.2	+17.0		+19.3	-0.9	+15.7
360	+18.5				+10.3			
1380		+19.8	-11.5	+16.9		+19.4	-1.2	+15.5
380	+19.6				+10.8			
1400		+20.1	-12.5	+17.0		+19.4	-1.6	+16.2
400	+19.8				+10.7			
1420		+19.5	-14.7	+19.2		+18.7	-2.9	+15.4
420	+20.3				+10.2			
1440		+20.0	-16.3	+17.7		+19.2	-3.2	+16.2
440	+21.3				+11.2			
1460		+19.0	-22.6	+16.1		+19.0	-7.9	+16.4
460	+15.2				+12.3			
1480		+19.2	-24.5	+16.1		+18.9	-8.8	+17.2
480	+2.4				+13.1			
	L47 and L48 removed from test at 1480 hrs - N40 and N42 added to test							
	D3	J29	N40	P48	K32	J28	N42	P49
1500		+18.7		+15.9		+18.6		+17.3
500	--				+13.3			
20			--				-23.8	

WEIGHT CHANGE DURING OXIDATION-EROSION TEST

TEST NUMBER 36, RIG NUMBER 2
1845° F MAXIMUM TEMPERATURE ALONG THE TRAILING EDGE

Exposure Time (hours)	Cumulative Weight Change (mg)							
	Specimen Number							
	N40 removed from test. E34 added for temperature control purposes							
	D3	J29	E34	P48	K32	J28	N42	P49
1520		+18.0		+15.0		+17.4		+17.3
520	-0.9				+12.7			
40							-28.2	
20			-3.0					
1540		+18.6		+15.4		+17.9		+18.1
540	+1.0				+13.8			
60							-29.7	
40			-2.4					
1560		+18.4		+15.5		+18.0		+18.7
560	+2.0				+14.3			
80							-30.8	
60			-3.1					
1580		+18.6		+15.8		+17.9		+19.0
580	+3.8				+14.9			
100							-31.5	
80			-4.1					

WEIGHT CHANGE DURING OXIDATION-EROSION TEST

TEST NUMBER 37, RIG NUMBER 1

2050° F MAXIMUM TEMPERATURE ALONG THE TRAILING EDGE

Exposure Time (Hours)	Cumulative Weight Change (mg)							
	Specimen Number							
	H38	B51	C48	F32	H56	B52	C54	F58
20	+15.1	+3.9	+6.7	+6.4	+16.8	+3.2	+8.4	-0.6
40	+19.2	+5.5	+10.5	+7.4	+19.4	+5.2	+11.7	+0.3
60	+20.8	+5.5	+11.7	+9.2	+20.4	+5.2	+12.6	+0.6
80	+23.8	+8.0	+15.3	+11.9	+23.4	+7.7	+15.8	+2.6
100	+24.6	+8.2	+15.2	+12.2	+24.0	+6.9	+15.7	+2.3
120	+24.6	+7.9	+14.5	+11.4	+23.4	+8.3	+16.3	+2.3
140	+25.4	+8.5	+14.5	+12.2	+25.4	+8.2	+15.5	+2.0
160	+27.5	+11.3	+16.2	+12.4	+26.6	+9.6	+16.7	+2.9
180	+28.9	+12.4	+17.2	+13.4	+27.2	+10.2	+17.8	+3.6
200	+29.4	+12.5	+17.2	+13.9	+27.4	+10.7	+18.3	+3.9
220	+27.3	+12.5	+14.1	+11.7	+25.6	+9.3	+16.4	+2.0
240	+26.9	+10.6	+13.1	+10.9	+24.8	+8.8	+15.0	+1.0
260	+26.2	+9.8	+12.1	+10.3	+23.7	+8.2	+14.1	+0.0
280	+26.3	+9.2	+12.4	+9.9	+23.8	+8.6	+14.1	+0.1
300	+27.0	+9.2	+12.7	+10.5	+24.1	+9.0	+14.6	+0.2
320	+26.3	+9.3	+11.4	+9.5	+23.1	+8.3	+13.3	-0.6
340	+26.3	+8.0	+10.4	+9.0	+22.5	+8.0	+13.4	-1.2
360	+26.2	+7.9	+10.0	+9.0	+22.6	+7.9	+12.3	-1.2
380	+25.2	+7.0	+9.0	+8.2	+21.7	+7.2	+11.1	-2.6
400	+24.1	+6.2	+7.8	+7.3	+20.7	+6.6	+10.0	-3.3
420	+24.2	+6.1	+8.0	+7.4	+20.5	+6.4	+9.8	-3.3
440	+24.7	+5.7	+7.4	+7.3	+20.2	+6.1	+9.1	-3.6
460	+25.0	+6.1	+7.9	+7.6	+20.4	+5.7	+9.9	-3.6
480	+25.8	+6.5	+8.2	+8.1	+21.5	+6.5	+10.3	-2.9
500	+26.1	+6.7	+8.8	+8.6	+21.3	+6.9	+10.7	-3.7
520	+25.7	+7.2	+9.7	+9.1	+21.5	+7.6	+11.3	-4.5
540	+22.3	+2.8	+3.2	+5.3	+17.3	+3.3	+4.7	-6.1
*	H38	B51	C48	F58	H56	B52	C54	F32
560	+21.8	+3.9	+3.5	-6.0	+17.4	+3.9	+5.3	+4.4
580	+20.8	+3.1	+4.6	-5.6	+18.5	+3.6	+4.5	+5.0
600	+21.8	+2.4	+1.5	-6.8	+16.3	+3.1	+3.8	+3.5
620	+22.0	+3.3	+2.7	-5.7	+17.2	+3.6	+4.9	+4.7

Notes: + denotes weight gain

* reversed specimens F32 and F58 in holder

WEIGHT CHANGE DURING OXIDATION-EROSION TEST
TEST NUMBER 37, RIG NUMBER 1
2050° F MAXIMUM TEMPERATURE ALONG THE TRAILING EDGE

Exposure Time (Hours)	Cumulative Weight Change (mg) Specimen Number							
	H38	B51	C48	F58	H56	B52	C54	F32
640	+21.9	+2.5	+1.1	-6.0	+15.8	+3.4	+3.8	+3.8
660	+21.5	+1.5	-0.3	-6.6	+15.2	+2.3	+2.5	+3.0
680	+20.7	+1.6	-0.1	-6.4	+15.0	+2.2	+2.1	+2.8
700	+21.7	+1.0	-1.3	-7.5	+14.7	+1.7	+1.2	+2.5
720	+20.6	+0.2	-1.5	-8.2	+13.7	+0.8	-0.1	+1.6
740	+20.6	-0.5	-3.3	-8.1	+13.2	-0.4	-0.7	+1.1
760	+19.7	-1.5	-4.5	-9.5	+12.2	-0.6	-2.2	0.0
780	+19.1	-2.0	-5.5	-10.0	+12.0	-0.9	-3.0	-0.5
800	+19.2	-2.2	-6.3	-10.4	+11.4	-1.6	-4.0	-1.2
820	+19.4	-2.0	-6.4	-10.2	+11.4	-1.6	-4.0	-1.1
840	+18.1	-3.5	-7.9	-11.2	+10.4	-2.5	-5.1	-2.0
860	+18.1	-2.9	-8.1	-11.0	+10.1	-3.2	-5.5	-2.3
880	+17.3	-4.7	-9.3	-11.8	+8.6	-4.4	-7.1	-3.5
900	+17.4	-4.4	-9.0	-11.6	+9.3	-4.2	-6.6	-2.7
920	+17.2	-4.5	-9.5	-11.2	+9.4	-3.7	-6.2	-2.6
940	+15.9	-4.3	-8.5	-11.3	+9.1	-5.7	-6.6	-2.5
960	+15.0	-5.6	-10.0	-12.0	+8.2	-7.2	-7.4	-3.6
980	+14.4	-6.6	-10.9	-12.8	+7.2	-8.5	-8.5	-4.1
1000	+13.4	-5.5	-10.0	-11.7	+8.1	-8.6	-7.4	-3.2
1020	+11.3	-6.6	-11.6	-12.8	+7.0	-11.7	-8.9	-4.3

Note: + denotes weight gain

WEIGHT CHANGE DURING OXIDATION-EROSION TEST
TEST NUMBER 37, RIG NUMBER 1
2050° F MAXIMUM TEMPERATURE ALONG THE TRAILING EDGE

	Cumulative Weight Change (mg)							
	Specimen Number							
	H38	B51	C48	F58	H56	B52	C54	F32
1040	+12.6	-5.8	-10.7	-11.7	+7.8	-12.4	-8.3	-3.6
1060	+13.0	-6.2	-11.1	-12.4	+7.2	-15.2	-8.5	-3.7
1080	+11.8	-7.8	-12.3	-13.7	+6.2	-18.9	-9.8	-4.7
1100	+12.9	-7.4	-12.1	-12.9	+6.4	-22.8	-9.2	-4.3
	B51 and B52 removed from test at 1100 hrs - G36 and G59 into test.							
	H38	G36	C48	F58	H56	G59	C54	F32
1120	+12.3	—	-12.9	-13.5	+6.3	—	-9.5	-4.2
20	—	+10.4	—	—	—	+5.9	—	—
1140	+12.4	—	-13.2	-13.6	+5.9	—	-10.1	-4.8
40	—	+15.4	—	—	—	+8.1	—	—
1160	+12.4	—	-14.1	-14.2	+5.0	—	-10.5	-5.2
60	—	+18.0	—	—	—	+8.7	—	—
1180	+11.2	—	-14.7	-14.5	+4.7	—	-11.3	-5.8
80	—	+19.9	—	—	—	+10.1	—	—
1200	+10.2	—	-16.6	-16.4	+2.6	—	+13.5	-7.6
100	—	+18.8	—	—	—	+8.8	—	—
1220	+10.4	—	-15.7	-14.9	+3.9	—	-12.8	-6.8
120	—	+21.4	—	—	—	+10.8	—	—
1240	+9.3	—	-16.3	-16.0	+2.6	—	-13.4	-7.8
140	—	+22.5	—	—	—	+11.1	—	—
1260	+11.6	—	-16.6	-16.0	+2.4	—	-13.8	-9.8
160	—	+23.1	—	—	—	+11.3	—	—
1280	+9.7	—	-17.6	-16.8	+1.6	—	-4.5	-9.8
180	—	+11.7	—	—	—	+11.5	—	—
1300	+7.9	—	-20.3	-19.3	+1.3	—	-15.9	-10.8
200	—	+6.2	—	—	—	+9.9	—	—

WEIGHT CHANGE DURING OXIDATION-EROSION TEST

TEST NUMBER 37, RIG NUMBER 1
2050° F MAXIMUM TEMPERATURE ALONG THE TRAILING EDGE

Exposure Time (hours)	Cumulative Weight Change (mg)							
	Specimen Number							
	H38	G36	C48	F58	H56	G59	C54	F32
1320	+8.1		-14.3	-18.0	-0.5		-16.3	-11.2
220		+2.8				+11.9		
1340	+7.8		-19.7	-18.0	-1.1		-16.5	-11.8
240		-2.5				+12.3		
1360	+4.5		-20.6	-19.0	-4.5		-17.4	-12.9
260		-10.4				+12.3		
1370			-21.3				-18.9	
	C48 and C54 removed from test at 1370 hrs; J21 and J50 added							
	H38	G36	J21	F58	H56	G59	J50	F32
1380	+7.2			-21.3	-7.0			-14.3
280		-16.8				+11.7		
10			+10.3				+10.7	
1400	+7.7			-18.9	-6.4			-13.4
300		-19.3				+12.9		
30			+13.4				+13.5	
	F58 and F32 removed from test at 1400 hrs; P38 and P50 added							
	H38	G36	J21	P38	H56	G59	J50	P50
1420	+8.0				-7.5			
320		-23.5				+13.2		
50			+14.8				+14.7	
20				+7.0				+6.9
1440	+6.6				-9.1			
340		-28.4				+12.3		
70			+13.9				+13.3	
40				+7.1				+6.5
1460	+9.4				-10.3			
360		-32.2				+12.1		
90			+13.3				+12.9	
60				+7.3				+6.6
1480	+7.6				-9.8			
380		-34.9				+13.2		
110			+14.1				+13.3	
80				+8.5				+6.3
1500	-3.1				-15.0			
400		-42.2				+11.5		
130			+10.4				+10.2	
100				+5.1				+2.3
1520	-3.5				-15.2			
420		-48.8				+12.5		
150			+10.5				+10.5	
120				+4.0				+1.1
1540	-3.7				-16.4			
440		-56.0				+12.4		
170			+8.1				+8.2	
140				+1.8				-3.2

WEIGHT CHANGE DURING OXIDATION-EROSION TEST

TEST NUMBER 37, RIG NUMBER 1
2050° F MAXIMUM TEMPERATURE ALONG THE TRAILING EDGE

Exposure Time (hours)	Cumulative Weight Change (mg)							
	Specimen Number							
	G36 removed from test at 440 hrs; D30 added to test							
	H38	D30	J21	P38	H56	G59	J50	P50
1560	-8.4				-18.1			
460						+11.7		
190			+6.2				+6.7	
160				-1.9				-5.9
20		+2.1						
1580	-11.0				-18.6			
480						+11.6		
210			+4.5				+4.1	
180				-5.2				-10.0
40		-2.0						
1600	-17.4				-19.4			
500						+12.0		
230			+3.2				+2.1	
200				-6.8				-12.7
60		-1.4						
1620	-20.1				-20.2			
520						+11.7		
250			+1.4				+0.4	
220				-8.9				-15.5
80		-0.4						